Mechanics of Fibroblast Migration

A Dissertation Presented
By

Steven Munevar

Submitted to the Faculty of the

University of Massachusetts Graduate School of Biomedical Sciences, Worcester

In partial fulfillment of the requirements for the degree of

DOCTOR OF PHILOSOPHY

(May 09, 2003)

Cellular and Molecular Physiology

MECHANICS OF FIBROBLAST MIGRATION

A Dissertation Presented

By

Steven Munevar

Approved as to style and content by;

_____
Thomas Honeyman, Chair of Committee

_____
Micah Dembo, Member of Committee

_____
Stephen Doxsey, Member of Committee

_____
Peter Grigg, Member of Committee

_____
Stephen Lambert, Member of Committee

_____
Yu-Li Wang, Dissertation Mentor

_____
Anthony Carruthers, Dean of
Graduate School of Biomedical Sciences

Department of Cellular
and Molecular Physiology

May 09, 2003

Copyright Notice

Parts of this thesis have appeared in the following publications:

Munevar, S., Y. L. Wang., and M. Dembo. ***Traction Force Microscopy of Migrating Normal and H-ras Transformed 3T3 Fibroblasts.*** *Biophysical Journal (2001) Vol. 80. p. 1744-1757.*

Munevar, S., Y. L. Wang., and M. Dembo. ***Distinct Roles of Frontal and Rear Cell-Substrate Adhesions in Fibroblast Migration.*** *Molecular Biology of the Cell (2001) Vol. 12. p. 3947-3945.*

Munevar, S., Y. L. Wang., and M. Dembo. ***Role of Stretch Activated Calcium Ion Channels During Fibroblast Migration.*** (Submitted).

Acknowledgments

I would like to thank Dr. Yu-Li Wang, Wang Lab members, and Dr. Micah Dembo for all of their help and insightful discussion. I would also like to thank Boston University Center for Scientific Computing for the use of their supercomputer facilities. Additionally I would like to thank the NIH NRSA for their support in the form of a predoctoral fellowship, GM-20749. Lastly I would like to thank my friends and most of all my family for all of their support and encouragement.

Abstract

Cell migration involves complex mechanical interactions between cells or between cells and the underlying substrate. Using a newly developed technique, "traction force microscopy", I have been able to visualize the dynamic characteristics of mechanical forces exerted by migrating fibroblasts such as magnitude, direction, and shear. For NIH 3T3 fibroblasts, I found that the lamellipodium provides nearly all of the force necessary for cell migration. A high shear zone separates the lamellipodium from the remainder of the cell body, suggesting that they are mechanically distinct entities. The timing of the tractions at the leading edge, as well as the spatial distribution, bears no apparent relationship to concurrent local protrusive activities, yet changes in traction force patterns often precede changes in migration direction. In H-ras transformed cells I found isolated regions of weak, transient traction forces in pseudopods all along the cell that appeared to act against one another. The resulting shear pattern suggested that there were multiple disorganized mechanical domains. These results support a frontal towing model for cell migration where the dynamic traction forces at the leading edge served to actively pull the cell body forward. In H-ras transformed cells, the weak poorly coordinated traction forces coupled with weak cell substrate-adhesions were likely responsible for the abnormal motile behavior of these cells. To probe the mechanical interactions beneath various regions of migrating fibroblasts, a cell substrate inhibitor (GRGDTP peptide) was locally applied while imaging stress distribution on the substrate utilizing traction force microscopy. I found that both spontaneous and GRGDTP induced detachment of the trailing edge resulted in extensive cell shortening with no change in overall traction force magnitude or cell migration. Conversely, leading edge disruption

resulted in a dramatic global loss of traction forces prior to any significant cell shortening. These results suggested that fibroblasts transmit their contractile forces to the substrate through two distinct types of adhesions. Leading edge adhesions were unique in their ability to transmit active propulsive forces whereas trailing end adhesions created passive resistance during cell migration and readily redistributed their loads upon detachment. I have also investigated how fibroblasts regulate traction forces based on mechanical input. My results showed that stretching forces applied through the flexible substrate induced increases in both intracellular calcium concentration and traction forces in fibroblasts. Treatment with gadolinium, a well known stretch-activated ion channel inhibitor, was found to inhibit both traction forces and cell migration without inhibiting cellular spread morphology or protrusive activities. Gadolinium treatment also caused a pronounced decrease in vinculin and phosphotyrosine concentrations from focal adhesions. Local application of gadolinium to the trailing region had no detectable effect on overall traction forces or cell migration, whereas local application to the leading edge caused a global inhibition of traction forces and an inhibition of migration. These observations suggest that stretch activated entry of calcium ions in the frontal region serves to regulate the organization of focal adhesions and the output of mechanical forces. Together my experiments elucidate how fibroblasts exert mechanical forces to propel their movements, and how fibroblasts utilize mechanical input to regulate their movements.

Table of Contents

List of Tables

List of Figures

Chapter 1 - Introduction

The Discovery of Cells and Cell Migration

In the year 1665, an Englishman Robert Hooke, using a crude microscope, reported that life's smallest structural units were small boxes or "cells" (Tortora G., 1995). This was one of the most important biological discoveries in history and marked the beginning of what was called the cell theory or the idea that all living things are composed of cells. The next advancement in the evolution of microscopy was brought about by a Dutch merchant and amateur scientist named Anton van Leeuwenhoek. Anton van Leeuwenhoek was probably the first person to see live microorganisms through the magnifying lens microscope he developed (Tortora G., 1995). Between the years 1673 and 1723 Leeuwenhoek detailed a series of letters to the Royal Society of London describing the "animalcules" he observed using his simple single lens microscope.

Since these early innovations in microscopy by Hooke and Leeuwenhoek, man has marveled at the multitude of microorganisms and single celled creatures that have since been discovered. One of the most exciting discoveries made by these early microscopists was that animal cells are capable of autonomous migration. As technology has advanced, so has our understanding of the mechanisms of cell movement. Yet a large number of questions still remain as to how exactly cells migrate and how cells in a multicellular organism coordinate their migration efforts.

According to Newton's law, in order for cells to move, they must exert some force onto something in their immediate surroundings. A second basic principle is that, in order to be functional, the cell must develop a polarity and a guidance mechanism to steer

the movement. Underlying these common principles are a wide variety of mechanisms. Some cells like bacterium in solution may exert propulsive forces using "spinner" like flagella structures. Bacterial flagella are composed of protein cylinders that curve smoothly and are about 20 nm in diameter and variable in lengths (on average 5-10μm in length). The base of the flagella is connected to a motor device through a short flagellar hook, which is a strong and resilient structure allowing the flagella to alter their rotation direction while still transmitting rotational forces. Flagellar motors can rotate on average about 100 revolutions per second and can reverse their direction of rotation on average in less than a tenth of a second. The motor is driven not by the hydrolysis of ATP as for eukaryotic motor proteins, but by a gradient of protons that move across the plasma membrane (Bray, 2001).

A similar mechanism, involving the beating of cilia and flagella, drives the locomotion of some eukaryotic cells. However, unlike prokaryotic flagella, which are filaments of protein projecting directly from the cell surface; eukaryotic flagella and cilia are microtubule-based projections encased in the plasma membrane. Both flagella and cilia structures in eukaryotic cells possess a diameter of approximately 0.25 μm. Cilia are approximately 10 μm in length. They tend to be large in number and dispersed across the cell surface. The collective forward-and-backward motion of cilia allows the cells to swim through the surrounding fluid, to move the surrounding fluid over the surface of the cell, or to sweep food particles into their oral cavity. Unlike cilia, flagella can be as long as 200 μm. They also differ from cilia in the pattern with which they beat (waveform). Flagella tend to be limited to one or two per cell and serve primarily a locomotive purpose (Bray, 2001).

Eukaryotic cilia and flagella are both composed of microtubules and associated proteins, collectively referred to as the axoneme. The microtubule component in the axoneme consists of a central pair surrounded by nine outer doublets. Anchoring the cilia and flagella to the cell is the basal body, into which the minus ends of the microtubules are inserted. The basal bodies also serve the important purpose of nucleating the growth of axonemal microtubules. The activity of cilia and flagella is driven by the microtubule motor protein dynein, which causes the outer microtubules doublets to slide relative to one another (Bray, 2001).

Theories of Amoeboid Movement

Some single-cell eukaryotic organisms such as amoebae utilize a method of locomotion that is distinct from those using cilia or flagella; they crawl by means of pseudopodia. Pseudopodia are extensions or protrusions of the plasma membrane approximately 100 μm or more in diameter. They require a time frame of minutes to extend or make noticeable changes in position. Amoebae migrate by extending pseudopodia in one direction that subsequently make contact with the underlying substrate, while other regions of the cell undergo retraction (Bray, 2001).

A number of biological events serve to support pseudopodial growth. As pseudopodia extend outward they are filled with a stream of fluid cytoplasm. The flow comes from the body of the cell via what appears to be a cylindrical, rigid wall of cytoplasm. Thus the pseudopodia can be subdivided into two distinct, interconvertible sections. The inner compartment, which is fluid, mobile and contains organelles, is the plasmasol (or endoplasm) whereas the outer layer, which is usually transparent and gel-like, is known as the plasmagel (or ectoplasm). The fluid plasmasol tends to congeal into

the gel-like plasmagel as the flow reaches the tip of the pseudopod. In areas of the cell where pseudopodia are being reabsorbed, the opposite process of solation takes place. These changes are believed to involve changes in the number, length, and degree of protein cross-linkages (Bray, 2001).

A number of hypotheses have been proposed concerning the locomotion of amoebae. One of the more widely accepted, supported by such researchers as Dujardin, Schulze, Eckert, and Wallich around 1835-1875, is that cytoplasmic streaming is driven by pressure. This hypothesis suggests that, in order to undergo locomotion, amoeboid cells contract their outer ectoplasm selectively in specific regions of the cell, thereby squeezing a stream of the more fluid endoplasm into an advancing pseudopod. Numerous hypotheses have also been proposed to explain how amoebae interact with the substrate to propel their forward migration. One popular theory is called the tail or trailing end retraction theory (Elson, 1999). In this hypothesis a migrating cell extends forward through pseudopodial formation and forms an adhesion with the underlying substrate. The cell body and trailing end remain adhered to the underlying substrate. As the cell continues to extend and form new substrate contacts at the leading edge, the cell body becomes elongated and tension starts to develop, which eventually overcomes the adhesions underlying the trailing region of the cell and allows the trailing end to snap forward.

A variation of the trailing end retraction theory suggests a more controlled mechanism (Sheetz et al., 1998). It proposes that, as cells elongate following the extension and adhesion of pseudopodia to the underlying substrate, enzymes at the rear of the cell serve to sever the linkages established there during earlier elongation steps (Bray,

2001). Thus cellular migration is a combination of extension and adhesion at the leading edge of the cell, controlled severing of substratum adhesions at the trailing edge, and retraction. An alternative mechanism, referred to as the frontal contraction theory, proposes that cell migration is driven primarily by anchorage near the leading edge combined with contractile forces that drag the cell body forward (Harris et al., 1980; Munevar et al., 2001a). The primary support for this theory is the observation that isolated cytoplasm from amoebae was capable of contraction and bi-directional locomotion (Allen, 1981). Since its inception this hypothesis has been the source of a great deal of controversy.

Cell Locomotion in Multicellular Organisms

The locomotion of cells in the body serves a myriad of important biological functions. Except for a small number of dedicated movers such as neutrophils, the relatively slow speed of migration and the sustained directionality suggest that cells may employ migration for purposes other than or in addition to transporting themselves. For example, fibroblasts are believed to serve a tissue remodeling function, where the large forces exerted by migrating cells remodel collagen fibers (Tomasek et al., 2002). Cell migration is also crucial for embryonic development, following specific biological cues over time and space. These events are mediated by movements of both individual cells and groups of cells moving together as sheets, which require a strong sense of cell-cell recognition and communication. It is likely that the movements, and the mechanical forces involved in cell movements, serve an important role in modulating both the extracellular environment and the intracellular signaling pathways.

Even in a fully developed body, cell locomotion remains a vital requirement of biological functions. For example, during wound healing cells must migrate into the wound and proliferate in order to generate new tissue (Tomasek et al., 2002). As cells move into a wounded area, they secrete the proteins to form the scaffold upon which the new tissue will be built (Tomasek et al., 2002). This scaffold also serves to assist cells of the immune system to migrate into the wounded region and ward off infections (Mutsaers et al., 1997).

In order for cells to correctly undergo directed migration they must be capable of sending and receiving a multitude of chemical and mechanical signals from both neighboring cells and surrounding matrices. Failure to respond to these cues may lead to abnormal proliferation and migration. Known as cancer, the abnormal proliferation of cells can take on a benign or malignant form. In the benign form a tumor, or abnormal proliferation of cells, stays in its location of origin never moving into neighboring or distant sites of the body. In the malignant form, tumors are able to invade neighboring tissues and move throughout the body via lymphatic and circulatory systems (Cooper, 1997). This in turn leads to serious pathological problems.

Locomotion of Cultured Cells

Even though most cells in intact tissues of a multicellular organism tend to be relatively immobile, being held in place via intercellular junctions and adhesions with the extracellular matrix, cells from many tissues are able to undergo spontaneous migration when dissociated and dispersed onto proper surfaces such as glass or charged plastic (Bray, 2001). Such cells often have the capacity to retain some of their differentiated characteristics. Examples are epithelial cells that can grow as sheets, nerve cells that

produce long axons, and myoblasts that can fuse into long, contractile multinucleate fibers (Bray, 2001).

Of the variety of adherent vertebrae cells that have been studied in culture, fibroblasts are among one of the most studied. While many cultured fibroblasts form striking lamellipodia and filopodia structures, other types of cells that have been dissociated into tissue culture also extend lamellipodia and filopodia structures. For example, dissociated neurons consist primarily of three main components: the cell body, the axon, and the growth cone. The cell body tends to stay in place whereas the growth cone migrates extensively. Attached to the cell body via its axon, the growth cone of many cultured neurons extends out flattened lamellipodia as well as long wispy filopodia that are seen to retract and extend much like the ruffling membranes of cultured fibroblasts. Highly mobile growth cones continue to move independently even if severed from the axon, suggesting that the motile machinery is self-sufficient. Another type of cultured cells often used in the study of cell migration is fish keratocytes (Anderson and Cross, 2000). These are non-pigmented epidermal cells from fish scales. They usually flatten into a fan shape as they adhere to the glass, and exhibit rapid, gliding movement at speeds of 10 μm/min or more (Bray, 2001).

Mechanism for the Locomotion of Cultured Cells

Locomotion of cultured cells is believed to share many common mechanisms with amoeboid movement described earlier. The two differ primarily with respect to the extent that cells adhere to the substrate, and the speed that the cytoplasm surges forward. In general locomotion of cultured cells may be divided into three distinct steps (Elson, 1999), which may take place simultaneously without a clear distinction of which is the

beginning or the end of the process. The first step is protrusion at the front end of the cell. This is followed by the formation of new adhesions near the site of protrusion onto the underlying substratum. At the opposite end, cells detach or retract its trailing edge from the underlying substratum, apparently as a result of contractions somewhere along the cell body. Such retraction is often coupled with a surge of forward movement (Chen, 1981). Although simple in principle, the mechanisms underlying these three basic steps remain largely a mystery. While the propulsion of the inner cytoplasm is generally viewed as being similar to that in amoeboid movement, albeit at a much lower rate, migration of cultured cells is believed to involve additional mechanisms for adhesion, de-adhesion, and retraction.

Migration of cultured cells is guided by both chemical and physical interactions with the environment. Many different cell types use chemical gradients to orientate their directional response (Bray, 2001). Various receptors on the cells surface serve to pickup different chemical signals which either attract or repel cells (Bray, 2001). Some cultured cells, such as fibroblasts, also show inhibition of migration upon the collision with other cells (Abercrombie and Dunn, 1975). This phenomenon is referred to as contact inhibition. The contact causes ruffling activities to cease, while the colliding cells appear to adhere to each other (Abercrombie and Dunn, 1975). Following collision alternate regions of the cells not in contact can continue to ruffle. Eventually the cells can separate from each other and start to migrate along new directions (Abercrombie and Dunn, 1975). Other cell types such as epithelial cells exhibit an even stronger contact inhibition of migration, as these cells will remain in contact following cell-cell collisions. Repeated collisions with additional cells can result in the formation of cell aggregates that

eventually develop into a contiguous sheet of cells such as those found in vivo (Abercrombie and Dunn, 1975).

In addition to cell-cell contact, other physical interactions with the environment can also serve to guide cell migration. When placed under mechanical tension, cultured endothelial cells are able to align themselves along the direction of the forces (Naruse et al., 1998). The mechanical stress may directly affect the direction of cell migration, or cause alignment of the underlying matrix proteins, which in turn guide cell migration. Cells can also respond to changes in substratum topography and surface adhesiveness; the guidance of cell migration by the gradient of surface adhesion strength has been referred to as haptotaxsis (Carter, 1967).

Detection of Mechanical Interactions during Cell Locomotion

One particular hurdle in understanding cell locomotion has been our limited ability to characterize the mechanical interactions between cells and the underlying substratum. The term most often used for this force is "traction". A number of methods have been developed for detecting traction forces, most of them using flexible artificial substrates. The technique developed some twenty years ago by Harris (Harris et al., 1980) involves culturing cells on thin films of silicone elastomer, polymerized from silicone fluid using a flame. As cells apply traction forces onto the silicone substrates, wrinkles visible under a light microscope would appear. This method was later optimized by substituting the flaming polymerization process with UV exposure, which yielded softer gels that allowed for an increased number of wrinkles and improved resolution and sensitivity (Burton and Taylor, 1997).

Despite improvements of the method with wrinkling silicone substrata, there are still a number of disadvantages. First, while this method can readily detect isolated regions of compression, with estimated sensitivity in the order of nano-newton, more complicated patterns of forces are not resolvable. Furthermore, it is extremely difficult to convert the patterns of wrinkles into vector maps of traction forces. Although the magnitude of compressive forces has been calculated based on the stiffness of the substrate and the length of wrinkle (Beningo et al., 2002), the results represent at best a crude estimate.

To allow quantitative measurements of traction forces, the silicone film method was improved by adhering the substrate along its edges to a cylindrical container, to prevent wrinkling, and by embedding it with beads that act as markers for local deformation (Oliver et al., 1998). The resulting non-wrinkling substrates detect traction forces as displacements of beads, and allow quantitative analysis of the magnitude and direction of traction forces using spring equations, even though the silicone substrates did not quite act as ideal springs (Oliver et al., 1998).

An alternative method uses fluorescence imaging to measure the deformation of micro patterned elastomers (Balaban et al., 2001). The procedure produces shallow patterns of a depth of 0.3 μm on the upper surface of the substratum, which is visible using phase contrast or fluorescence microscopy (Balaban et al., 2001). This pattern allows direct visualization of the displacement and facilitates quantification of the forces (Balaban et al., 2001). Forces can be calculated based on the elasticity theory, using measured displacements, the spring constant, and the location of the focal adhesions as input parameters. GFP-vinculin, a well-known focal adhesion protein, serves as the

marker for focal adhesions (Balaban et al., 2001). The precision that can be achieved is determined by the size of the micro-patterned array; smaller dot arrays with a diameter of approximately 0.8 μm and a pitch of 2 μm were found to yield more precise measurements (Balaban et al., 2001). This novel approach has been used to measure the forces applied by stationary cells to the substratum. However, its reliability is affected by the requirement of a precise knowledge of the distribution of focal adhesions, such that failure to include small focal adhesions near the leading edge may lead to significant errors.

Another novel method involves the use of micro machined cantilevers on silicone wafers as the force transducer (Galbraith and Sheetz, 1997). This system works by using a light microscope to detect displacements of micrometer-sized pads at one end of the flexible cantilever. Forces applied by the cell are confined to the individual cantilevers and thus the magnitude of these forces can be calculated by multiplying the spring constant of the cantilever with the displacement distance. Drawbacks to this system are the difficulty in constructing the system, and potential effects of surface topography on cell migration. Also the spatial resolution of the system is limited by the density of the cantilevers and only forces perpendicular to the axis of the cantilever can be detected.

Traction Forces Exerted by Migrating Fish Keratocytes

Due to the simple shape of the cell and the lack of complicated steps of tail retraction, fish keratocytes have been used as a favorite model system for studying cell locomotion. They tend to crawl with little change in cell shape or migration speed due to the tight coupling between leading edge protrusion and trailing edge retraction (Burton et al., 1999). These cells appear to glide along the surface, as if propelled by wings, moving

quickly and changing directions readily. In the leading edge the predominant cytoskeletal protein is actin. The trailing edge of the cell and the regions around the nucleus contain mainly intermediate filaments and microtubules (Bray, 2001). It has also been shown that regions of the leading edge, when separated from the cell either spontaneously during retraction or as a result of micromanipulation, were able to migrate with the same speed as that of the intact cell (Bray, 2001), indicating that the leading edge contains all the essential components for cell migration.

Traction forces generated by migrating keratocytes have been studied extensively by Jacobson and colleagues (Dembo et al., 1996; Lee et al., 1994; Oliver et al., 1995) using the non-wrinkling silicone substratum method as discussed previously. The results revealed acto-myosin dependent "pinching" forces in steadily migrating keratocytes. Since the forces detected were perpendicular to the migration direction, it was initially unclear how these cells generated the propulsive forces for forward migration.

This puzzle was resolved using keratocytes whose trailing edge became transiently stuck to the substratum. These cells produced approximately 1 μdyn of propulsive thrust at the lateral "wings" (Oliver et al., 1999). However no propulsive thrust was detected at the leading edge even as the cell was pulling on its transiently stuck trailing edge (Oliver et al., 1999). The observations lead to the hypothesis that the propulsive tractions that drive the locomotion of keratocytes are usually cancelled by the adhesive tractions that resist locomotion. This in turn leaves only the equatorial or pinching tractions as detectable forces (Oliver et al., 1999). In addition, cells undergoing tight turns showed a markedly different pattern of traction forces from the normal pinching pattern (Oliver et al., 1999). This difference could be explained by the idea that

turning is accomplished through asymmetrical contractions at opposing lateral sides of the keratocyte (Oliver et al., 1999).

Measurements of Traction Forces with Polyacrylamide Substrata

An alternative method for the measurement of traction forces, which will be used extensively in this thesis, is based on substrata made from flexible polyacrylamide sheets. These sheets are easily prepared and possess superior mechanical and optical properties (Pelham and Wang, 1997). The optical properties allow for high resolution imaging through the gel, while the porous nature of the gel creates an environment that is more physiological in nature than plastic or glass. The polyacrylamide gel itself is inert thus interactions between cells and the gel are mediated by extracellular matrix proteins covalently linked onto the surface during preparation.

One of the most beneficial features is that the gel shows a nearly ideal elasticity over a wide range of applied forces. In addition the flexibility of the polyacrylamide gels can be readily regulated by varying the acrylamide and/or bisacrylamide concentration, without changing the chemical properties of the gel. Lastly by embedding the gels with fluorescent beads, it becomes possible to track the deformation of the gel in response to exerted forces with a sub-micron resolution. The distribution of forces may then be calculated based on the theory of elasticity.

The calculation of traction stress (forces per unit area), as developed by Dembo (Dembo et al., 1996), is based on the deformation of the substrate, as measured by the displacement of markers near the surface of the substrate, the boundaries of the cell, the spring constant (Young's modulus, E), and the compressibility of the material (defined by

the Poisson ratio, (v). The displacement $\boldsymbol{d}$ at a given position **p**, $\boldsymbol{d}_{p\alpha}$ as a result of traction stresses $\mathbf{T}_\beta(\boldsymbol{r})$ exerted over the surface, may be expressed as:

$$d_{p\alpha} = \iint g_{\beta\alpha}(m_p - r)T_\beta(r)dr_1 dr_2$$

where α and β denote the directions along Cartesian axes, and m_p denotes the position vector at p, taking into account the uncertainty of the measurement. The integration is confined within the spread area of the cell, since the traction forces were exerted only at cell-substratum contact points.

The nine functions $g_{\beta\alpha}(\boldsymbol{m}\text{-}\boldsymbol{r})$, derived by Boussinesq, define the displacement of the substratum in the direction α at location $\boldsymbol{m}$, in response to a concentrated force acting at location $\boldsymbol{r}$ and in the direction of β. The thickness of the polyacrylamide substrate for this analysis is assumed to be infinite as compared to the maximal displacement of the marker beads. The actual equations are as follows:

$$g_{11} = \frac{1+\nu}{2\pi E}\left(\frac{(2(1-\nu)r - x_3)}{r(r-x_3)} + \frac{(2r(\nu r - x_3) + x^2{}_3)x^2{}_1}{r^3(r-x_3)^2}\right)$$

$$g_{21} = \frac{1+\nu}{2\pi E}\left(\frac{((2r(\nu r - x_3) + x^2{}_3)x_1 x_2)}{r^3(r-x_3)^2}\right)$$

$$g_{31}=\frac{1+\nu}{2\pi E}\left(\frac{x_1x_3}{r^3}+\frac{(1-2\nu)x_1}{r(r-x_3)}\right)$$

$$g_{12}=\frac{1+\nu}{2\pi E}\left(\frac{\left((2r(\nu r-x_3)+x^2{}_3\right)x_1x_2}{r^3(r-x_3)^2}\right)$$

$$g_{22}=\frac{1+\nu}{2\pi E}\left(\frac{\left(2(1-\nu)r-x_3\right)}{r(r-x_3)}+\frac{(2r(\nu r-x_3)+x^2{}_3)x^2{}_2}{r^3(r-x_3)^2}\right)$$

$$g_{32}=\frac{1+\nu}{2\pi E}\left(\frac{x_2x_3}{r^3}+\frac{(1-2\nu)x_2}{r(r-x_3)}\right)$$

$$g_{13}=\frac{1+\nu}{2\pi E}\left(\frac{x_1x_3}{r^3}+\frac{(1-2\nu)x_1}{r(r-x_3)}\right)$$

$$g_{23}=\frac{1+\nu}{2\pi E}\left(\frac{x_2x_3}{r^3}+\frac{(1-2\nu)x_2}{r(r-x_3)}\right)$$

$$g_{33}=\frac{1+\nu}{2\pi E}\left(\frac{2(1-\nu)}{r}+\frac{x^2{}_3}{r^3}\right)$$

The Boussinesq theory predicts that at or near the surface of an incompressible substratum (Poisson ration = 0.5), there is negligible coupling of the in-plane displacements to the out of plane tractions.

A maximum likelihood analysis is then applied to calculate the resulting traction forces. To begin this analysis, the cell is divided into quadrilaterals with the use of a paving algorithm. The values of the x and y components of the traction force at each node of this mesh is then determined by maximizing the total Bayesian likelihood of the predicted marker displacements, defined as exp $[-(\chi^2 + \lambda C^2)]$, in conjunction with the following constraints:

1. There can be no forces outside of the boundary of the cell.
2. There can be no net force.
3. There can also be no net torque.
4. Lastly there must be minimal complexity.

In the equation χ^2 measures the deviation of calculated substrate displacement from the actual measurement, while C^2 denotes the complexity of the given traction map, and λ is an empirical parameter. Beginning with $\lambda = 0$ followed by progressively larger values of λ, the distribution of traction stresses that maximizes the Bayesian likelihood is determined. As λ increases, the relative weight of complexity in determining the likelihood increases while the relative weight of deviation, as reflected by χ^2, decreases. This eventually leads to a threshold point where the deviation becomes unacceptably large. The traction stress distribution just before this point represents the distribution of minimal complexity that satisfies the Boussinesq equations within an acceptable error.

Proteins Involved in Cell Locomotion

The multiple steps of cell locomotion, as addressed earlier, involve a number of proteins. The most crucial among them is actin, which is also the most abundant intracellular protein in most eukaryotic cells. Globular actin monomers, 43 kDa in molecular weight (375 amino acids), carry two self-assembly sites that allow it to undergo head-to-tail polymerization with two other actin monomers. The resulting actin filaments are polarized double helical structures, with the two ends referred to as the plus and minus ends respectively. The polarity serves important functions in defining the preferred site of assembly (at the plus end) as well as the direction of movement as a result of interactions with myosin motors (toward the minus end for most myosins). The bias in assembly also leads to the creation of a flux of subunits that assemble continuously at the plus end and disassemble at the minus end. This process has been referred to as treadmilling (Wang, 1985).

Cellular actin filaments are assembled into different structures. These structures can take the form of bundles or meshwork, each serving a different function. Actin bundles are cross-linked parallel arrays of filaments. Microvilli consist of closely packed parallel actin filaments, which serve to support plasma membrane projections. The actin filaments in these bundles are of a uniform polarity with their plus ends directed towards the plasma membrane. There are also bundles of actin filaments, such as stress fibers and the contractile ring during cytokinesis that are more loosely packed and able to contract. Actin networks generally serve to underlie the plasma membrane and thus support the surface of the cell. They are also involved in a variety of cell surface activities such as endocytosis.

The formation of these diverse structures involves interactions of actin filaments with a large number of accessory proteins. Such proteins are involved in actin filament nucleation (Arp 2/3 complex), cross linking (α-actinin and fascin), severing (gelsolin, cofilin), and stabilization (tropomyosin) (Borisy and Svitkina, 2000). Upon activation by such proteins as WASP family proteins or the bacterial equivalent ActA, the Arp 2/3 complex has been shown to bind existing actin filaments along their sides and to nucleate new actin filaments. The complex remains associated with the pointed end of the new filament, resulting in the formation of a Y-junction with a characteristic angle of ~ 70° (Borisy and Svitkina, 2000). This configuration has been found in lamellipodia. Following activation of the Arp 2/3 complex, the activator protein dissociates from the complex allowing them to activate additional nucleating events.

Other protein components that may promote treadmilling are Actin Dissociating Factor (ADF), cofilin, and profilin (Borisy and Svitkina, 2000). Under steady state conditions in vitro, the binding of ADF/cofilin to an actin-ADP filament increases dissociation from the pointed end by 25-fold. This interaction has been shown to speed up the movement of Listeria in extracts (Borisy and Svitkina, 2000), while shrinking the length of their actin "rocket tails", consistent with the notion that ADF/cofilin accelerates the turnover of actin filaments (Borisy and Svitkina, 2000). Working in conjunction with ADF/cofilin is the actin binding protein profilin, which has the unique ability to bind to actin monomers and promote the incorporation of actin subunits into the barbed but not the pointed end (Borisy and Svitkina, 2000). In addition profilin also suppresses spontaneous actin nucleation, thus maintaining a pool of actin subunits that are capable of

adding only to the barbed end. Thus profilin acts synergistically with ADF/cofilin to promote actin treadmilling (Borisy and Svitkina, 2000).

Working in conjunction with actin filaments are the myosin motor proteins. Myosin is responsible for numerous cellular movements in eukaryotic cells (Volkmann and Hanein, 2000). These motors are capable of moving actin filaments as well as vesicles (or cargo) along actin filaments. Although most myosins move actin filaments toward their pointed ends, some myosins have an opposite polarity of force production (Wells et al., 1999). In addition to the contraction of muscles, members of the myosin superfamily participate in diverse cellular functions such as membrane trafficking (Mermall et al., 1998), cell adhesion (Tuxworth et al., 2001), phagocytosis (Diakonova et al., 2002), cell motility (Mermall et al., 1998), cytokinesis (Glotzer, 2001), organelle transport (Mermall et al., 1998), and signal transduction (Mermall et al., 1998). At least some of these functions involve direct interactions of myosin with the microtubule motor kinesin, linking the functions of actin- and microtubule-based cytoskeleton systems (Volkmann and Hanein, 2000).

Myosins are ATPases, which generate forces as a result of actin-activated ATP hydrolysis (Volkmann and Hanein, 2000). For myosin to move along the actin filament it needs to undergo cycles of attachment and detachment from the actin filament (Volkmann and Hanein, 2000). Kinetic analyses have shown that ATP is hydrolyzed while myosin is detached from the actin filament (Volkmann and Hanein, 2000). The release of ADP and (Pi) is accelerated in the presence of actin, and is coupled to the generation of forces and formation of an actomyosin rigor complex (Volkmann and

Hanein, 2000). Myosin then detaches from actin following ATP binding, allowing another cycle of force production to begin (Volkmann and Hanein, 2000).

In addition to actin filaments, microtubules are also important components of the cellular cytoskeleton. Microtubules are rigid, hollow, rod-like structures approximately 25 nm in diameter. The structures are composed of protein subunits called tubulin, which exists as a dimer of α-tubulin and β-tubulin. These dimers polymerize in a head-to-tail fashion into tubular structures of 13 parallel protofilaments. As for actin, microtubules have a fast-growing plus end and a slow-growing minus end and undergo dynamic assembly-disassembly in the cell. This polarity, as for the polarity of actin filaments, is very important in determining the direction of movements upon interactions with motors. In addition to treadmilling, microtubules show alternating periods of growth and disassembly, a process referred to as dynamic instability. Microtubules are known to interact with actin filaments in cells. Although the mechanism is unclear, this interaction is believed to assist in determining cell shape and stabilizing the polarity of cell movements.

Actin Structures Involved in Cell Locomotion

During motility some of the essential actin containing structures are lamellipodia, filopodia, and focal adhesions. Studies have shown that microinjected fluorescently labeled actin becomes quickly incorporated in the peripheral lamellipodia, after which it is found to localize to focal contacts near the cell front. Lastly and much later it is found to incorporate into stress fiber bundles and in the arc-shaped actin arrays observed along the dorsal surface of the cell (Small et al., 1998). Evidence suggests that the tips of lamellipodia and filopodia serve to localize and harness actin polymerization for cell

locomotion (Small et al., 2002), and that actin polymerization is sufficient to account for the forces of protrusion (Abraham et al., 1999). Given a polymerization driven mechanism of motility, the system must be capable of both steady state maintenance and transient responses. Actin undergoes treadmilling in the lamellipodium (Wang, 1985). It is believed that steady state is achieved through a balance of elongation at the barbed end and shortening at the pointed end. At steady state though the growth at the barbed end is ultimately limited by dissociation of subunits from the pointed end, which is slow for pure actin filaments suggesting that additional components are required to accelerate the dissociation from the pointed end. ADF/cofilin and profilin are two components that are believed to accelerate the treadmilling process (Borisy and Svitkina, 2000).

Given the cell type and/or the substrate conditions, the lamellipodia may be made up of a homogenous actin filament network or a network that is covered with a varying number of radialy arranged actin bundles (Small et al., 1998). These bundles are referred to as filopodia when extending significantly beyond the edge of the lamellipodium, or microspikes when only extending marginally (Small et al., 1998). These actin bundle structures have been suggested to come from the convergence of actin filaments in the lamellipodium meshwork (Pollard and Borisy, 2003) and are controlled by the lateral filament flow as well as the activity of actin bundling proteins such as fascin (Small et al., 1998).

During fibroblast migration, ventral stress fibers extend from an anchorage site (focal adhesions are discussed later) close to the cell edge, to the perinucleur region. The assembly of stress fibers consists of two major steps. The first is the establishment of a focal adhesion, and the second is the recruitment of actin and actin associated proteins

into a contractile bundle at the focal adhesion (Small et al., 1998). This process of stress fiber assembly has been previously been shown to be initiated through the Rho signaling pathways (Small et al., 1998).

On the dorsal surface of cells undergoing migration or spreading, convex arc shaped arrays of actin filaments can be found just behind the lamellipodia. These arcs of actin protein are not anchored at focal adhesions but rather are contractile. They have been suggested to drive the centripetal flow of cortical receptors (Small et al., 1998). Actin arcs form at the convex of lamellipodia and contain a mixed polarity of actin filaments thus allowing them to be contractile (Small et al., 1998). It has been suggested that the delivery of actin filaments of mixed polarity from filaments of uniform polarity in the lamellipodium involve sweeping in both directions along the lamellipodium, laying down their trailing ends parallel to its base (Small et al., 1998). The breakage of these filaments from the lamellipodium would release the sheath of filaments and allow the rearward flow driven by acto-myosin interactions (Small et al., 1998). It has been suggested that the assembly of stress fibers is coupled to the formation of actin arcs (Small et al., 1998). Specifically stress fibers may grow between the base of the lamellipodium and the actin arcs, as the arcs move dorsally towards the perinuclear region (Small et al., 1998).

Cell-Substrate Adhesions

As stated earlier, for cells to undergo migration they must adhere to the underlying substratum. Such adhesions function as the anchor, onto which force is exerted to propel the cell forward (Beningo et al., 2001). A very useful technique for the analysis of cell substrate adhesions is interference reflection microscopy. Devised by

Curtis in 1964 this technique utilizes the medium between the cell membrane and the cover glass as a thin film to produce an interference pattern in reflected light (Izzard and Lochner, 1976). Based on the colors produced when using white light, or the intensities generated when using monochromic light, one can gain information concerning the closeness of the contacts between the cell and the underlying substrate (Izzard and Lochner, 1976). In general a migrating cell shows two distinct regions of contacts. First there is a broad zone of grayish close contact under the leading lamella (Izzard and Lochner, 1976). Secondly there are spindle-shaped dark areas of very close contacts, or focal adhesions, in the peripheral regions of the leading lamella and other extended regions of the cell (Abercrombie et al., 1971; Izzard and Lochner, 1976). The distance between the cell membrane and the glass is estimated to be within 10-15 nm at focal adhesions and approximately 30 nm at close contacts. By comparing the adhesion pattern with actin organization it was found that focal adhesions are located at the termini of actin stress fibers.

Focal adhesions are derived from focal complexes, smaller adhesion contacts located at the end of extending protrusion (Petit and Thiery, 2000). The formation of a focal adhesion begins with the clustering of integrins as they bind the extracellular matrix. As the cell moves forward the focal complexes mature, enlarge, and incorporate numerous additional proteins (Petit and Thiery, 2000). Recent studies, conducted concurrently with this thesis research, indicated that focal complexes are primarily responsible for the exertion of propulsive forces (Beningo et al., 2001). Once the focal adhesions mature, the cell no longer exerts strong forces through them and they seem to act as glue to hold the cell body onto the substrate (Beningo et al., 2001).

During locomotion it is crucial to establish a balance of adhesion and de-adhesion. Detachment from the substratum occurs both under the cell body and at the rear of the cell (Cox and Huttenlocher, 1998). It has been observed that a significant portion of integrins and their associated membrane are physically detached from the cell and left behind on the substratum. The integrins that remain have been found to either translocate as aggregates and form new adhesion sites or disperse back into the cell membrane (Petit and Thiery, 2000).

Protein Organization at Focal Adhesions

At the core of focal adhesions are the transmembrane proteins known as integrins. Integrins are comprised of a large family of αβ heterodimeric glycoprotein receptors that serve to adhere to extracellular matrix proteins such as fibronectin and collagen (Hynes, 1992). To date there are eighteen α and eight β subunits that combine to form twenty four known adhesion receptors. For both the α and the β subunits, the larger extracellular domain is involved in recognizing extracellular membrane proteins, while the smaller cytoplasmic regions are responsible for interacting either directly or indirectly with the cytoskeleton network. Although the majority of integrins can bind to more than one extracellular matrix proteins, genetic studies have shown that certain integrins potentially have special and irreplaceable functions (Beauvais-Jouneau and Thiery, 1997). Besides integrins other transmembrane proteins, such as syndecans and tetraspanins have been shown to localize at cell substratum adhesion sites and participate in the process of adhesion and migration (Petit and Thiery, 2000).

On the cytoplasmic side, mature focal adhesions are complexes of a large number of proteins. Vinculin and α-actinin are two of the major structural proteins involved in

the formation of focal adhesions (Geiger, 1979). VASP, localized at focal adhesions as well as along some stress fibers and at the edge of spreading lamellipodia, was first identified as a substrate for cGMP and cAMP dependent protein kinases (Haffner et al., 1995; Reinhard et al., 1992; Rottner et al., 1999a). VASP has been reported to act as a regulator of actin assembly at the barbed end during membrane extension (Bear et al., 2000). Another focal adhesion protein is zyxin, localized at the sites of both cell-cell and cell-substrate adhesions (Beckerle, 1997). Zyxin has been shown to interact with other focal adhesion proteins such as VASP, α-actinin, and the nucleotide exchange factor Vav (Crawford et al., 1992; Hobert et al., 1996; Reinhard et al., 1995). Zyxin has been shown to localize VASP at focal adhesions and may facilitate dynamic changes of the actin cytoskeleton that are important for cell motility (Beckerle, 1997; Drees et al., 1999). Other important components of focal adhesions include tensin, talin, and paxillin which may act as adaptor or scaffold proteins for the structure or as signaling proteins (Petit and Thiery, 2000). In addition, through a poorly understood process know as "inside out signaling", proteins on the cytoplasmic side are able to respond to signals and modulate the affinity of the extracellular domain of integrins for extracellular matrix proteins (Takagi et al., 2002).

Focal adhesions are associated with a number of signal transduction enzymes. For example, calpain is a calcium dependent cysteine protease (Beckerle et al., 1987), believed to be involved in focal adhesion and stress fiber formation or turnover (Huttenlocher et al., 1997; Kulkarni et al., 1999; Perrin and Huttenlocher, 2002). Its potential substrates include a number of focal adhesion proteins such as FAK, talin, and integrins. Focal adhesions also contain a large number of protein kinases and substrates.

Focal adhesion kinase (p125FAK) (Hanks et al., 1992; Schaller et al., 1992), was first identified as a substrate of the tyrosine kinase, Src. It in turn phosphorylates paxillin, which mediates the recruitment of another protein kinase PAK (p21 GTPase-activated kinase) (Turner et al., 1999). FAK also interacts with p130Cas, talin, Graf, as well as other proteins that contain SH2 binding sites (Chen et al., 1995; Harte et al., 1996; Hildebrand et al., 1995; Hildebrand et al., 1996). FAK has been implicated in a variety of cellular events such as spreading, migration, and cell proliferation. Another important regulatory protein at focal adhesions is PI3-K, which phosphorylates the D3 location of the inositol ring of phosphoinositides (PtdIns) to convert PtdIns 4-p to PtdIns 3,4-p and PtdIns 4,5-p_2 (PIP2) to PtdIns 3,4,5-p_3 (Carpenter et al., 1990; Petit and Thiery, 2000). PI3-K may be involved in intracellular traffic, migration, cytoskeletal regulation, and cell survival (Carpenter and Cantley, 1996).

Also found at focal adhesions is the family of serine/threonine kinases, protein kinase C (PKC; (Dekker and Parker, 1994)). Although PKC has various putative target proteins, the best characterized are MARCKS (myristylated, alanine-rich, C-kinase substrates), which colocalize with PKC at the sites of adhesion and serve to regulate the remodeling of the cytoskeleton (Rosen et al., 1990). Potential targets of PKC also include vinculin, paxillin, and talin (De Nichilo and Yamada, 1996; Hyatt et al., 1994). A second serine/threonine protein, integrin-linked kinase (ILK), was initially found to interact with β1 integrin. Recently studies have shown that it also localizes to focal adhesion (Hannigan et al., 1996).

Important Questions to Address

The study of cell locomotion has both challenged and intrigued scientists for many years. Cell migration is a crucial component of biological functions that range from embryogenesis to immune function to wound healing. Loss of proper control of cell migration causes severe problems such as cancer metastasis. Important questions yet remain about how cells undergo migration, and how cells regulate locomotion in response to environmental cues. During cell migration, complex mechanical interactions occur at sites of cell-cell and cell-substrate adhesion. In order to better understand the mechanism of locomotion, it is important to resolve the temporal and spatial pattern of these mechanical interactions.

Over the years various theories have been put forward to explain how the mechanical interactions between cells and substrates act to generate sustained migration. These theories although differing are not necessarily mutually exclusive. Cells have been hypothesized to migrate via a tug-of-war type of action between the leading edge and the cell body. It has also been suggested that the elastic nature of many cell types serve to produce a rubber band type of effect where, protrusion at the leading edge stretches the cell until the trailing edge retracts like the snapping of a rubber band. An alternative migration model suggests that cells migrate through a frontal towing mechanism. In this model it is postulated that the leading edge acts to generate the propulsive force necessary for forward migration, towing behind it the passive cell body as cargo. Very important insight can be gained by determining not only the distribution but also the nature of traction forces relative to cell morphology and migration. For example, forces exerted onto the substrate by migrating cells could be either active contractile forces or passive

resisting to forces, and it would be the active forces that drive the forward migration of the cell.

Recent advances in cell migration studies have lead to the identification of many molecular components involved in cell migration, yet little is known about the mechanism that propels and regulates cell migration. In addition to generating mechanical forces, cells must also be able to sense mechanical signals such as fluid shear, stretching forces, and varying substrate rigidities. In response to these environmental cues, cells must be able to change such functions as rate of cell growth, cell morphology, and migration activity. Thus it is equally important to understand the mechanism for translating environmental cues into intracellular signals.

Chapter 2 - Traction Force Microscopy of Migrating Normal and H-ras Transformed 3T3 Fibroblasts

Abstract

Mechanical interactions between cell and substrate are involved in vital cellular functions from migration to signal transduction. A newly developed technique, "traction force microscopy", makes it possible to visualize the dynamic characteristics of mechanical forces exerted by fibroblasts, including the magnitude, direction, and shear. In the present study such analysis is applied to migrating normal and transformed 3T3 cells. For normal cells, the lamellipodium provides almost all the forces for forward locomotion. A zone of high shear separates the lamellipodium from the cell body, suggesting that they are mechanically distinct entities. Timing and distribution of tractions at the leading edge bear no apparent relationship to local protrusive activities. However, changes in the pattern of traction forces often precede changes in the direction of migration. These observations suggest a frontal towing mechanism for cell migration, where dynamic traction forces at the leading edge actively pull the cell body forward. For H-ras transformed cells, pockets of weak, transient traction scatter among small pseudopods and appear to act against one another. The shear pattern suggests multiple disorganized mechanical domains. The weak, poorly coordinated traction forces, coupled with weak cell-substrate adhesions, are likely responsible for the abnormal motile behavior of H-ras transformed cells.

Introduction

Complex mechanical interactions take place at cell-substrate and cell-cell adhesion sites. Forces generated at these sites are involved in determining the cell shape and supporting cell migration, allowing cells to perform such important functions as wound healing and embryonic morphogenesis (Galbraith and Sheetz, 1998). These mechanical interactions likely involve a combination of substrate anchorage and contraction (Elson, 1999; Lauffenburger and Horwitz, 1996; Sheetz et al., 1998). Counter forces exerted by the substrate onto cells then cause the cell or part of it to move forward. By coordinating the magnitude of forces and the strength of adhesions in different regions, the cell is able to extend or migrate in a specific direction (Elson, 1999; Lauffenburger and Horwitz, 1996; Sheetz et al., 1998). To address the mechanism of cell locomotion, it is important to determine the spatial and temporal pattern of cell-cell and cell-substrate mechanical interactions. For many decades cultured fibroblasts have been used as a model for studying cell migration and cell-substrate interactions. In addition, fibroblasts transfected with oncogenes such as H-ras manifest typical cancer phenotypes such as anchorage independent growth and metastasis (Bondy et al., 1985; Brown et al., 1989; Byers et al., 1991; Egan et al., 1987; Varani et al., 1986), making them ideal candidates for studying the effects of oncogenic transformation on cell-substrate mechanical interactions.

Traction stresses generated by fibroblasts were first investigated using thin silicone rubber substrata (Harris et al., 1980; Leader et al., 1983), where wrinkles appear as a result of compression and stretching. However since wrinkling is an inherently nonlinear and chaotic process, there is no known theoretical method for predicting the

wrinkles that will occur in a substratum as a result of complex loading. While significant efforts have been made to develop alternative methods for force detection (Galbraith and Sheetz, 1997), and to improve the silicone rubber technique for better quantification and versatility (Burton et al., 1999; Burton and Taylor, 1997; Oliver et al., 1998), quantitative mapping of traction stresses during fibroblast migration has yet to be accomplished.

In the present study we have acquired images depicting the dynamics of various characteristics of the forces at the cell-substratum interface. The new approach, referred to as traction force microscopy, is based on our recently developed polyacrylamide substrates (Wang and Pelham, 1998) and on the application of computational procedures to convert measurements of substrate deformation into a maximum likelihood estimate of the traction stresses (Dembo and Wang, 1999). Improvements in data collection, analysis, and rendering have now made it possible to generate time-lapse images and shear fields of traction stress at a high spatial and temporal resolution. We have applied this approach to analyze the dynamics of cell-substrate mechanical interactions for normal and transformed cells. Our results indicate that normal NIH 3T3 cells exert strong, dynamic propulsive forces within a discrete zone near the leading edge, which are likely responsible for towing the cell body forward during cell migration. In contrast, H-ras transformed cells display transient, weak, and poorly coordinated traction stress all along the cell perimeter. Our observations allow us to propose a frontal towing model for fibroblast migration.

Materials and Methods

Preparation of Polyacrylamide Substrates

Thin sheets of polyacrylamide gel were prepared from acrylamide (Bio-Rad, 40% w/v) and N,N-methylene-bis-acrylamide (BIS, Bio-Rad, 2% w/v) and adhered to activated coverslips, as described in detail previously (Wang and Pelham, 1998). All the substrates used in this study contained 5% acrylamide, 0.1% BIS, and 1:100 dilution of fluorescent latex beads (0.2 μm FluoSpheres, Molecular Probes, Eugene, OR). Fifteen μls of the acrylamide solution were spread onto the surface of an activated large coverslip (45x50 mm) and contained under a 22 mm diameter circular cover slip. Type I collagen was covalently attached to the surface of the polyacrylamide gel using photoactivatable heterobifunctional reagent sulfo-SANPAH (sulfosuccinimidyl 6 (4-azido-2-nitrophenyl-amino) hexanoate), as described previously (Wang and Pelham, 1998).

Characterization of Substrates

Steady state thickness of the polyacrylamide sheets at 37° C was estimated to be ~75 μm, by focusing a microscope with a calibrated focusing knob from the glass surface to the surface of the polyacrylamide gel. Young's modulus of the polyacrylamide sheets was determined based on the Hertz theory, similar to the method used in atomic force microscopy (Radmacher et al., 1992). Briefly, a steel ball (0.64-mm diameter, 7.2 g/cm^3; Microball Company, Peterborough, NH) was placed onto the polyacrylamide sheets embedded with fluorescent beads. The resulting indentation was measured by following the vertical position of surface fluorescent beads under the center of the steel ball with the microscope focusing mechanism. Young's modulus was calculated as $Y=3(1-v^2)^2f^2/4d^{3/2}r^{1/2}$, where f is the buoyancy-corrected weight of the steel ball, d is the

indentation of the substrate, r is the radius of the steel ball, and v is the Poisson ratio of polyacrylamide assumed to be 0.3 in this study; (Li, 1993). This method yielded a Young's modulus of 28 x 10^3 N/m^2 for the substrates.

Cell Culture and Microscopy

Polyacrylamide substrates were equilibrated with the culture medium for approximately thirty minutes at 37° C. NIH 3T3 cells and a metastatic line of H-ras transformed NIH 3T3 cells, PAP2, were kindly provided by Dr. Ann Chambers (Bondy et al., 1985; Hill et al., 1988). The cells were cultured in DMEM (Sigma, St. Louis, MO), supplemented with 10% donor calf serum (JHR Biosciences, Lenexa, KS), 2 mM L-glutamine, 50 μg/ml streptomycin, and 50 U/ml penicillin (Gibco-BRL).

Phase images of cells, fluorescent images of substrates-embedded beads, and combined phase/fluorescence images were collected with a Zeiss 40X, NA 0.65 Achromat phase objective on a Zeiss IM-35 microscope. The microscope was equipped with a stage incubator. Bead images of relaxed substrates were collected at the end of time-lapse recordings by microinjecting cells with Gc-globulin, a known actin cytoskeleton inhibitor (Goldschmidt-Clermont et al., 1985; Lee and Galbraith, 1992; Van Baelen et al., 1980). All images were collected with a cooled CCD camera (TE/CCD-576EM; Princeton Instruments, Trenton NJ) and processed for background subtraction using custom programs.

Calculation and Rendering of Traction Magnitude and Shear

Deformation of the substrate by cultured cells was determined relative to the relaxed substrate, based on pattern recognition using a cross-correlation algorithm. Briefly, a force-loaded bead image was first divided into small square areas. The

computer program then tried to match the bead pattern in each small square against the pattern in different regions of the null-force image, searching for a best match. Deformation vectors were then drawn from the position in the null-force image to the position in the force-loaded image with the best match. The degree of match was scored with a normalized cross-correlation equation, which yielded a value of 1 for a perfect match and 0 for no similarity. No vector was assigned if this value fell below a user-defined threshold. In regions where the deformation was larger than one pixel, additional vectors were generated at a progressively shortened distance from each other to provide a higher density of data. The size of the square, the distance for the pattern search, and the threshold for positive identification were determined empirically, in order to generate an optimal set of vectors that matched visual assessment of substrate displacement when the null and force loaded images were displayed in quick succession. Cell boundaries were drawn manually using phase images and a custom interactive program. Coordinates defining the deformation field and cell boundary were then input into a supercomputer and analyzed with a maximum likelihood algorithm, which generates traction vectors at pre-assigned nodes throughout the cell (Dembo and Wang, 1999). Average compressive stress was calculated by averaging the absolute values of stress vectors projected onto specified directions. The projection was obtained by multiplying the magnitude of the vector with the cosine of the angle between the vector and the direction of projection. The traction magnitude, *mag*, and shear, *shr*, are defined as follows:

Equation 1

$$mag(\mathbf{T}) = |\mathbf{T}| \equiv \left[T_x^2 + T_y^2\right]^{1/2}$$

Equation 2

$$shr(\mathbf{T}) \equiv \left[2(\partial_x T_x)^2 + (\partial_y T_x + \partial_x T_y)^2 + 2(\partial_y T_y)^2\right]^{1/2}$$

where $\mathbf{T}=[T_x(x,y), T_y(x,y)]$ is the continuous field of traction vectors underlying the cell. One should notice that shr(**T**) essentially measures the magnitude of the spatial derivatives of the traction field with a combination of derivatives. Spatial derivatives of the traction field are of biological interest because, potentially, they can identify locations where there are sudden qualitative changes in contractility or adhesion. For purposes of comparing such changes across different cells and between different regions of the same cell, one is mainly interested in the changes relative to the prevailing background of traction. Thus it is useful to normalize the shear fields by dividing with the corresponding traction magnitude. The ratio will be referred to as normalized shear. Pseudo-color images were obtained by first determining the magnitude of the scalar or vector at each pixel within the cell boundary by interpolation, then converting the magnitude into different RGB color combinations.

Results

Traction Force Microscopy

The basic approach for mapping traction stresses has been described in Dembo and Wang (1999). The method is based on the use of flexible polyacrylamide substrates, coated with extracellular matrix proteins (type I collagen in the present study) for cell adhesion and embedded with fluorescent beads for tracking the deformation as a result of exerted forces. Several modifications were made to improve the spatial resolution and to facilitate the visualization of calculated results. First, substrate stiffness was optimized for the detection of deformation by NIH 3T3 cells, by systematically adjusting the concentrations of acrylamide and bis-acrylamide until the maximal traction generated 10-15 pixels of bead displacement. Too stiff a substrate yielded small deformation and large errors; too soft a substrate caused problems with maintaining the plane of focus. Second, the concentration of fluorescent beads was increased by 50-100% (Fig. 1A), which minimized areas devoid of fluorescent marker beads and allowed the generation of a higher density of deformation vectors. Third, deformation was analyzed not by tracking individual beads but by pattern recognition (see **Materials and Methods – Chapter 2**). This allowed a more uniform distribution of deformation vectors. To further increase the amount of useful information, the density of deformation vectors was increased automatically where significant bead displacements were found, by generating additional vectors at a progressively shorter distance from each other (Fig. 1B). Calculated traction stresses were displayed either as arrows (Fig. 1C) or as a pseudo-color images of the magnitude (*mag*(**T**); Fig. 1D).

Figure 1. Traction Force Microscopy

A) Fluorescent microspheres embedded in polyacrylamide substrates, used for the detection of substrate surface deformation as a result of forces exerted by a NIH 3T3 fibroblast. The image was recorded with simultaneous illumination for phase contrast and epi-fluorescence. Arrow indicates the direction of cell migration. B) Deformation vectors, plotted over the phase image of the cell. Deformation was determined by comparing the distribution of microspheres before and after force relaxation. Regions devoid of vectors either contained few fluorescent beads or went out of focus as a result of traction. C) Field of traction stresses, shown as vectorial arrows within the boundary of the cell. D) Field of traction stresses, rendered as a color image after mapping the magnitude of stress into different colors that range from violet (9.20×10^2 dynes/cm^2) to red ($>= 3.60 \times 10^5$ dynes/cm^2). The segmented scheme of pseudo-color mapping, as shown along the right edge, allowed the visualization of both the magnitude of stress and the iso-magnitude contours. E) Normalized shear of traction that ranges from violet (2.02×10^2 cm^{-1}) to red (5.53×10^4 cm^{-1}), reflecting the local complexity of traction forces. Areas of uniformly low shear most likely represent mechanically integrated domains. Bands of high shear most likely represent boundaries between these domains. Scale bar, 20 μm.

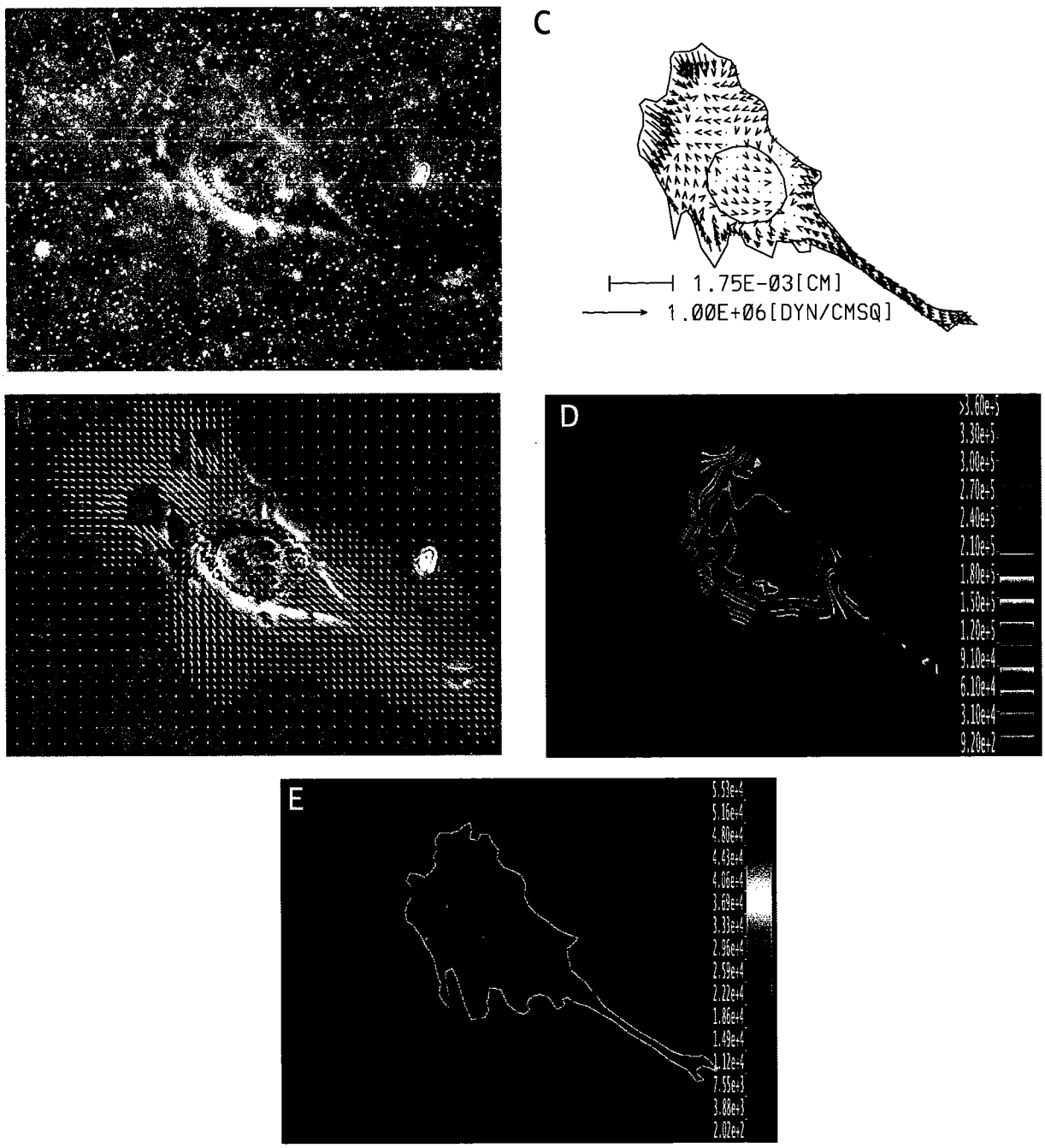

Figure -1 Traction Force Microscopy

The scheme of pseudo-color, shown in Fig. 1D, sacrifices directional information of the vectors but facilitates the visualization of magnitudes and iso-magnitude contours.

One major advance in the current study is our ability to obtain time-lapse sequence of traction forces. The increase in the speed of data processing makes it practical to collect data at short intervals, to analyze the traction maps frame by frame, and to render the pseudo-color images as motion pictures. We have currently achieved a temporal resolution of up to ~40 seconds and an estimated spatial resolution of 3-4 microns, which are more than adequate for studying the relationship between traction forces and the slow migration of 3T3 cells. Furthermore, local protrusions were on average ~9 microns in diameter, with each cycle lasting on average for 55 seconds (± 39 seconds S.D.). Thus it is also practical to address the relationship between traction forces and protrusive activities.

In addition to magnitude and direction we have calculated *shr*(**T**), which reflects the local spatial derivative of the traction vectors (see Equation 2 in **Materials and Methods – Chapter 2** for definition). Since spatial fluctuations in traction are meaningful only in comparison to the average traction in a local area, we found it most informative to normalize *shr*(**T**) against *mag*(**T**) in a pixel-by-pixel fashion (Fig. 1E). Thus, within a region where tractions are relatively constant in proportion to the background, the normalized shear values should be low. Along the boundaries of discrete mechanical domains, the ratio *shr*(**T**)/*mag*(**T**) should be high and unstable. This allows us to detect discrete domains in a cell.

Characteristics of Traction Forces Generated by Normal NIH 3T3 Cells

Most NIH 3T3 cells underwent steady migration on polyacrylamide substrates, with stable, well-defined leading and trailing edges that persisted for up to 2 hours (Fig. 2A). Small protrusions sometimes appeared along the sides (Fig. 1D). These protrusions were short-lived in most cases but occasionally were able to expand and replace an existing leading edge, causing a change in the direction of migration (discussed later). In agreement with our previous studies (Dembo and Wang, 1999; Pelham and Wang, 1999), all the significant traction forces were directed toward the interior of the cell. From the general organization of the traction field, one can conclude that essentially all the propulsive forces for forward migration were concentrated at the leading edge (Figs 1C, 1D and 2B), while strong foci of retarding traction were sometimes present in the tail region (Fig. 3). The overall average of traction stresses was 3.03×10^4 dyne/cm^2 with a standard deviation of 2.13×10^4 dyne/cm^2 (Table I). When average compressive stresses were calculated along different directions, we found that there was a strong bias along the long axis of a steadily migrating 3T3 cell (Fig. 2C).

Time-lapse analysis revealed that, in most cases, cells undergoing steady migration maintained a band of strong traction forces at the lamellipodium. Sub-regions within the leading lamellipodium showed large spatial and temporal variations in traction forces. Pockets of strong forces appeared and disappeared constantly throughout this region, with each pulse of traction lasting on average 24 minutes (Fig. 3E-H). Transient strong traction forces, comparable in magnitude to those in the lamellipodia, were also found at lateral protrusions. However, they covered a smaller area and appeared as isolated pulses rather than recurring events.

Table 1. Average Traction Stress for Migrating Normal NIH 3T3 and H-ras Transformed Fibroblasts

	Average Traction Stress (dyns/cm^2)	
Cell Number	3T3	Pap2
1	1.07×10^4	1.43×10^4
2	1.81×10^4	7.80×10^3
3	2.67×10^4	9.95×10^3
4	4.17×10^4	7.81×10^3
5	3.69×10^4	
6	8.08×10^4	
7	2.21×10^4	
8	1.67×10^4	
9	1.94×10^4	
Mean	3.03×10^4	9.97×10^3
Standard Deviation	2.13×10^4	3.06×10^3

Table 1 Average Traction Stress for Migrating Normal NIH 3T3 and H-Ras Transformed Fibroblasts

Figure 2. Spatial organization of traction stress generated by a migrating normal 3T3 fibroblast

A) Phase contrast image of a migrating normal 3T3 fibroblast. The cell showed a well-defined leading edge and trailing edge during migration. Arrow indicates the direction of cell migration. B) Magnitude of traction stress rendered as a color image, with traction stress ranging from violet (9.20×10^2 dynes/cm^2) to red (>= 3.60×10^5 dynes/cm^2). Strong tractions, denoted in red, were constrained to a thin band along the leading edge of the cell. C) Angular distribution of average compressive stress. Arrowhead denotes the orientation of the long axis of the cell. Scale bar, 20 μm.

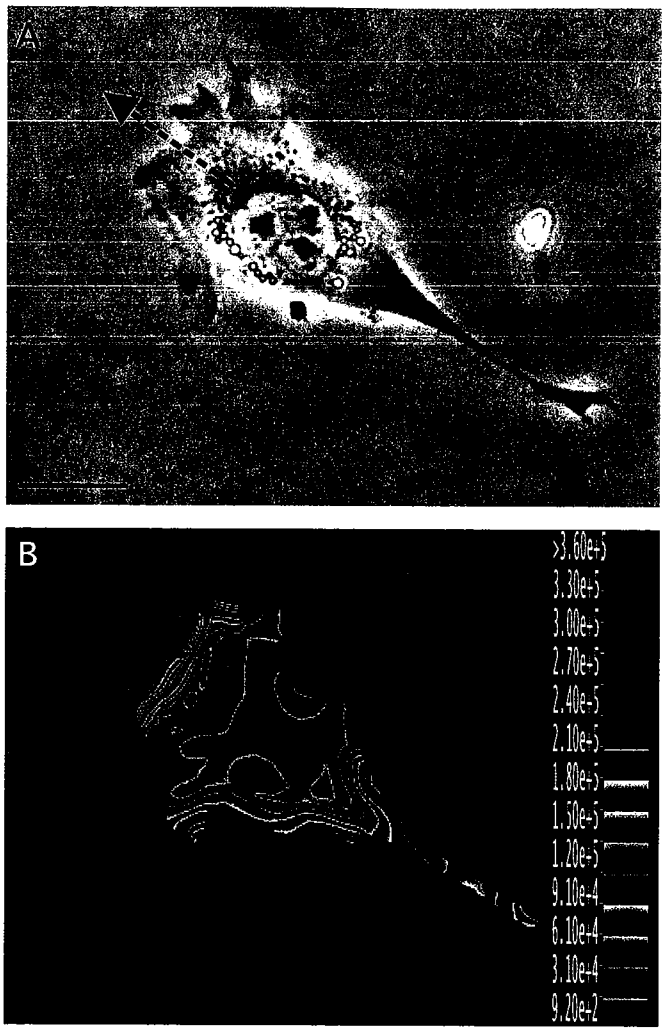

Figure 2. Spatial organization of traction stress generated by a migrating normal 3T3 fobroblast

Further insights were provided by rendering images of normalized shear values of the stress (Fig. 3I-L). In cells migrating at steady state, a band of high shear values, as denoted by the bright region in color rendering, was found just behind the lamellipodium, where traction forces dropped sharply in magnitude and reversed in direction. This suggests that the frontal region and the rest of the cell are mechanically distinct domains. The lamellipodium region at times can be divided into multiple small domains separated by regions of high shear. In contrast, normalized shear values in the trailing end were typically low, as denoted by the darkness in color rendering, despite the presence of strong forces there in some cells (Fig. 3E and 3I). The rest of the cell body can be grouped into a few large domains: a band of significant shear was typically found beneath the nucleus, where weak forces from the two lateral sides collided.

Relationship between Traction Forces and Cell Migration

To determine the role of traction forces in cell migration, we first examined the relationship between frontal traction stress and local protrusive activities. As shown in Fig. 4A-D, during cell migration membrane protrusion and retraction occurred rapidly and dynamically along the leading edge. These events showed no apparent correlation with the appearance or disappearance of local traction forces (Fig. 4).

A second possibility is that frontal traction is related to the migration of the cell body, as suggested by the tight correlation between the distribution of forces and the polarity of the cell (Fig. 2). We have therefore focused on cells that changed the direction of migration during the period of observation (N = 9). As shown in Fig. 5, redistribution of traction forces can take place well in advance of the change in cell polarity.

Figure 3. Dynamics of traction stress generated by a migrating normal 3T3 fibroblast

A-D) Phase contrast images of a migrating NIH 3T3 fibroblast at t = 0, 6 min 27 sec, 12 min 46 sec, and 19min 14 sec. Arrows in (A) and (D) indicate the direction of cell migration at the beginning and end of the experiment respectively. E-H) Color rendering of the corresponding magnitude of traction stress, which ranges from violet (5.00×10^2 dynes/cm^2) to red (>= 2.00×10^5 dynes/cm^2). The strongest tractions, in red, were located at the leading edge as a sharply defined band. These forces were highly dynamic as was the leading edge itself (white arrowheads). The trailing end of this cell also showed strong traction. However no significant traction was present around the nucleus. I-L) Color rendering of the corresponding normalized shear that ranges from violet (7.43×10^1 cm^{-1}) to red (6.50×10^4 cm^{-1}). A band of high shear separates the leading edge from the main body of the cell. Scale bar, 20 μm.

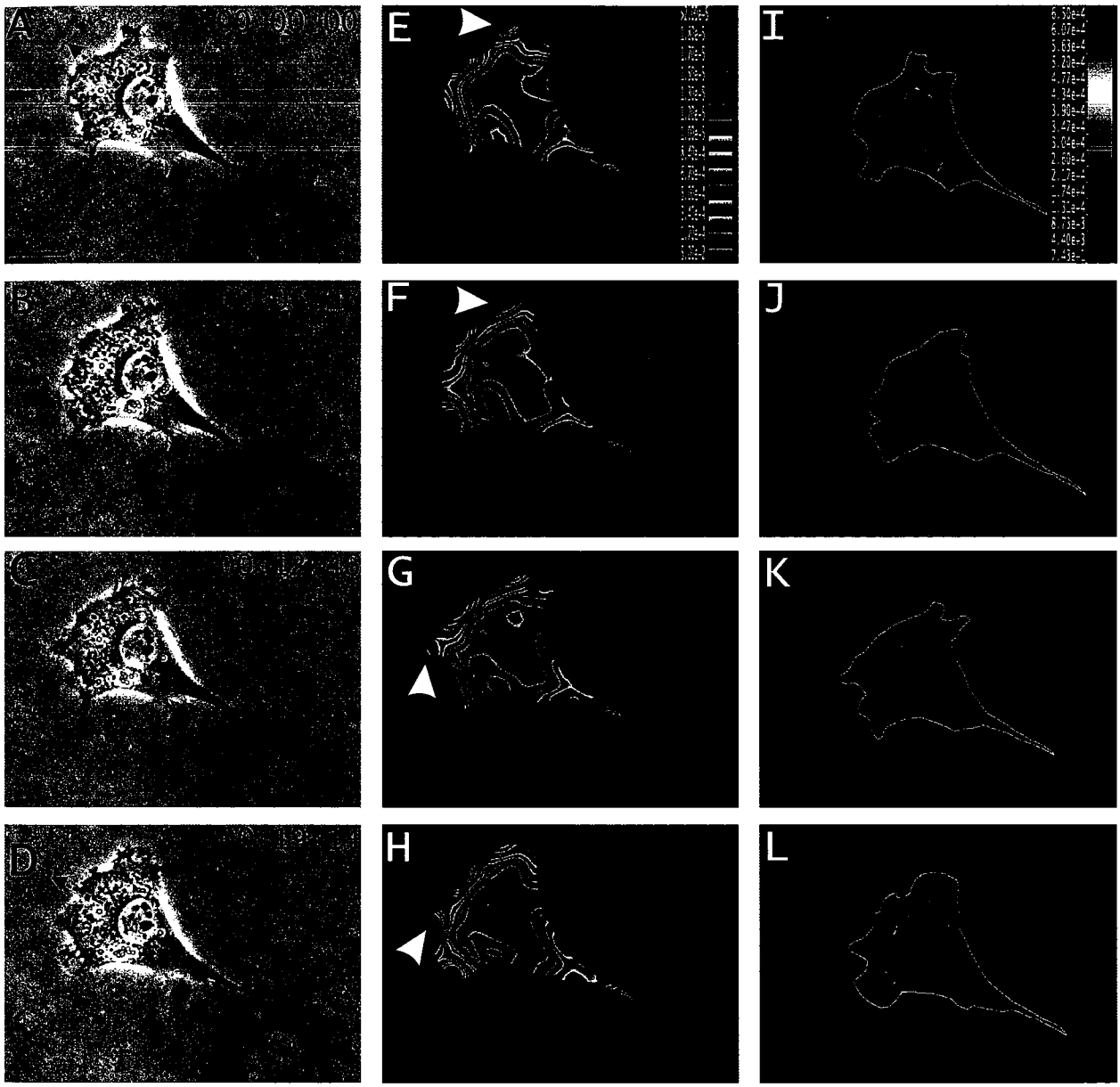

Figure 3. Dynamics of traction stress generated by a migrating normal 3T3 fibroblast

Figure 4. Membrane protrusion and traction stress at the leading edge of a migrating normal 3T3 fibroblast

A-D) Phase contrast images of a migrating NIH 3T3 fibroblast at t = 0, 44 sec, 1 min 27 sec, and 2 min 6 sec. The outline of the cell at the previous time point is drawn as white lines in panels B-D. Open arrowheads indicate the sites of retraction and closed arrowheads identify the sites of protrusion. E-H) Color rendering of the corresponding magnitude of traction stress, which ranges from violet (2.30×10^2 dynes/cm^2) to red (>= 1.55×10^5 dynes/cm^2). Arrowheads indicate protrusive/retraction activities as in phase images. Lamellipodial protrusion/retraction can take place both during the peak of local traction stress and during a period without significant traction forces. Circular white traces indicate the position of the nucleus E-H. Scale bar, 20 μm

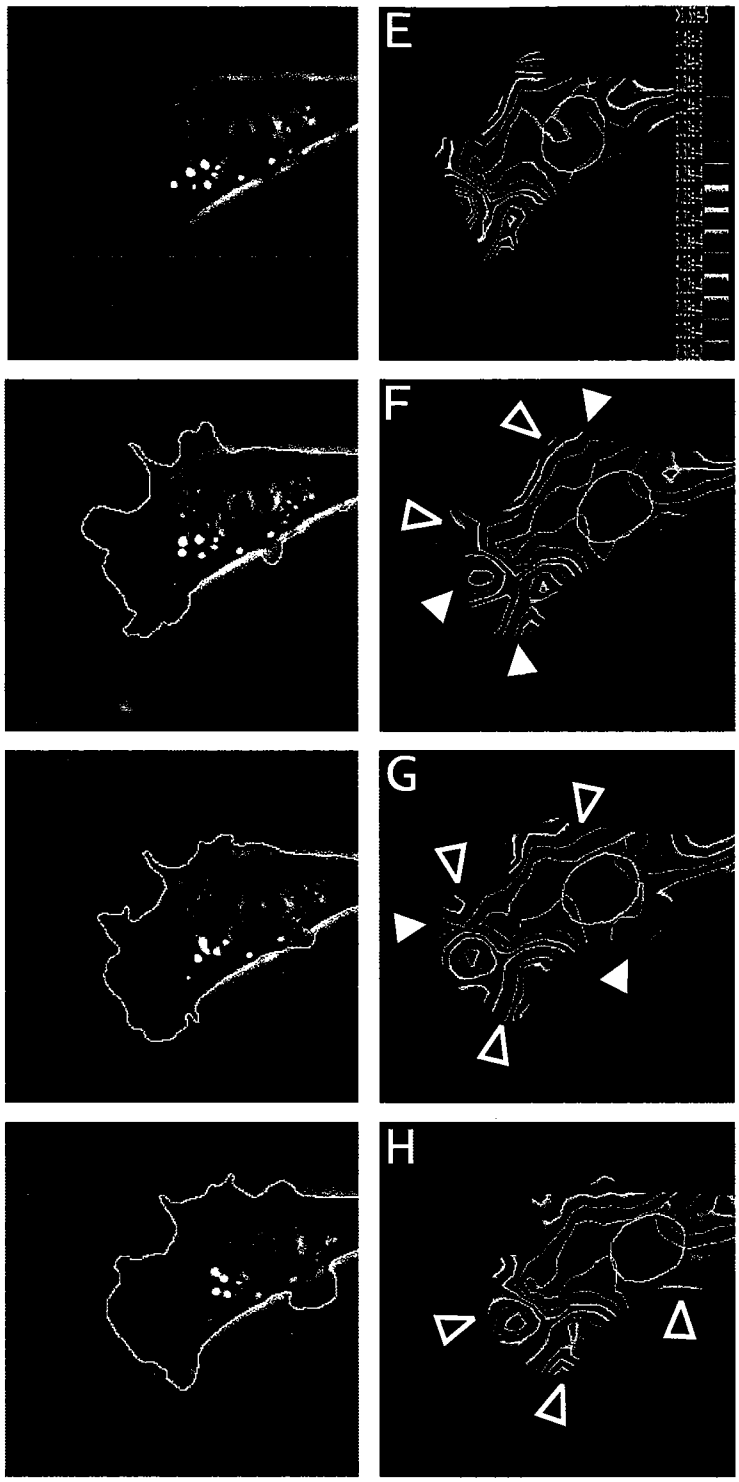

Figure 4. Membrane and traction stress at the leading edge of a migrating normal 3T3 fibroblast

The original leading edge maintained its ruffling activity for an extended period of time with no significant local traction forces, while strong sustained traction forces started to develop in the region that subsequently became the leading edge (Fig. 5D-F). These observations support the notion that the spatial and temporal pattern of traction forces dictates the direction of cell migration.

Traction Forces Generated by H-ras Transformed NIH 3T3 Cells

To determine the impact of oncogenic transformation on traction forces, we used an H-ras transformed clone of NIH 3T3 cells (PAP2 cells), originally selected for their ability to metastasize in chick embryos (Bondy et al., 1985; Egan et al., 1987). Morphologically PAP2 cells were poorly polarized, exhibiting multiple transient protrusions instead of a well-defined lamellipodium (Fig. 6A). Cell migration was effected by these protrusions, which appeared to drag the cells in a disorganized fashion. These cells migrated with a poor directional stability yet at a higher average speed of 0.31 μm/min, as compared to 0.19 μm/min for normal cells.

While the traction stresses exerted by PAP2 cells were generally directed inward as in normal cells, significant forces were found only in small pockets near the tip of multiple scattered protrusions (Fig. 6B). Furthermore, there was no region that could be unambiguously identified as the trailing end, based on either the morphology or force characteristics. The average traction magnitude, 9.97×10^3 dyne/cm^2 with a standard deviation of 3.06×10^3 dyne/cm^2 (Table I), was markedly reduced as compared to that for normal cells ($P < 0.02$). In addition, traction forces generated by PAP2 cells showed no angular directionality, in contrast to what was observed in normal cells (Fig. 6C).

Figure 5. Traction stress generated by a migrating normal 3T3 fibroblast during directional change

A-C) Phase contrast images of a migrating NIH 3T3 fibroblast at t ~ 0, 18 min 55 sec, and 121 min 26 sec. Arrows in (A) and (C) indicate the direction of cell migration. The outline of the cell at the previous time point is drawn as white lines in panels B and C. The cell shows a 90-degree change in direction. D-F) Color rendering of the corresponding magnitude of traction stress, which ranges from violet (1.07×10^2 dynes/cm^2) to red (>= 1.90×10^5 dynes/cm^2). White arrowheads identify pockets of strong traction stress. Changes in the overall distribution of traction stress become apparent before the cell changes its polarity (E). One end of the cell shows strong traction before developing into a leading edge (E, arrowhead). Some protrusive activities persist at the original leading edge while the local traction stress drops to a very low level (B, E). Circular white traces indicate the position of the nucleus D-F. Scale bar, 20 μm

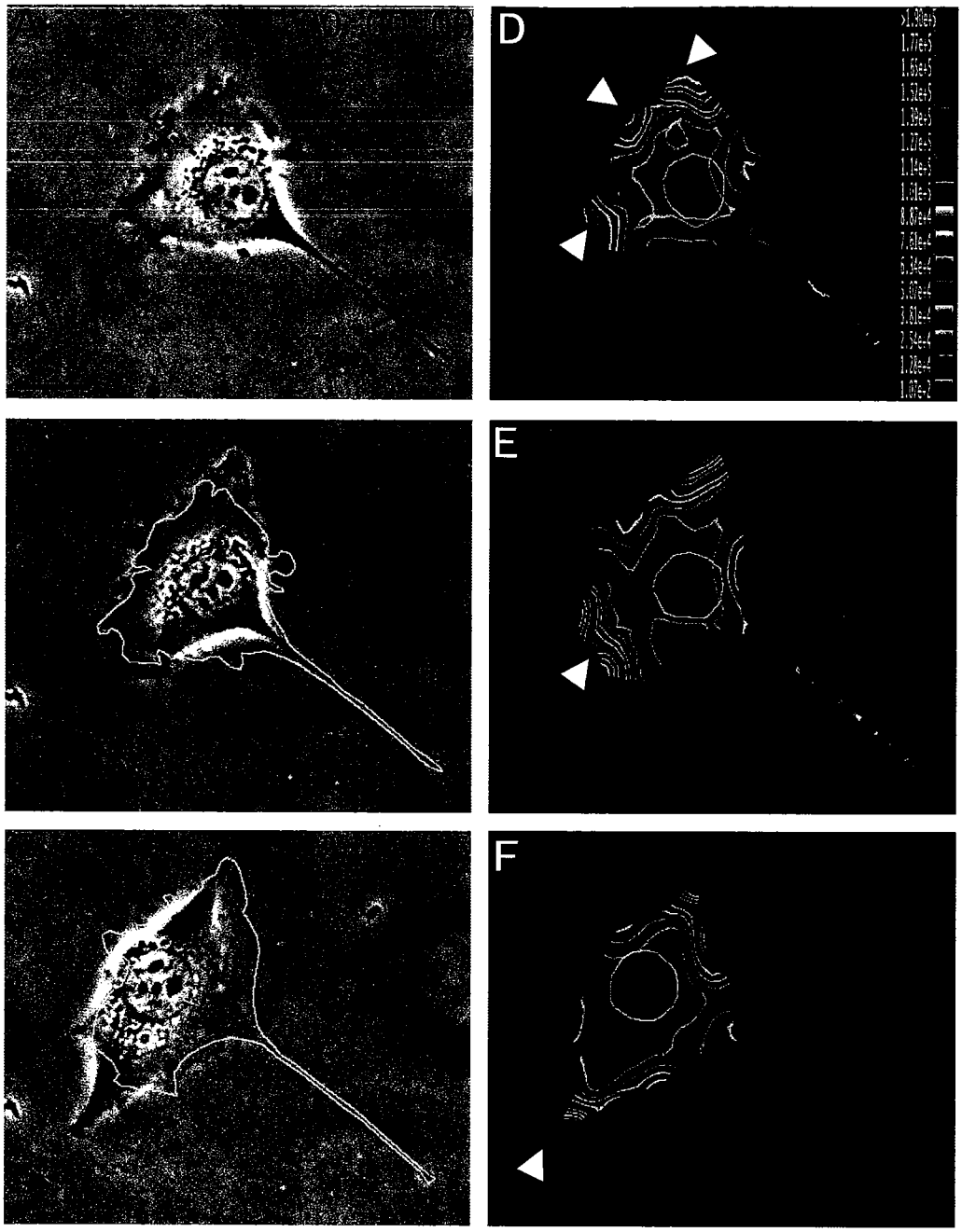

Figure 5. Traction stress generated by a migrating normal 3T3 fibroblast during directional change

Figure 6. Spatial organization of traction stress generated by a migrating H-ras transformed NIH 3T3 fibroblast

A) Phase contrast image of a migrating H-ras transformed NIH 3T3 fibroblast. Arrow indicates the direction of cell migration. Note the absence of a well-defined leading edge and trailing edge. B) Color rendering of the corresponding magnitude of traction stress, which ranges from violet (9.20×10^2 dynes/cm^2) to red (>= 3.60×10^5 dynes/cm^2), using the same color-mapping scheme as that for normal cells in Fig. 2. Compared to normal fibroblasts, the overall magnitude of traction stress is markedly reduced, as is the spatial organization. C) Angular distribution of average compressive stress, showing the lack of angular asymmetry in contrast to what is seen in Figure 2. Scale bar, 20 μm.

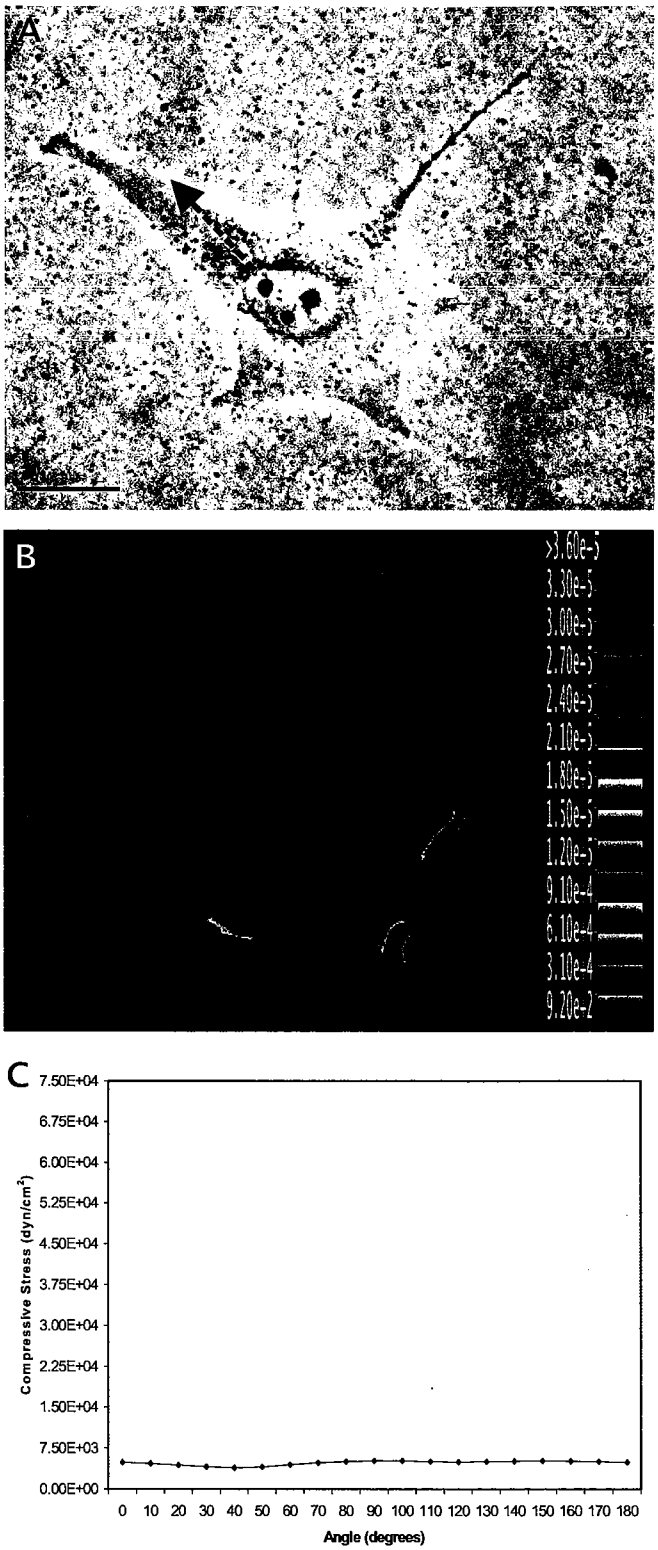

Figure 6. Spatial organization of traction stress generated by a migrating H-ras transformed NIH 3T3 fibroblast

Time-lapse analysis of the traction stress indicated that the distribution of forces in PAP2 cells was very unstable (Fig. 7E-H). Although the average duration of each traction event, 22-23 minutes, was similar to that in normal cells, no region was able to develop a concentration of traction forces or to maintain the activity for any extended period of time. In contrast to normal cells where a band of high shear was present at the base of lamellipodia, pockets or bands of high shear values scattered in numerous locations and migrated chaotically (Fig. 7I-L). Therefore, transformed cells were able to develop transient protrusions and tractions, but were unable to turn them into a stable lamellipodium.

Figure 7. Dynamics of traction stress generated by a migrating H-ras transformed NIH 3T3 fibroblast

A-D) Phase image of a migrating H-ras transformed NIH 3T3 fibroblast at t = 0, 6 min, 12 min, and 18 min. Arrows in (A) and (D) indicate the direction of cell migration. Note the multiple "leading-edge" like protrusions. E-H) Color rendering of the corresponding magnitude of traction stress, which ranges from violet (5.00×10^2 dynes/cm^2) to red (>= 2.00×10^5 dynes/cm^2) using the same color scheme as in Figure 3. The magnitude of traction was sharply reduced as compared to that in normal cells. In addition, traction stress was exerted at small, highly unstable pockets along the perimeter of the cell (arrowheads). I-L) Color rendering of the corresponding normalized shear that ranges from violet (5.80×10^1 cm^{-1}) to red (2.00×10^4 cm^{-1}). The unstable, complex pattern of shear bands suggests a mechanically fragmented cell body. Scale bar, 20 μm.

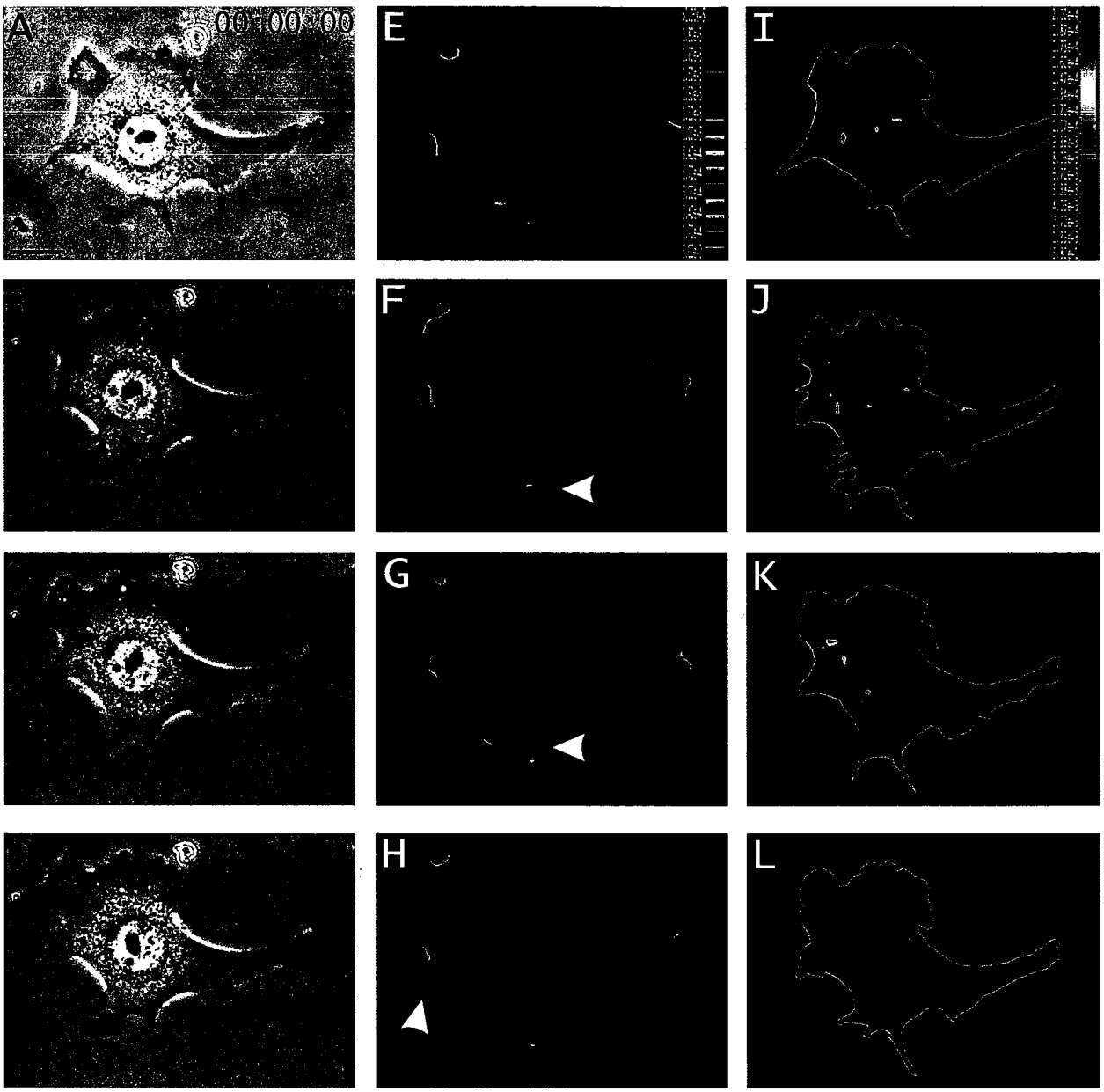

Figure 7. Dynamics of traction stress generated by a migrating H-ras transformed NIH 3T3 fibroblast

Discussion

We have developed a new imaging technique, traction force microscopy, to map mechanical forces generated by normal and H-ras transformed fibroblasts. This approach combines flexible substrates, digital imaging, and computation to "deconvolve" substrate deformation into the distribution of mechanical forces. The use of automatic deformation determination algorithm, the improved spatial and temporal resolution, and the color rendering of traction parameters, have greatly increased the efficiency and power of this approach beyond its predecessor or other force mapping techniques (Dembo and Wang, 1999). New features in the present study include time-lapse analysis of traction field relative to cell migration, the generation of shear pattern for identifying discrete mechanical domains, and the elucidation of differences in substrate mechanical interactions of normal versus transformed cells.

Traction Forces Exerted by Normal Cells on the Substrate: A Frontal Towing Model for 3T3 Cell Migration

Our results showed that all traction forces generated by NIH 3T3 cells are pointed toward the center of the cell, with the strongest forces concentrating near the very tip of the lamellipodia and dropping precipitously toward the central region. These observations generally agree with what we reported with Swiss 3T3 cells using static methods (Dembo and Wang, 1999; Pelham and Wang, 1999). Furthermore, new results from this study indicate that traction at the leading edge does not correlate directly with local protrusive activities, but with the overall direction of cell migration. As shown in Figure 2C, although traction forces are generated at scattered sites, the direction of maximal compressive stress generally lies parallel to the long axis of steadily migrating

cells. In addition, the distribution of traction forces changes prior to changes in the direction of cell migration. Protrusive regions that show persistent traction forces develop into dominant lamellipodia, while those with only transient traction activities retract quickly. Therefore, the polarity of cell migration is not determined by membrane protrusion *per se* but by the subsequent development of firm adhesion and traction forces, which may play a role in sustaining the local protrusive activities and in pulling the cell body forward. This mechanism allows the cell to send local protrusions in various directions to probe the environment while maintaining a steady course of movement.

In addition, the shear field of traction indicates that normal cells can be divided into mechanically discrete segments or zones. The lamellipodium is separated from the rest of the cell by a high shear zone (Fig. 3). The rest of the cell consists of one or several domains, which generate resisting forces against the forward movement. These dragging forces spread across a large region of the cell and sometimes show a strong focus at the tail. Together, these results can be explained with a frontal towing model for cell migration (Fig. 8A and 8C). We propose that the leading lamellipodium consists of one or more transient towing units, which adhere firmly and transmit strong retrograde forces to the substrate. The body of the cell adheres more weakly to the substrate, allowing it to be dragged forward by the frontal towing zone as a mechanically coherent cargo. The towing zone is connected to the cell body via an elastic transition zone, as suggested by a band of high shear in the lamella region, which facilitates the transmission of contractile forces from the cell body to the leading edge. The generation/transmission of contractile forces in this elastic transition zone, combined with the firm anchorage at the front, provides the forces responsible for towing the cargo.

Figure 8. Model for the migration of normal and H-ras transformed NIH 3T3 fibroblasts

A) Structural model of normal NIH 3T3 fibroblasts. We propose that normal 3T3 cells consist of three distinct mechanical regions, towing zone, elastic transition zone, and cargo zone. Towing zone is located at the front lamellipodium where propulsive traction forces are exerted on the substrate. It is also the region for the assembly of new actin cytoskeleton. The main body of the cell composes the cargo zone. It is connected to the towing zone through an elastic transition zone, which is located in the lamella region. This transition region serves the important function of generating and/or transmitting the contractile forces for cell migration. In addition, active centripetal cortical flow in this region incorporates new cytoskeleton formed in the towing zone into the cell body. Adhesions under the cargo zone and at the trailing end generate the dragging force and have to be released for sustained cell migration. B) Structural model of H-ras transformed 3T3 fibroblasts. H-ras transformation of 3T3 cells results in the formation of multiple, small towing zones. A combination of multiple towing zones and disorganized elastic transition zones gives rise to complex, unstable traction forces and erratic cell movement. As a result the cargo zone becomes highly fragmented. Weakened adhesions likely account for the increased speed of movement. C) Frontal towing model of 3T3 cell migration, broken down into discrete steps. Triangles represent substrate adhesion sites. Arrows represent the direction of movement relative to the substrate. Waved lines represent the flexible transition zone between the frontal towing zone (red outline) and the cargo zone (blue outline). In reality these steps probably take place simultaneously; i.e. new towing zones are assembled as existing ones are exerting traction forces.

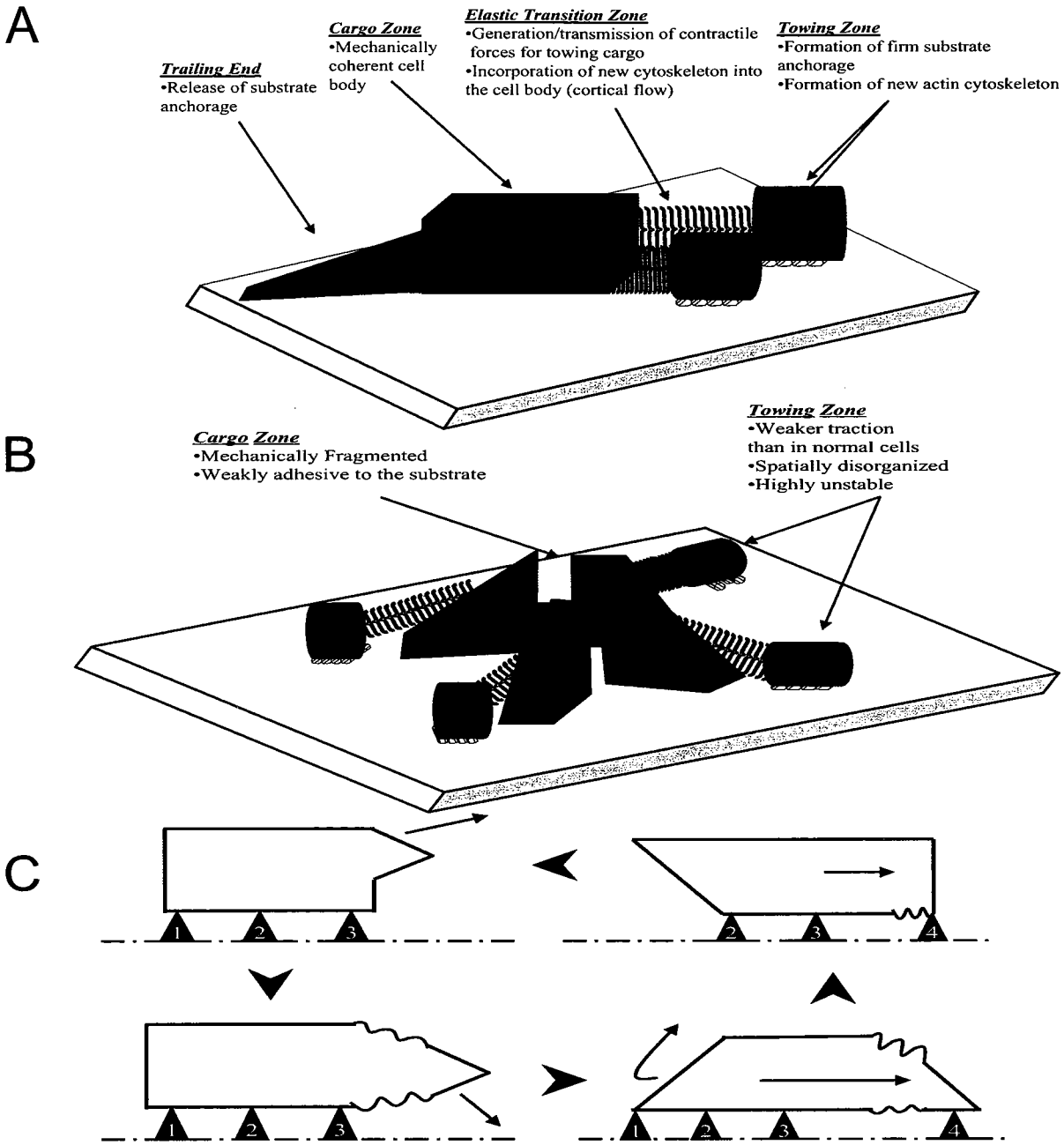

Figure 8. Model for the migration of normal and H-ras transformed NIH 3t3 fibroblasts

To maintain a steady state, this mechanism must be sustained by the continuous formation of new towing units at the leading edge, driven by the assembly of new actin filaments and adhesion sites (DePasquale and Izzard, 1987; Small et al., 1998; Wang, 1985). Furthermore, the detachment, transport, and incorporation of "aged" towing zones into the cargo zone likely gives rise to the retrograde flow of membrane and cortical components, commonly observed in the lamella region (Heath, 1983).

This frontal towing model is supported not only by the present results but also by a number of past observations. A similar mechanism has been previously speculated by (Harris et al., 1980), based on the compression of silicone substrates behind the leading edge. In addition, the existence of a transition zone between the lamellipodium and the cell body is consistent with the organization of actin and myosin II (Svitkina et al., 1997), and the unique behavior of membrane proteins in this region (Ishihara et al., 1988). The idea that the frontal region contains sufficient components for driving cell migration is further supported by the autonomous movement of small cytoplasmic fragments derived from the lamella (Albrecht-Buehler, 1980; Malawista and De Boisfleury Chevance, 1982; Verkhovsky et al., 1999). However, important questions remain concerning the molecular mechanisms for the generation and transmission of mechanical forces. Our previous studies indicated that these forces are generated predominantly by actin-myosin II based contractions (Pelham and Wang, 1999). Where the forces are generated and how the contractions are regulated remains unclear.

Also of great importance is the characterization of substrate adhesions (DiMilla et al., 1991). Since large focal adhesions are typically localized behind the region of strong traction (Pelham and Wang, 1999), we speculate that small, nascent adhesions at the

leading edge are more active in transmitting traction forces. Moreover, since the rate of cell migration is determined by a combination of traction forces and adhesiveness, a complete picture would require the determination of the strength and regulation of cell adhesion. Finally, it is important to note that the pattern of traction forces for 3T3 cells differs significantly from that for fish keratocytes and possibly other cell types such as leukocytes (Burton et al., 1999; Oliver et al., 1999). Thus different types of cells, or cells under different conditions or morphologies, may use different mechanisms for their migration.

What Went Wrong in H-ras Transformed 3T3 Cells

Previous studies with silicone substrates have indicated drastic reductions in the number of wrinkles generated by transformed fibroblasts (Harris et al., 1981; Leader et al., 1983). However, due to the poor resolution of the approach, it was difficult to determine if the effects were due to weakening of the forces, the disorganization of forces, or rapid changes in the distribution of forces. The present study has identified a number of striking differences between the traction forces of normal and H-ras transformed cells. In H-ras transformed cells the magnitude of traction stresses is reduced as compared to that in normal cells, although the duration of local traction activities at the protrusion remains similar. Furthermore, forces exerted by H-ras transformed cells become radialy symmetric and scatter among small pockets, which likely gives rise to the loss of a defined polarity.

The disorganization of traction forces in transformed cells is further demonstrated by the drastically different shear images. Compared to the shear images of normal cells, those of H-ras transformed cells show multiple small, unstable towing domains along the

cell perimeter, with neither an organized front nor a well-defined tail. These disorganized towing domains appear to act against one another, trying to drag the cell body in multiple directions. Combined with the weak substrate adhesion of H-ras transformed cells (Shin et al., 1999), these changes in mechanical activities can easily contribute to the erratic, invasive motile behavior of PAP2 cells.

What might lead to the drastic changes in traction forces in transformed cells? We notice that similar transient protrusions are present in both normal and transformed cells. However in normal cells lateral protrusions are short lived while those along the direction of cell migration amplify into a wide expanse of lamellipodium. Therefore an attractive possibility is that the polarity in normal cells is maintained by a local positive feedback mechanism that amplifies and maintains adhesion sites and traction activities at the leading edge, and possibly by a distal negative feedback mechanism that suppresses the protrusive/adhesion activities elsewhere. Such coordination mechanism may be impaired in transformed cells due to defects in signal transduction. Previous studies have suggested potential interactions between signaling pathways mediated by H-ras and the small GTP binding proteins, including rac and rho, which are known to modulate both actin organization and myosin II contractility (Hall, 1998; Narumiya et al., 1997; Rottner et al., 1999a). In addition, H-ras may disrupt the state of protein tyrosine phosphorylation, particularly the focal adhesion kinase (FAK) and paxillin, which are associated with focal adhesion and believed to play a role in regulating adhesion-activated transmembrane signals (Ilic et al., 1997; Parsons, 1996).

In addition to cell migration, traction forces are likely to play a role in the loss of growth regulation in transformed cells. The exertion of active traction stresses induces

strains and hence structural modifications within the cell-substratum linkages, the cell membrane, or the cytoskeleton. These structural changes could in turn modulate the catalytic activity of enzymes, the susceptibility of substrates and/or the conductance of ion channels (Boudreau and Jones, 1999; Giancotti and Ruoslahti, 1999; Gumbiner, 1996; Schoenwaelder and Burridge, 1999; Schwartz and Baron, 1999). Accumulating evidence from mechanical stimulation and fluid shear experiments indicates that mechanical forces can affect gene expression, cell cycle, and apoptosis (Davies, 1995; Grinnell et al., 1999; Sadoshima and Izumo, 1993; Schwartz and Baron, 1999). By exerting weaker, disorganized forces to the substrate, PAP2 cells would also receive weaker, disorganized mechanical input and respond with altered growth behavior (Lukashev and Werb, 1998). While the pathways leading to altered motility and loss of growth control are likely different, the common root in mechanical interactions explains why the two are usually coupled in cancerous transformation.

The capacity of cells to use traction forces for the regulation of motility and growth bear far reaching implications on such biological phenomenon as contact inhibition, wound healing, and development. Future studies utilizing this novel traction force mapping technique will serve to further our understanding of the mechanical interaction between cells and their environment, as well as the impact of this interaction on a wide spectrum of cellular functions.

Chapter 3 – Distinct Roles of Frontal and Rear Cell-Substrate Adhesions in Fibroblast Migration

Abstract

Cell migration involves complex physical and chemical interactions with the substrate. To probe the mechanical interactions under different regions of migrating 3T3 fibroblasts, we have disrupted cell-substrate adhesions by local application of the GRGDTP peptide, an inhibitor of cell attachment, while imaging stress distribution on the substrate with traction force microscopy. Both spontaneous and GRGDTP-induced detachment of the trailing edge caused extensive cell shortening, without changing the overall level of traction forces or the direction of migration. In contrast, disruption of frontal adhesions caused dramatic, global loss of traction forces before any significant shortening of the cell. While traction forces and cell migration recovered within 10-20 minutes of transient frontal treatment, persistent treatment with GRGDTP caused the cell to develop traction forces elsewhere and reorient toward a new direction. We conclude that contractile forces of a fibroblast are transmitted to the substrate through two distinct types of adhesions. Leading edge adhesions are unique in their ability to transmit active propulsive forces. Their functions cannot be transferred directly to existing adhesions upon detachment. Trailing end adhesions create passive resistance during cell migration, and readily redistribute their loads upon detachment. Our results indicate the distinct nature of mechanical interactions at the leading versus trailing edges, which together generate the mechanical interactions for fibroblast migration.

Introduction

The migration of cultured fibroblasts has been studied in detail for many decades (Abercrombie et al., 1970; Harris et al., 1980). The process consists of cycles of frontal extension and tail retraction, coupled to complex mechanical interactions between the cellular contractile apparatus and the substrate through integrin-mediated adhesion sites (De Beus and Jacobson, 1998; Horwitz and Parsons, 1999; Lauffenburger and Horwitz, 1996; Sheetz et al., 1998; Yamada and Miyamoto, 1995). It is generally agreed that frontal protrusion serves as a means to extend forward and establish new adhesion structures, while the transmission of contractile forces to the substrate at adhesion sites causes the cell body to move (Burton et al., 1999; Lauffenburger and Horwitz, 1996; Sheetz et al., 1998; Svitkina and Borisy, 1999). However the exact mechanism of fibroblast migration remains controversial.

To begin to understand the physical principle of cell migration, it is important to characterize the spatial and temporal pattern of mechanical interactions between the cell and the substrate. We have recently developed a method, traction force microscopy, for imaging the distribution of mechanical stresses exerted by a cultured cell (Dembo and Wang, 1999). Traction images of migrating 3T3 cells indicated a general centripetal pattern of forces, with strong stresses located at the leading edge, lateral protrusions, and sometimes at the trailing edge (Dembo and Wang, 1999; Munevar et al., 2001a). There are also weak, diffuse forces distributed under most of the cell body with a forward bias. These observations indicate that the cell body is indeed under tension and that constant mechanical cross talk takes place among widely separated regions of the cell.

From the centripetal pattern of traction forces, one can conclude that propulsive actions for cell migration are concentrated at the leading edge (Dembo and Wang, 1999; Munevar et al., 2001a). However, unregulated centripetal contractions would simply cause the cell to collapse. Sustained cell migration can take place only through a tight coordination of the protrusive activities, the assembly and disassembly of adhesion structures, and the distribution of traction forces (Galbraith and Sheetz, 1997; Oliver et al., 1999; Svitkina et al., 1997). Different theories, not necessarily exclusive of one another, emphasize different mechanical aspects and differ with respect to the scenario of events. In a simple tug-of-war mechanism, peripheral regions of the cell try to walk away from the cell center, and the region that generates the strongest forces determines the overall polarity. Thus forces in different regions are qualitatively identical but differ in their magnitudes. From the retraction of tails coupled to the surge in protrusion (Chen, 1981), it has also been suggested that the elasticity of the cell body may play a role in cell migration, by storing potential energy like a rubber band. The direction of cell migration is determined primarily by the preferential rupture of adhesive bonds at the tail, followed by the conversion of stored potential energy in a stretched cell body into kinetic energy for forward migration. In the "frontal towing" mechanism, the leading edge represents a unique region that provides active forces for dragging a passive cell body across the substrate. This model contends that mechanical interactions at the leading edge differ both quantitatively and qualitatively from those under the rest of the cell body.

Important insights into the mechanism of fibroblast migration can be gained by determining not only the distribution but also the nature of traction forces in relation to the cell morphology and migration. Forces exerted on the substrate could reflect either

active pulling or passive resistance to forces exerted elsewhere, and it is the active forces that drive the migration of the cell. In the present study, we combined traction force microscopy with focal release of the GRGDTP peptide, a competitive inhibitor of integrin-ECM binding, to disrupt cell adhesions at defined regions. The results indicate the distinct nature of mechanical interactions at the leading versus trailing edges and suggest that the frontal towing mechanism plays a major role in fibroblast migration.

Material and Methods

Preparation and Characterization of Polyacrylamide Substrates

Thin sheets of polyacrylamide gel were prepared from acrylamide (Bio-Rad, 40% w/v) and N,N-methylene-bis-acrylamide (BIS, Bio-Rad, 2% w/v) and adhered to activated cover slips as described previously (Wang and Pelham, 1998). All the substrates used in this study contained 5% acrylamide, 0.1% BIS, and 1:100 dilution of fluorescent latex beads (0.2 μm FluoSpheres, Molecular Probes, Eugene, OR). Fifteen μls of the acrylamide solution were spread onto the surface of an activated large rectangular cover slip (45x50 mm) and induced to polymerize under a 22 mm diameter circular cover slip. Type I collagen was covalently attached to the surface of the polyacrylamide gel using photoactivatable heterobifunctional reagent sulfo-SANPAH (sulfosuccinimidyl 6 (4-azido-2-nitrophenyl-amino) hexanoate), as described previously (Wang and Pelham, 1998).

Steady state thickness of the polyacrylamide sheets at 37° C was estimated to be ~75 μm, by focusing a microscope with a calibrated focusing knob from the glass surface to the surface of the polyacrylamide gel. Young's modulus of the polyacrylamide sheets were determined as described previously (Lo et al., 2000), using a method based on the Hertz theory (Radmacher et al., 1992). This method yielded a Young's modulus of 2.8 x 10^4 N/m^2.

Calculation and Rendering of Traction Stress

Traction force microscopy was performed as described recently (Munevar et al., 2001a). Briefly, deformation of the substrate caused by cellular traction forces was determined relative to the relaxed substrate using a pattern recognition algorithm.

Coordinates defining the deformation field and cell boundary were analyzed with a Bayesian method to determine maximum likelihood traction vectors at pre-assigned nodes throughout the cell (Dembo and Wang, 1999). Pseudo-color images were obtained by first determining the magnitude of the traction stress at each pixel within the cell boundary and then converting the magnitude into different RGB color combinations.

Cell Culture and Microscopy

Polyacrylamide substrates were equilibrated with culture medium for approximately 30 minutes at 37° C. NIH 3T3 cells were cultured in DMEM (Sigma, St. Louis, MO), supplemented with 10% donor calf serum (JHR Biosciences, Lenexa, KS), 2 mM L-glutamine, 50 μg/ml streptomycin, and 50 U/ml penicillin (Gibco-BRL). Phase images of cells, and fluorescent images of substrates-embedded beads were collected with a 40X/NA 0.75 Plan-Neola phase objective on a Zeiss Ax overt S100TV microscope equipped with a custom stage incubator. Bead images of relaxed substrates were collected at the end of time-lapse recording by removing the cell with a microneedle. All images were collected with a cooled CCD camera (ST133 controller with an EEV Type57 back-illuminated frame-transfer CCD chip; Roper Scientific, Trenton, NJ) and processed for background subtraction using custom programs.

Local Application of GRGDTP Peptide

A synthetic peptide Gly-Arg-Gly-Asp-Thr-Pro (GRGDTP; Sigma-Aldrich Chemical G-5646, St. Louis, MO) was used to disrupt cell substrate attachment (Dedhar et al., 1987; Gehlsen et al., 1988). An inactive synthetic peptide Gly-Arg-Gly-Glu-Ser-Pro (GRGESP; Bachem H-3136, Torrance, CA) was used as a control (Pytela et al., 1986). Both peptides were dissolved to a concentration of 5 mg/ml in PBS containing 5

mg/ml rhodamine dextran (Molecular Probes), which served as an inert fluorescent marker for visualizing the distribution of the released solution. Application of the rhodamine dextran marker alone had no discernable effect on migrating cells.

Focal release of GRGDTP was carried out as described in (O'Connell et al., 2001). The peptide was loaded into a release microneedle connected to a source of regulated compressed air. A suction micropipette was prepared by breaking and fire-polishing the broken tip of a microneedle using a microforge (Narishige), and was then connected to a regulated source of vacuum. The release and suction micropipettes were mounted on a custom micromanipulator that allowed both precise relative positioning of the two needles and their simultaneous movements. Generally the suction pipette was positioned 20-40 μm behind the release needle at a slightly higher elevation. Because of the continuous liquid flow, the distribution of GRGDTP was determined by the flow pattern rather than its diffusion. By balancing the rates of release and suction, the distribution of GRGDTP was maintained in a region 10-15 μm in diameter as judged by the distribution of fluorescent rhodamine dextran.

Results

Imaging and Manipulating Cell-Substrata Mechanical Interactions

The basic approach for mapping traction stresses was described in Dembo and Wang (1999), and was recently modified by Munevar et al. (2001a). The method is based on the use of flexible polyacrylamide substrates, coated with extracellular matrix proteins (type I collagen in the present study) for cell adhesion and embedded with fluorescent beads for tracking the deformation caused by exerted forces. The magnitude of the traction stress was calculated at each pixel and displayed as pseudo-color images or movies.

Although the substrate was coated with type I collagen, it is possible that additional components such as fibronectin were recruited to the surface. Cell-substrate interactions were disrupted by focal release of the GRGDTP peptide (see ***Materials and Methods – Chapter 3***), which was reported to inhibit cell attachment to fibronectin, vitronectin, and type 1 collagen (Dedhar et al., 1987; Gehlsen et al., 1988), and caused the detachment of 3T3 cells in a highly controlled and localized manner. This manipulation served two purposes. The first was to probe the coordination of activities in different regions, by determining if detachment of one region leads to changes in cell length or protrusive activities in other regions. The second purpose was to classify traction forces in specific areas. Since traction forces are globally balanced over the cell, local disruptions of adhesions must be compensated by changes in traction forces at distant sites. One possibility is that local disruption causes an immediate *decrease* in the magnitude of distal stresses pointing in the opposite direction. This occurs when the disrupted adhesions are directly connected to a contractile apparatus that acts on the rest

of the cell, and will be referred to as "active" tractions. Alternatively, local disruptions may not impair the average traction output, but are compensated by an *increase* in the magnitude of proximal stresses that point at a similar direction. This happens when a group of adhesions share the job of resisting contractile forces generated elsewhere, and will be referred to as "passive" or "reactive" tractions.

Responses of Traction Forces and Cell Migration to Spontaneous and Induced Tail Retraction

Most NIH 3T3 cells migrated on polyacrylamide substrates with stable, well-defined leading and trailing edges (Fig. 9A). We first tested the involvement of the elasticity of cell body in cell migration. As predicted by some of the models such as the "elastic cell body" model (see ***Introduction – Chapter 3***), traction forces should increase in proportion to the cell length and decrease precipitously upon tail retraction. Contrary to this idea however, we observed no change in the average magnitude of traction stress during cell elongation. Furthermore, spontaneous tail retraction was actually associated with a slight increase in frontal traction forces (Fig. 9E-H).

To substantiate the results with spontaneous tail retraction, we induced tail retraction with focal release of GRGDTP (n = 8 cells). This treatment again caused a dramatic decrease in cell length (> 40%) accompanied by a slight increase in frontal traction stress (Fig. 10E-H), while the average magnitude of traction stress showed no significant change (Fig. 10I). Both spontaneous and induced tail releases caused a transient increase in the rate and no change in the direction of cell migration. Application of GRGESP, a control peptide, caused no discernable detachment of the cell or change in substrate deformation.

Figure 9. Response of traction forces to spontaneous tail retraction

Panels A-D show phase contrast images of a migrating NIH 3T3 fibroblast, recorded at time points indicated at the upper right corner. Arrow in (A) indicates the direction of cell migration. E-H), color rendering of the corresponding magnitude of traction stress, which ranges from violet (9.15×10^2 dynes/cm^2) to red ($> 8.50 \times 10^5$ dynes/cm^2). Note the increase in traction stress at the leading edge following retraction of the trailing edge. In addition, traction at the tail shifted to a region not affected by the retraction (G-H, arrowhead). I) Average magnitude of traction stress (■) and cell length (♦) during spontaneous tail retraction. Letters A-H mark the corresponding panels. Note that there was no loss of average traction force as the cell shortened to less than 50% of the original length. Scale bar, 20 μm.

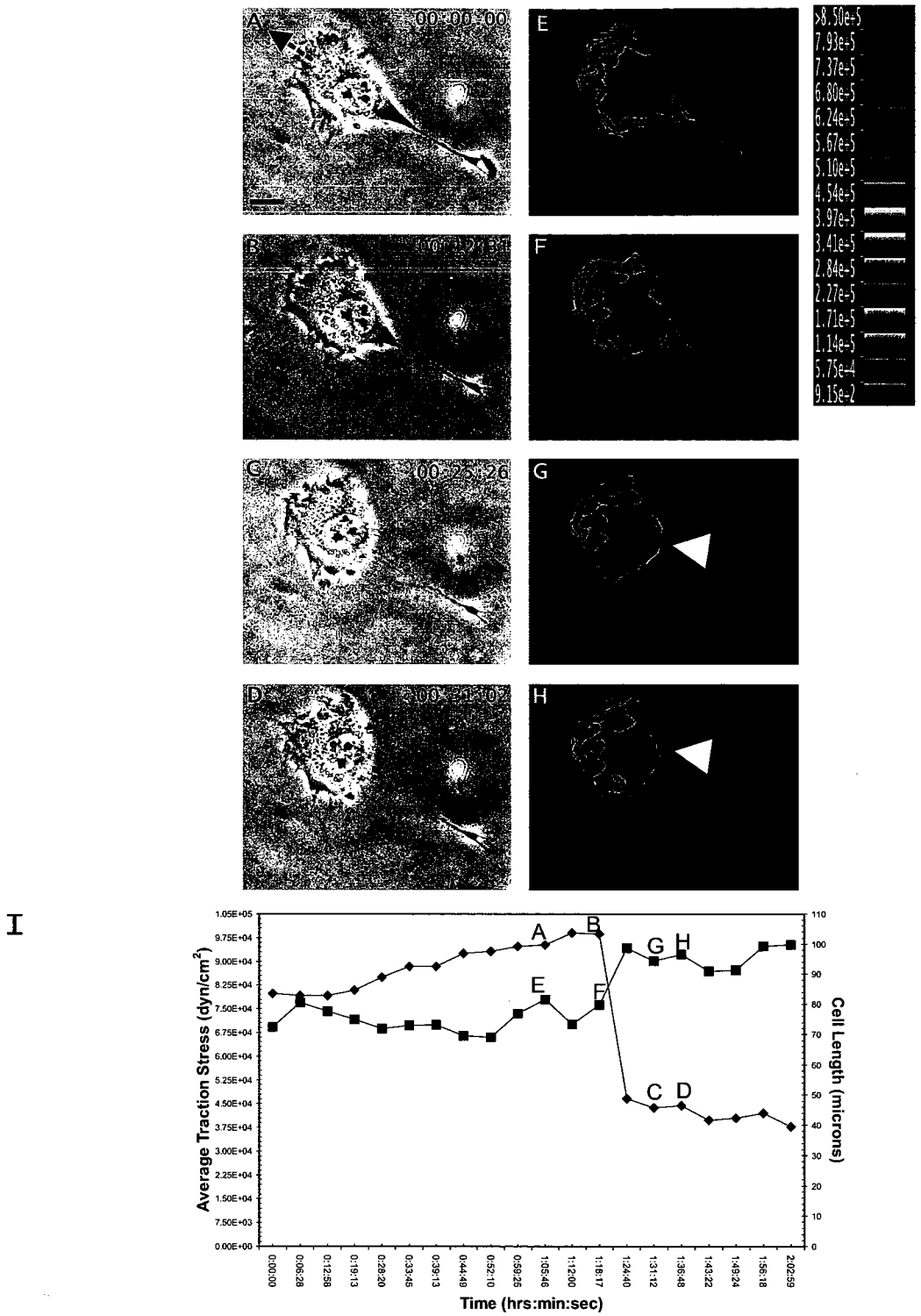

Figure 9. Response of traction forces to spontaneous tail retraction

Figure 10. Response of traction forces to GRGDTP-induced tail retraction

Panels A-D show phase contrast images of a migrating NIH 3T3 fibroblast, recorded at time points indicated at the upper right corner. The needle releasing GRGDTP is seen in panels B and C. Arrow in (A) indicates the direction of cell migration. Panels E-H show color rendering of the corresponding magnitude of traction stress, which ranges from violet (1.88×10^1 dynes/cm^2) to red ($> 2.00 \times 10^5$ dynes/cm^2). Note the increase in traction stress at the leading edge following GRGDTP-induced retraction of the tail. I) Average magnitude of traction stress (♦) and cell length (■) during GRGDTP-induced tail retraction. Letters A-H mark the corresponding panels. The arrowhead indicates the time when the GRGDTP peptide was locally applied to the trailing edge. Scale bar, 20 μm.

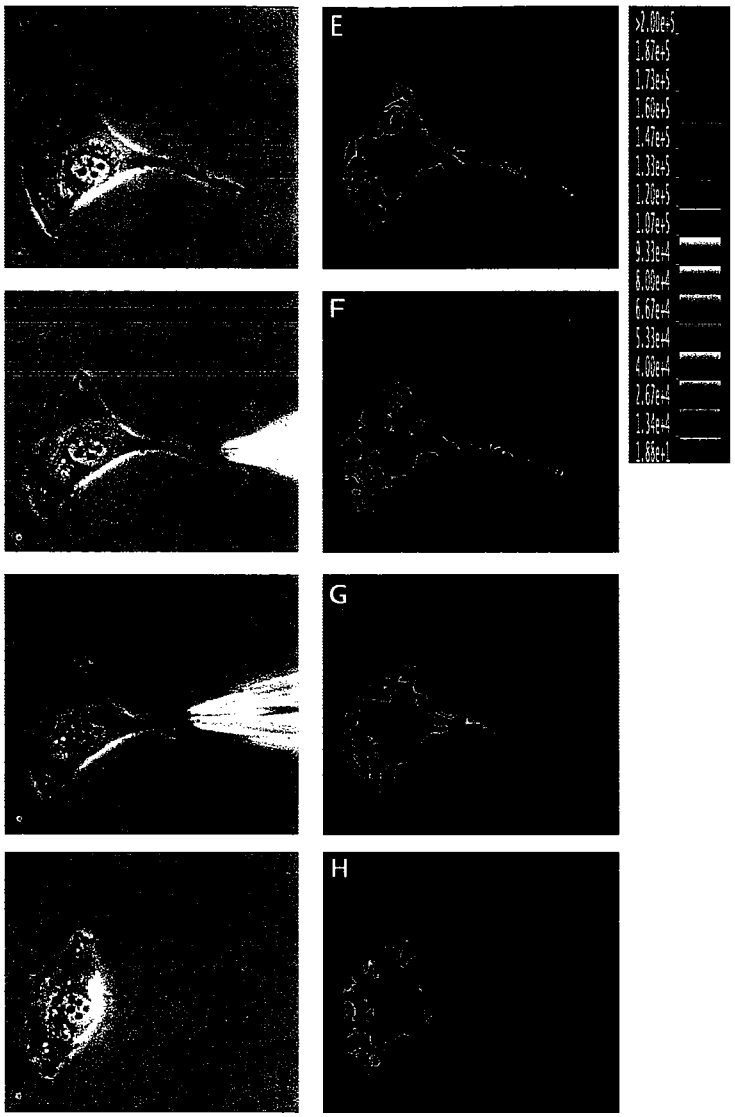

I

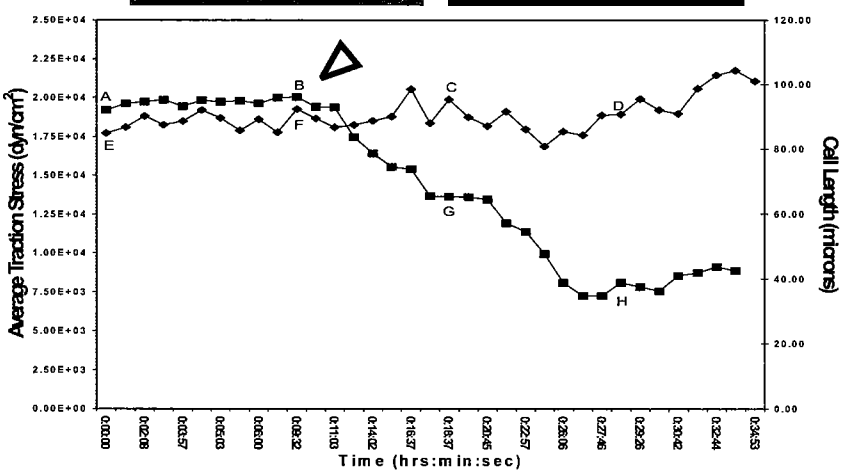

Figure 10. Response of traction forces to GRGDTP-induced tail retraction

Upon the loss of adhesion and traction forces at the tail, global balance was maintained by an immediate increase of tractions in other trailing regions (Fig. 9G-H, arrowheads). Together, these observations indicate that traction forces near the tail of a locomoting 3T3 cell are of the passive or reactive type.

Responses of Traction Forces and Cell Migration to Induced Frontal Retraction

The results with tail release indicated that a large portion of tail forces may be actively generated elsewhere, while the tail serves only as a site of passive anchorage. A similar approach with GRGDTP was thus applied to assess the effects of frontal release on traction forces and cell migration (n = 11 cells).

Limited detachment of the leading edge, induced by transient application of the GRGDTP peptide near the tip of the cell, resulted in an immediate and global decrease in traction stress by as much as 90%, before any significant decrease in cell length (Fig. 11D-F). Although the treatment caused the leading edge to collapse, upon removal of the peptide the lamellipodium and the traction forces returned within 10-20 minutes and cell migration resumed along the previous direction (Fig. 11G). Sustained applications of GRGDTP caused the cell to switch its direction of migration by establishing a new leading lamellipodium in a distal area (Fig. 12A-D). Application of the control peptide GRGESP again had no effect. These results indicate that traction forces were actively applied to the protrusive regions of the cell independent of the length or elastic properties of the cell. Furthermore, unlike tail detachment, the loss of frontal adhesion cannot be compensated by simply shifting the traction forces to other preexisting adhesion sites. These "active" traction forces appeared to reestablish only by the formation of new adhesion sites.

Figure 11. Response of traction forces to GRGDTP-induced frontal release

Panels A-C show phase contrast images of a migrating NIH 3T3 fibroblast, recorded at time points indicated at the upper right corner. The needle releasing GRGDTP is located near the bottom of panels B and C. Arrow in (A) indicates the direction of cell migration. Panels D-F show color rendering of the corresponding magnitude of traction stress, which ranges from violet (1.12×10^2 dynes/cm^2) to red ($> 1.80 \times 10^5$ dynes/cm^2). G) Average magnitude of traction stress (♦) and cell length (●) during GRGDTP-induced frontal release. Letters A-F mark the corresponding panels. The first arrowhead indicates the time when GRGDTP peptide was locally applied to the leading edge, causing a sharp drop in the average traction stress. The second arrowhead indicates the time when the needle releasing GRGDTP was removed. Note that upon local detachment of the leading edge, traction stress decreases dramatically across the entire cell while the length of the cell decreased only slightly (G; time ~11:00). The average traction stress recovers to the previous level over a period of 10-20 min. Scale bar, 20 μm.

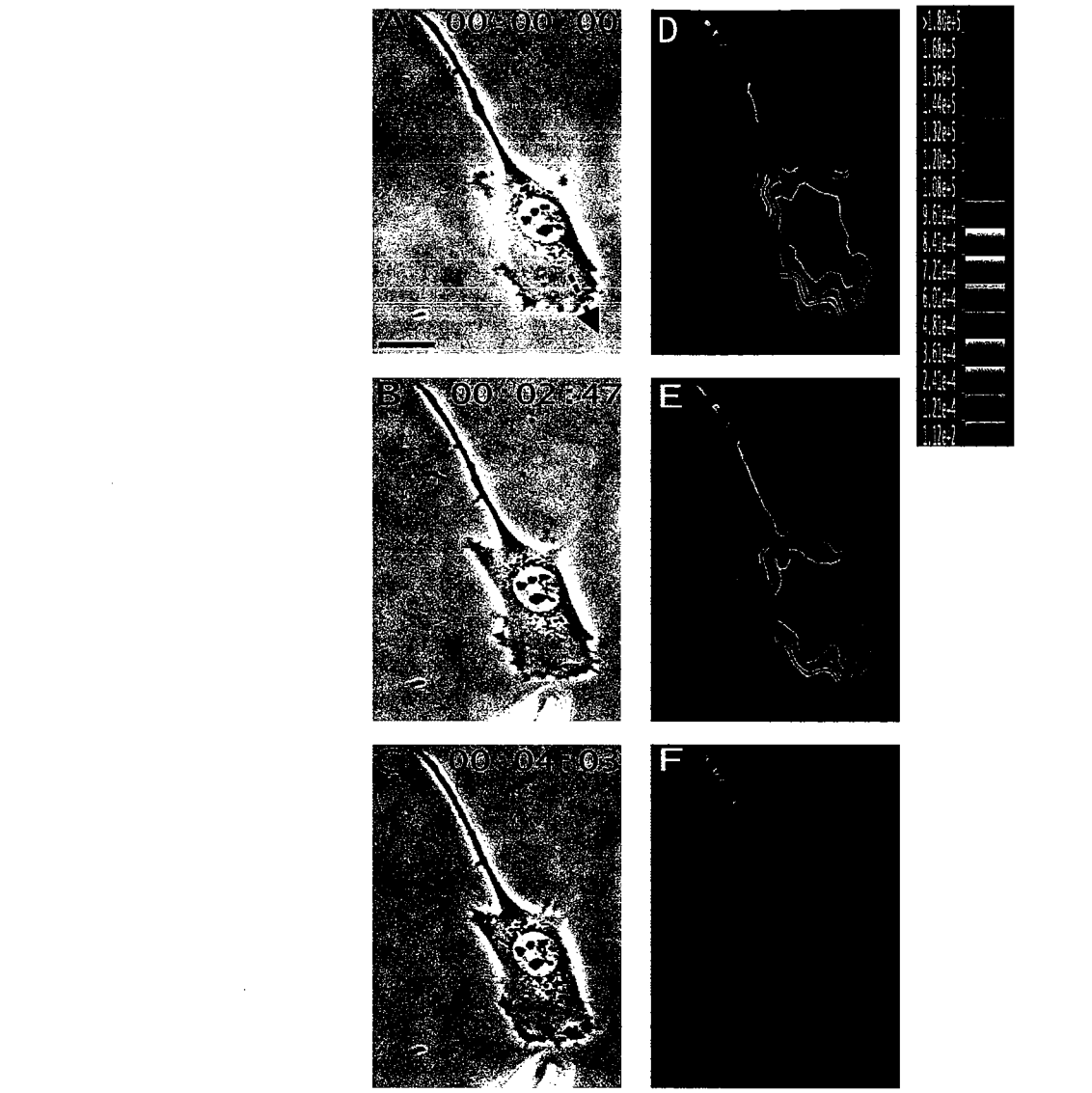

Figure 11. Response of traction forces to GRGDTP-induced frontal release

Figure 12. Redirection of cell migration following persistent treatment of the GRGDTP peptide at the front

Panels A-D show phase contrast images of a migrating NIH 3T3 fibroblast, recorded at time points indicated at the upper right corner. Arrows in (A) and (D) indicate the initial and final direction of cell migration respectively. Panels E-H show color rendering of the corresponding magnitude of traction stress, which ranges from violet (1.89×10^2 dynes/cm^2) to red ($> 1.50 \times 10^5$ dynes/cm^2). The cell changes its direction of migration following persistent frontal treatment with GRGDTP. A region near the original tail expands into a new lamellipodium with a concomitant increase in traction stress. Scale bar, 20 μm.

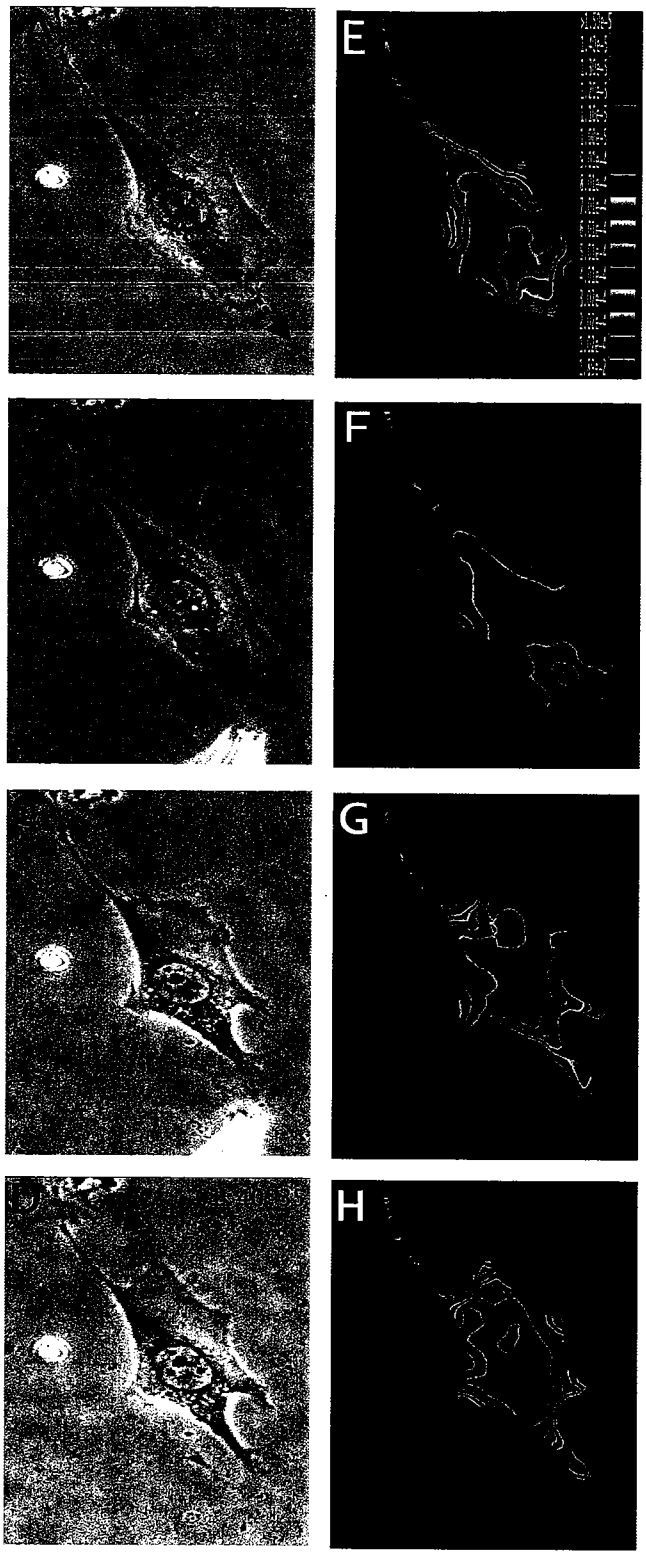

Figure 12. Redurection of cell migration following persistant treatment of the GRGDTP peptide at the front

Discussion

The first step toward a mechanistic understanding of cell migration is to determine the dynamic distribution of traction forces at the cell-substrate interface in relation to cell migration. We have extended the elastic substrate approach (Harris et al., 1980; Pelham and Wang, 1999; Wang and Pelham, 1998), by introducing computational methods capable of converting substrate displacements into high-resolution fields of traction vectors (Dembo et al., 1996; Dembo and Wang, 1999). As currently implemented, this methodology is capable of providing dynamic images of the traction stress under live cells, with a maximum temporal resolution on the order of few seconds and an estimated spatial resolution of 5-6 microns (Beningo et al., 2002; Munevar et al., 2001a). Analysis of polarized migrating 3T3 fibroblasts indicated that strong inward tractions were localized at the leading edge, lateral protrusion, and sometimes at the trailing edge of the cell. However, while these images clearly indicated that the cytoskeleton is under tension and that propulsive actions are concentrated at the front, they shed limited light on where forces are actively exerted and how they are converted into directional cell migration.

To probe into the functional role of traction forces in different regions, we have coupled traction force microscopy with focal release of GRGDTP. The responses of traction stress and cell migration to localized disruption of cell-ECM adhesions allowed us to gain unique insight into the mechanism of fibroblast migration. Our results indicated fundamental differences between traction forces at the front and rear of a 3T3 fibroblast. Release of frontal adhesions caused a drastic, global decrease in traction forces, indicating that integrins and the associated cytoskeleton in this region are rather

specialized in their abilities to transmit active forces and to maintain the general tension throughout the cell. Moreover, the force generating mechanism cannot be rapidly recycled to pre-existing adhesion sites upon detachment, but appeared to function only on new adhesion sites in the protrusive region. Conversely release of adhesions at the tail caused no decrease in traction forces elsewhere, indicating that they are passive anchors resisting forces generated in other regions and transmitted through the cell body. Furthermore, although tensile stresses along the cell body were often focused disproportionately onto a small subset of adhesion sites at the tail, these resistive forces were spread dynamically among multiple adhesion sites and were able to redistribute immediately upon the formation and dissociation of substrate adhesions. This may ensure a high degree of mechanical leverage for tail retraction and could be an important factor in maintaining the front-back asymmetry that enables the cell to migrate forward.

Our results further indicate that frontal and rear adhesion sites play different roles in maintaining the cell length. Dissociation of frontal adhesions caused a drastic loss of traction forces before any cell shortening becomes apparent. Conversely, both spontaneous and induced tail retraction caused striking shortening without a concomitant decrease in the overall traction stress. These observations may be explained if the elongated cell body is maintained by anchoring sites located at the tail and along the cell body, while the leading edge itself constitutes a mechanically distinct entity that exerts strong forces to tow this anchored cell body forward (Munevar et al., 2001b).

The present results also help address several potential mechanisms in cell migration (Bray, 2001). One common notion is that the cell consists of a network of contractile fibers attached to the substrate at various places. Directional migration arises

as a result of differential distribution of traction forces. This "tug-of-war" mechanism predicts that disruption of frontal attachments should not cause a dramatic, global decrease in tension, but simply cause the cell to contract towards the center until the tension is taken up by remaining adhesions, much like the detachment of the tail. This is clearly at odds with our findings. To account for tail retraction, some models place the emphasis on the elastic characteristics of the cell body, and use the conversion between potential and kinetic energies as an important part of the migration mechanism. However, the present results showed no evidence for the correlation between cell length and traction forces, or the storage of a significant amount of elastic energy for propelling cell movement, although such changes in cell length and cytoskeletal tension may serve an indirect function in regulating the rate or direction of cell movements (Chen, 1981). Our observations are generally in accord with the notion that the tension in the cell body is the result of continuous contraction, maintained at a more or less constant level regardless of cell length.

The present results are consistent with our recent finding that nascent focal adhesions near the leading edge are involved in generating transient propelling forces (Beningo et al., 2001), possibly coupled to the assembly of myosin II ribbons and minifilaments observed previously in this area (McKenna et al., 1989; Svitkina et al., 1997; Verkhovsky and Borisy, 1993). Important questions remain concerning the molecular interactions responsible for the generation and transmission of mechanical forces, the nature of chemical signals regulating the "active" and "passive" traction forces in different regions, and the possible differences between the migration of fibroblasts and other types of cells. This interface between physical forces and chemical signals lies at

the very heart of the mechanism that drives the directed cellular migration in a physiologically responsive fashion.

Chapter 4 - Regulation of Mechanical Interactions between Fibroblasts and the Substrate by Stretch-Activated Calcium Entry

Abstract

Calcium ions have long been implicated in regulating various aspects of cell movements. We found that stretching forces applied through flexible substrates induced increases in both intracellular Ca^{2+} concentration and traction forces of NIH 3T3 fibroblasts. Conversely, application of gadolinium (Gd^{3+}), an inhibitor of stretch-activated ion channels, or removal of extracellular free Ca^{2+} caused inhibition of traction forces. Gadolinium treatment also inhibited cell migration without affecting the spread morphology or protrusive activities. Local application of Gd^{3+} to the trailing region had no detectable effect on the overall traction forces, while local application to the leading edge caused a global inhibition of traction forces and cell migration, suggesting that stretch-activated channels function primarily at the leading edge. Immunofluorescence microscopy indicated that Gd^{3+} caused a pronounced decrease in vinculin and phosphotyrosine concentrations at focal adhesions. Our observations suggest that stretch-activated calcium entry in the frontal region regulates the organization of focal adhesions and the output of mechanical forces. This mechanism likely plays an important role in sustaining cell migration and in mediating active and passive responses to mechanical signals.

Introduction

Cell migration is important to many crucial biological functions such as embryogenesis, immune responses, wound healing, and cancer metastasis (Stossel, 1993). The process involves a number of well-orchestrated steps including protrusion, adhesion, contraction, and de-adhesion (Galbraith and Sheetz, 1998; Horwitz and Parsons, 1999; Lauffenburger and Horwitz, 1996). Although rapid advances have been made recently in identifying molecular components involved in cell migration, little is known about the mechanism that propels and regulates the movement.

Central to this problem are mechanical interactions between cells and the underlying substrate (Chicurel et al., 1998). Mechanical forces generated by the cell provide the traction for forward migration. For adherent cells such as fibroblasts, strong contractile forces are also required for the detachment of adhesions underneath the cell body and for organizing the extracellular matrix (Cox and Huttenlocher, 1998; Tomasek et al., 2002). In addition to the generation of mechanical forces, an equally important aspect is the ability of cells to sense mechanical signals, such as fluid shear, stretching forces, and substrate rigidity (Geiger and Bershadsky, 2001), and to respond by changing their growth rate, morphology, and migratory characteristics (Lo et al., 2000; Sai et al., 1999; Tzima et al., 2001; Wang et al., 2000). This interplay between the input and output of mechanical forces likely provides an essential feedback mechanism for guiding cell migration (Munevar et al., 2001a).

Calcium ions have long been recognized as an important second messenger for biological processes. In addition to the well-characterized troponin/tropomyosin system of striated muscles, there are multiple Ca^{2+}-sensitive pathways that may play an equally

effective role in regulating non-muscle contractility. For example, an earlier study has demonstrated a surge of Ca^{2+} as the eosinophils switch their direction of migration (Brundage et al., 1991). Potential downstream effectors include myosin light chain kinase (Kamm and Stull, 2001), caldesmon (Huber, 1997), gelsolin (Sun et al., 1999), and the Ca^{2+}-activated protease calpain (Glading et al., 2002). In addition, without a dedicated Ca^{2+} delivery system, such as the T-tubules and sarcoplasmic reticulum in skeletal muscle (Ebashi, 1991), an equally important question is how non-muscle cells regulate Ca^{2+} release for their contractile functions.

Of particular interest with regard to mechano-sensing are the stretch-activated ion channels. Although the molecular identity of these channels is still unclear, electrophysiological studies have clearly demonstrated the entry of extracellular Ca^{2+} upon mechanical stimulation of the plasma membrane (Guharay and Sachs, 1984). A common characteristic of these channels is their dose-dependent sensitivity to the heavy metal blocker gadolinium (Gd^{3+}) (Yang and Sachs, 1989). The presence of stretch-activated channels has been demonstrated in migrating fish fibroblast-like cells, which respond to stretching forces with a surge in cytoplasmic Ca^{2+} concentration (Lee et al., 1999). A similar Gd^{3+}-sensitive Ca^{2+} surge was observed with human gingival fibroblasts upon mechanical stimulations (Ko et al., 2001). Such stretch-activated channels represent an appealing candidate for mediating mechano-sensitive regulation of mechanical forces, by stimulating contractile forces in response to mechanical forces. Since stretch-activated Ca^{2+} surge appeared to correlate with cell retraction, it was further speculated that stretch-activated channels may function primarily along the cell body, to mediate the retraction and de-adhesion processes (Lee et al., 1999).

We have recently developed traction force microscopy to map mechanical interactions between migrating cells and the underlying substrate (Munevar et al., 2001a). Cells were cultured on flexible substrates impregnated with fluorescent beads, and mechanical forces exerted on the substrate were calculated based on the displacements of beads (Beningo et al., 2002). The flexibility of the substrate also facilitated the application of mechanical forces, by stretching the substrate with a blunted needle near the cell. In the present study we have applied this technique to characterize the responses of migrating NIH3T3 fibroblasts to stretching forces. We demonstrate that stretching forces stimulate profound increases in intracellular Ca^{2+} concentration, traction forces, and cell migration. Furthermore, Gd^{3+} applied locally to the frontal region of the cell causes a strong inhibition of traction forces and cell migration, while release at the tail has no detectable effect. Our study suggests that a major role of stretch activated channels is to regulate contractile activities and adhesion structures near the leading edge.

Materials and Methods

Preparation and Characterization of Polyacrylamide Substrates

Thin sheets of polyacrylamide gel were prepared from acrylamide (40% stock w/v; Bio-Rad Laboratories, Hercules, CA) and N,N-methylene-bis-acrylamide (BIS, 2% stock w/v; Bio-Rad) and adhered to activated cover slips as described previously (Beningo et al., 2002; Wang and Pelham, 1998). All the substrates used in this study contained 5% acrylamide, 0.1% BIS, and 1:100 dilution of fluorescent latex beads (0.2 μm FluoSpheres, Molecular Probes, Eugene, OR). The surface was coated covalently with type I collagen using photoactivatable heterobifunctional reagent sulfo-SANPAH (sulfosuccinimidyl 6 (4-azido-2-nitrophenyl-amino)(hexanoate; Pierce Chemicals, Rockford, IL), as described previously (Beningo et al., 2002; Wang and Pelham, 1998).

Steady state thickness of the polyacrylamide sheets at 37° C was estimated to be ~75 μm, by focusing a microscope with a calibrated focusing knob from the glass surface to the surface of the polyacrylamide gel. Young's modulus of the polyacrylamide sheets was estimated as 2.8×10^4 N/m^2 as described previously (Lo et al., 2000).

Measurement of Traction Stress and Application of Mechanical Forces

Traction force microscopy was performed as described recently (Munevar et al., 2001a). Briefly, deformation of the substrate caused by cellular traction forces was determined relative to the relaxed substrate using a pattern recognition algorithm. Coordinates defining the deformation field and cell boundary were analyzed with a Bayesian maximum likelihood method, which yielded traction vectors at pre-assigned nodes throughout the cell (Dembo and Wang, 1999). Pseudo-color images were generated by determining the magnitude of the traction stress at each pixel within the cell

boundary through interpolation and converting the magnitude into different RGB color combinations. For the application of mechanical stimulation, a blunted microneedle was inserted into the polyacrylamide substrate ~60 μm from a cell, and pulled away from the cell for ~ 15 min. The force caused displacement of the proximal region of the cell by ~20 μm.

Cell Culture and Microscopy

NIH 3T3 cells were cultured in DMEM (Sigma-Aldrich Chemical, St. Louis, MO), supplemented with 10% donor calf serum (JHR Biosciences, Lenexa, KS), 2 mM L-glutamine, 50 μg/ml streptomycin, and 50 U/ml penicillin (Gibco-BRL, Rockville, Maryland). Polyacrylamide substrates mounted in open coverslip chambers (McKenna and Wang, 1989) were equilibrated with the culture medium for approximately 30 minutes at 37° C before plating the cells. Phase images of cells, and fluorescent images of substrates-embedded beads were collected with a 40x/NA 0.75 Plan-Neofluar phase objective lens on a Zeiss Axiovert S100TV microscope, equipped with a custom stage incubator. Bead images on relaxed substrates were collected at the end of time-lapse recording by removing the cell with a microneedle and micromanipulator (Leitz, Wetzlar, Germany). All images were collected with a cooled CCD camera (ST133 controller with an EEV Type 57 back-illuminated frame-transfer CCD chip; Roper Scientific, Trenton, NJ) and processed for background subtraction using custom programs.

Interference reflection microscopy (IRM) was performed using a standard epifluorescence illuminator with the emission filter removed. Fluo-4-dextran (Molecular Probes) was used to monitor intracellular Ca^{2+} ion concentration. Cells were

microinjected with Fluo-4-dextran at 5 mg/ml in 10 mM Tris-Acetate (Sigma-Aldrich) and allowed to recover for 30 minutes before the analysis.

Pharmacological Analysis

Gd^{3+} was prepared as 100 mM stock solution from $Gd^{3+}Cl_3$ (Sigma-Aldrich). Manganese was prepared as 25 mN stock solution from $Mn^{2+}Cl_2$ (Sigma-Aldrich). The stock solutions were diluted into a modified Hank's balanced salt solution (Lee et al., 1999), to obtain working solutions of 100 μM and 500 μM respectively. Niphedipine (10 μM; Sigma-Aldrich), and EGTA (10 mM; Sigma-Aldrich) were prepared with the same balanced salt buffer. The culture medium was replaced with the drug solution by direct pipeting, and cells were imaged for approximately one hour.

Focal release of Gd^{3+} solution was carried out with a microneedle as described previously (O'Connell et al., 2001). A suction micropipette held 20-40 μm behind the release needle maintained the distribution of Gd^{3+} to a region 10-15 μm in diameter. Rhodamine dextran (Molecular Probes) at 5 mg/ml was added to the Gd^{3+} solution to allow monitoring of the distribution of the released solution. Applications of the rhodamine dextran marker alone had no discernable effect on migrating cells.

Immunofluorescence Staining

Cells treated with Gd^{3+} or Mn^{2+} for 30 min were rinsed with warm PBS with (for phosphotyrosine staining) or without (for vinculin staining) 1 mM sodium orthovanadate (Fisher Scientific, Pittsburgh, PA), and fixed with 4% paraformaldehyde (EM Sciences, Washington, PA) and 0.1% Triton X in warm PBS for 10 minutes. Fixed cells were blocked with 1% bovine serum albumin (BSA; Boehringer Mannheim, Indianapolis, IN), and incubated with vinculin monoclonal antibodies (Vin-11-5, Sigma-Aldrich), or

phosphotyrisine monoclonal antibodies (4G10; Upstate Technologies, Lake Placid, NY) at a dilution of 1:100 for one hour at 37 °C. After thorough washing with 1% BSA in PBS, cells were then incubated with Alexa 546-conjugated goat anti-mouse antibodies (Molecular Probes) at a dilution of 1:100 for 45 minutes at 37 °C. Counterstaining with flourecien phalloidin (Molecular Probes) for actin filaments was performed according to manufacturer's procedure. The intensity of phosphotyrosine staining was quantified by manually defining the boundary of the cell and integrating the fluorescence intensities within the boundary.

Results

Effects of Stretching Forces on Traction Forces and Intracellular Calcium

We found previously that stretching forces act as an effective means for guiding NIH 3T3 cell migration (Lo et al., 2000). To determine if this process involves an increase in traction forces, we stretched cells on flexible substrates by pulling on the substrate with a microneedle. As shown in Figure 13, the cell turned toward the direction of stretching forces, accompanied by an increase in traction stress near the leading edge. By comparing the average traction stress magnitude before and after stretching, we found a 52% increase in traction stress (n = 3). We also observed an acceleration of migration from ~0.2 μm/minute to ~0.4 μm/minute, based on the centroid of the nucleus of cells with (n = 3) and without stretching (n = 6). Furthermore, using cells loaded with the Ca^{2+} indicator Fluo-4, we found that stretching induced an increase in cytoplasmic Ca^{2+} concentration (Figure 13G and I). These observations suggest that mechanical signals affect the intracellular Ca^{2+} concentration, which may in turn regulate the output of traction forces.

Involvement of Stretch-Activated Channels in Calcium Entry and Traction Forces

To address if stretch-activated channels were involved in the mechanical force-induced increase in Ca^{2+}, we treated cells with 100 μM Gd^{3+}, a known blocker of stretch-activated channels (Yang and Sachs, 1989). The treatment inhibited stretch-activated increase in Ca^{2+} concentration (Figure 13H and J) (Lee et al., 1999), suggesting that the response must rely on the entry of extracellular Ca^{2+} through stretch-sensitive channels.

Figure 13. Increases in traction forces and intracellular Ca^{2+} following the application of stretching forces

Mechanical forces were applied to a migrating NIH3T3 cell by stretching the flexible substrate near the leading edge with a microneedle. Arrows (B, C) indicate the direction of stretching. Phase contrast (A-C) and traction stress (D-F) images were recorded prior to (A, D) and following the removal of the needle, at time points indicated (B, C, E, F). Asterisks mark a fiduciary reference point on the substrate (A-C). Traction stress images were rendered with different colors representing the magnitude from violet (2.50×10^1 dynes/cm^2) to red (> 3.99×10^4 dynes/cm^2). To detect the calcium concentration, cells loaded with Fluo-4-dextran were recorded before (G, H) or after (I, J) the application of stretching forces. While the cell stretched in control balanced salt solution showed a clear increase in fluorescence intensity ~10 minutes after stretching (G, I), the cell stretched in 100 μM Gd^{3+} showed a slight decrease in fluorescence intensity (H, J). Bars, 20 μm.

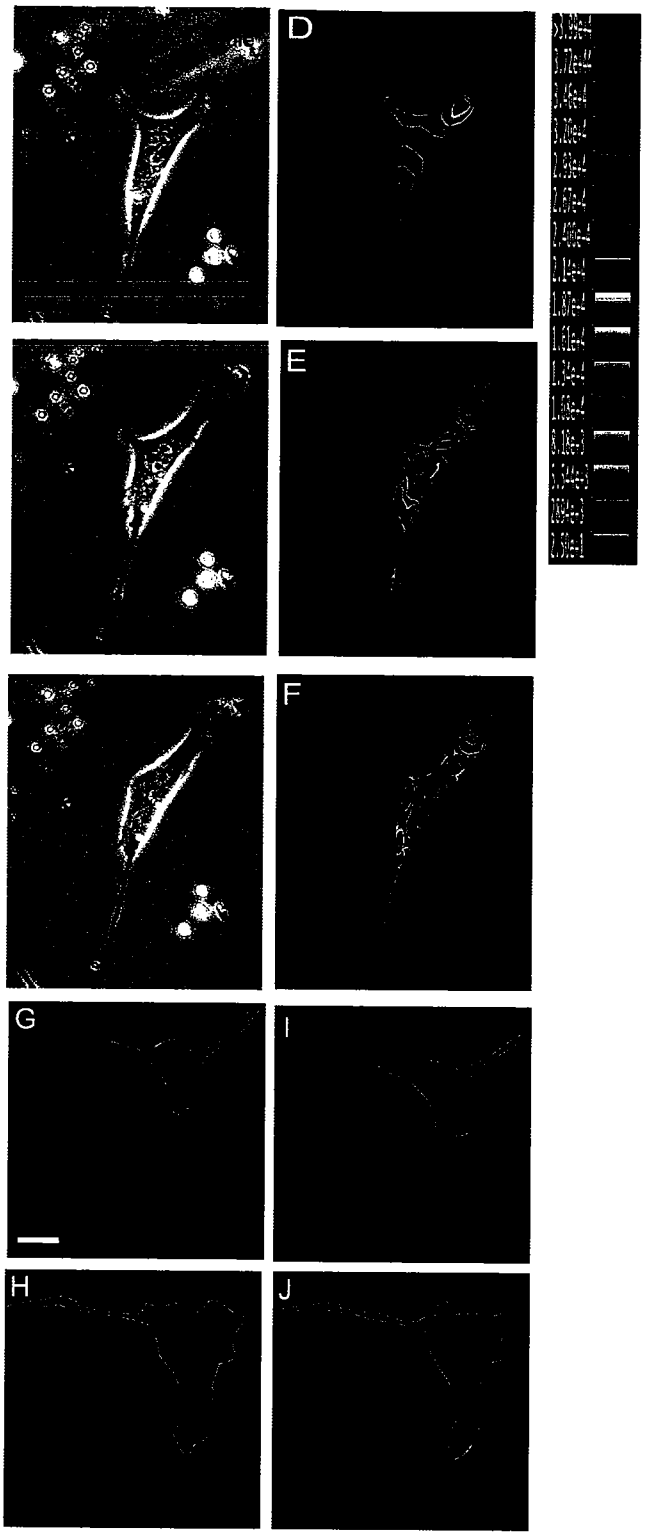

Figure 13. Increase in traction forces and intracellular calcium following the application of stretching forces

Figure 14. Response of cell migration and traction forces to the application of Gd^{3+}

Phase contrast images (A-C) of a migrating NIH3T3 fibroblast, recorded immediately before and at specified time points after the application of 100 μM Gd^{3+}, showed no apparent effect on the spread morphology or local protrusive activities (arrows). However, forward migration of the cell was inhibited. Asterisks mark a fiduciary reference point on the substrate. The corresponding traction stress images (D-F), with different colors representing the magnitude from violet (1.04×10^2 dynes/cm^2) to red (> 1.00×10^5 dynes/cm^2), showed a striking decrease in traction stress following Gd^{3+} application. Scale bar, 20 μm

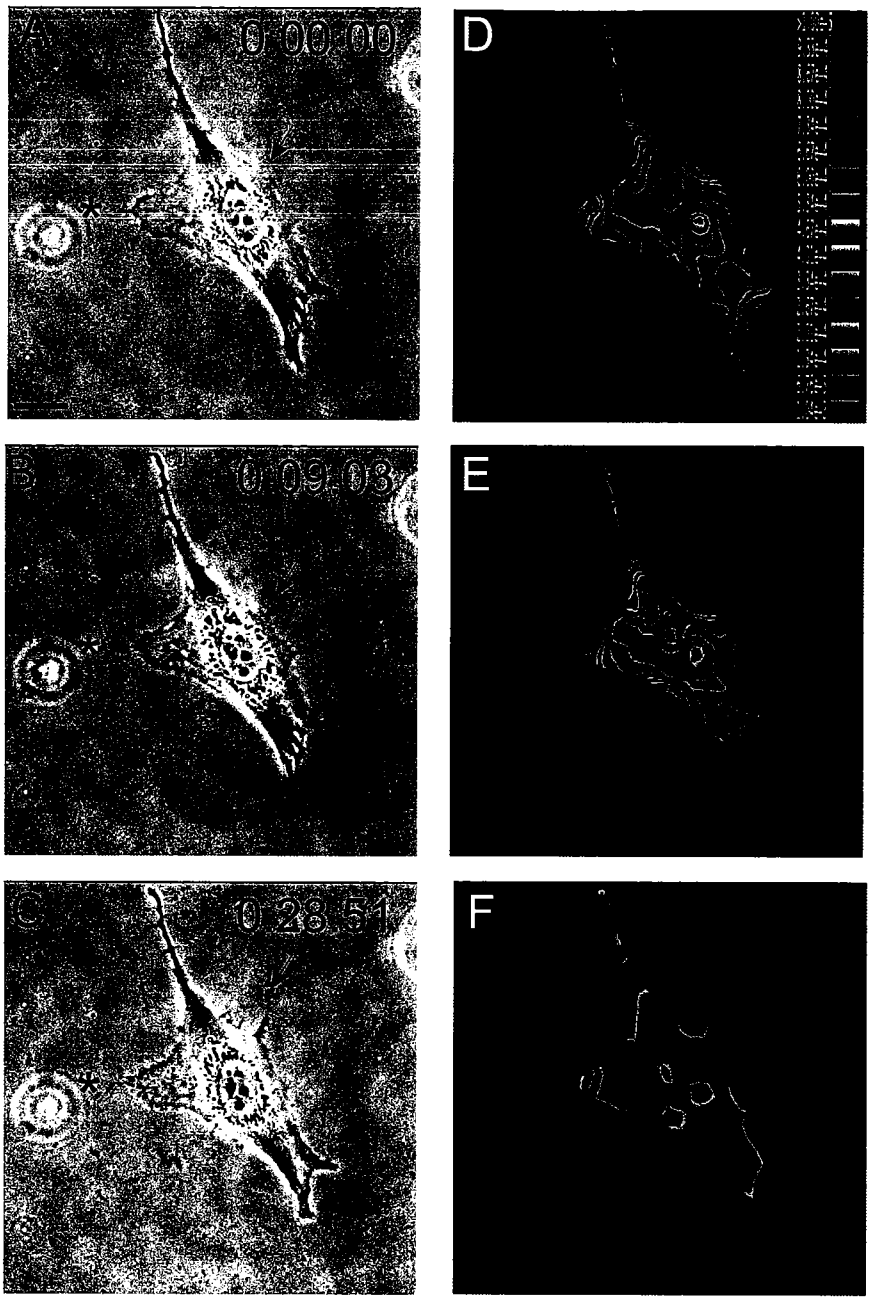

Figure 14. Response of cell migration and traction forces to the application of Gadolinium

Figure 15. Average migration speed in response to inhibition of stretch-activated Ca^{2+} entry

NIH3T3 cells incubated globally in gadolinium ion showed a marked decrease in average migration speed as compared to control cells. Cell migration speed also decreased sharply upon application of Gd^{3+} to the leading edge, but not when applied to the trailing edge. Global application of EGTA similarly caused a sharp decrease in average migration speed. Error bars indicate standard error.

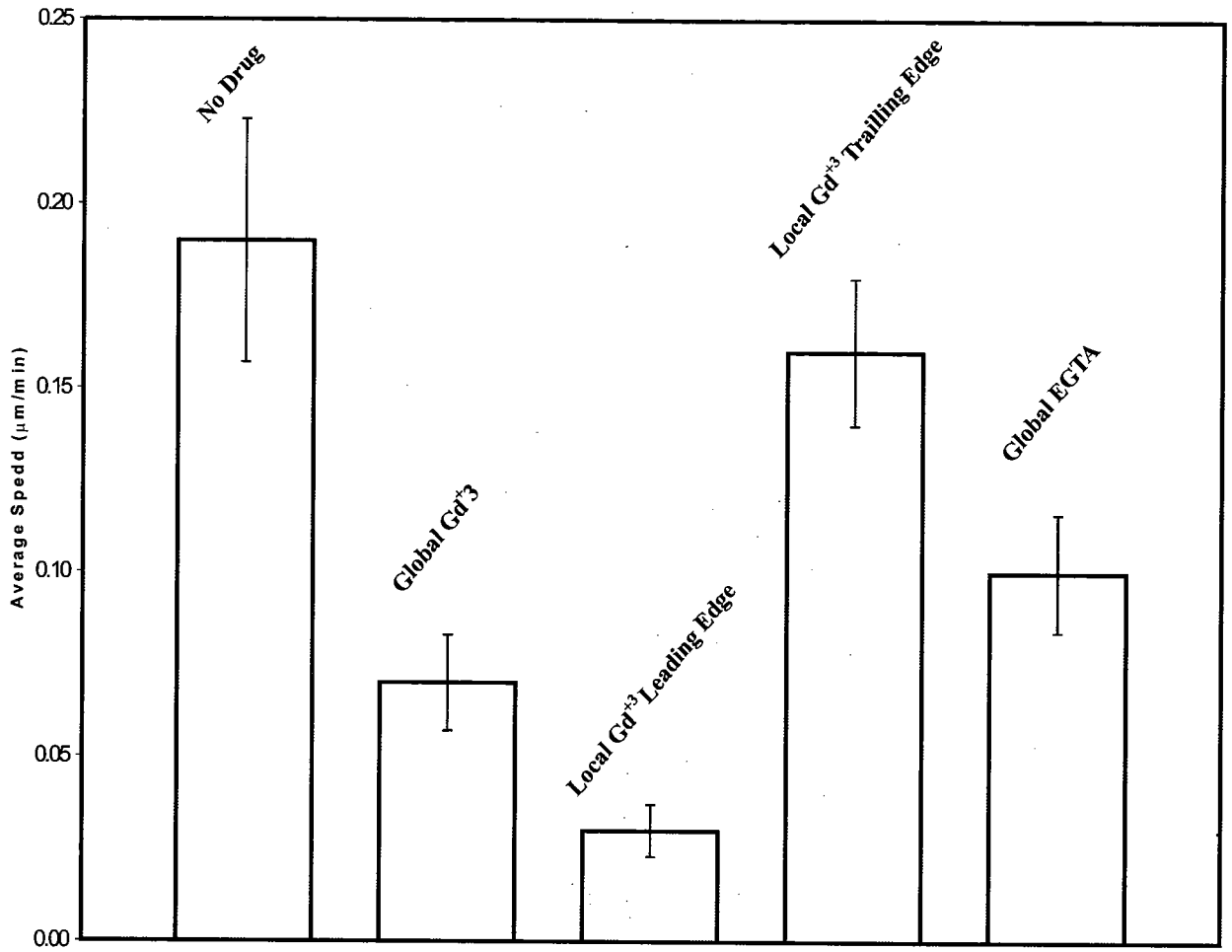

Figure 15. Average migration speed in response to inhibition of stretch-activated Calcium entry

Treated cells maintained their spread morphology and localized ruffling activities (Figure 14C), however the rate of migration decreased as compared to non-treated cells (Figure 15). In addition, Gd^{3+} caused traction forces to drop sharply to a basal level within 30 minutes (n = 4; Figure 14D-F), suggesting that Ca^{2+} entry is required for the generation and/or maintenance of traction forces. Cells cultured in balanced salt buffer alone showed no inhibition of traction forces (not shown).

Since Gd^{3+} may affect other cellular mechanisms, we have investigated the effects of Ca^{2+} depletion from the medium, which should induce similar effects as those caused by channel blockage. As for Gd^{3+}, chelation of extracellular Ca^{2+} with EGTA caused a sharp decrease of traction forces to a basal level (Figure 16F; n = 3), consistent with the notion that entry of extracellular Ca^{2+} is essential for maintaining traction forces. However, EGTA also caused inhibition of ruffling activities and partial retraction of the cell, as expected from the involvement of Ca^{2+} in integrin-ECM interactions (Leitinger et al., 2000). Treatment with 10 μM niphedipine, an inhibitor of L-type Ca^{2+} channels, caused no consistent decrease in either traction forces or motility (not shown). Together, these results suggest that the entry of extracellular Ca^{2+} is tightly regulated through specific pathways during cell migration, and that stretch-activated channels play a major role in this process.

Previous studies suggested that stretch-activated channels may be involved in regulating the retraction and de-adhesion along the cell body, in response to periodic changes in tension during cell migration (Lee et al., 1999). To determine the site of action of stretch-activated channels, we applied Gd^{3+} locally to different regions of migrating cells with a microneedle while simultaneously monitoring the traction forces.

Characterization of this technique with fluorescent markers indicated that the released solution was confined to a region ~15 μm in diameter (O'Connell et al., 2001).

Figure 16. Response of cell migration and traction forces to the application of EGTA

Phase contrast images (A-C) of a migrating NIH3T3 fibroblast, recorded immediately before (A) and at specified time points after the application of 10 mM EGTA (B-C), showed inhibition of local protrusive activities (arrow, C) and partial retraction. Asterisks mark a fiduciary reference point on the substrate. The corresponding traction stress images showed a striking decrease in traction forces (D-F). Different colors representing the magnitude of traction stress, from violet (9.5×10^1 dynes/cm^2) to red (> 1.00×10^5 dynes/cm^2). Scale bar, 20 μm.

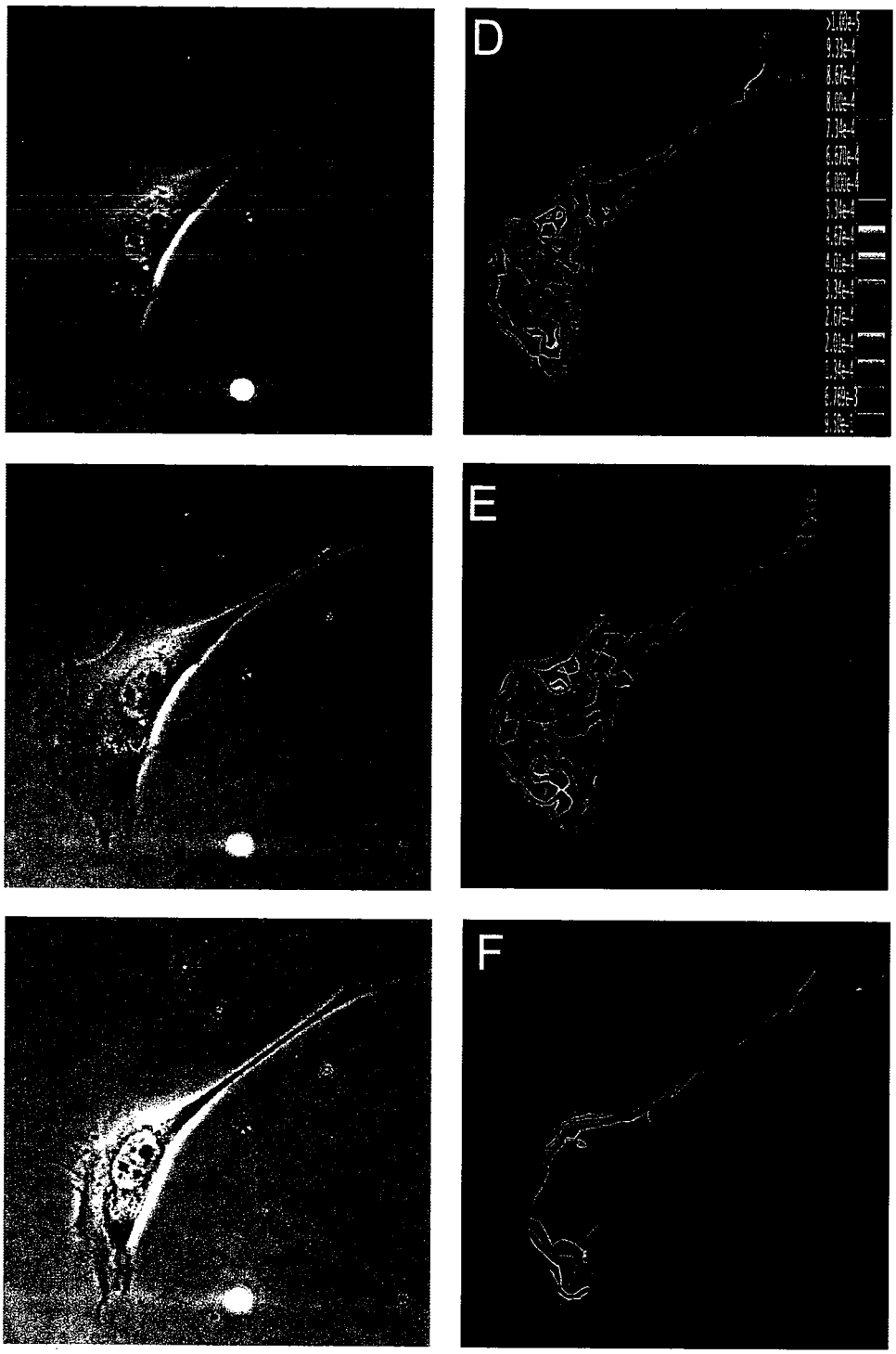

Figure 16. Response of cell migration and traction forces to the application of EGTA

Figure 17. Response of cell migration and traction forces to local application of Gd^{3+} near the leading edge

Phase contrast images (A-C) of a migrating NIH3T3 fibroblast, recorded immediately before (A) or at specified time points after the application of 100 μM Gd^{3+} near the leading edge (arrows, B-C), showed no inhibition of local protrusive activities (arrows), although the cell body failed to migrate forward. Asterisks mark a fiduciary reference point on the substrate. The corresponding traction stress images (D-F), with different colors representing the magnitude from violet (4.25×10^1 dynes/cm^2) to red ($> 4.50 \times 10^4$ dynes/cm^2), showed a global decrease in traction stress following the local Gd^{3+} application. Scale bar, 20 μm.

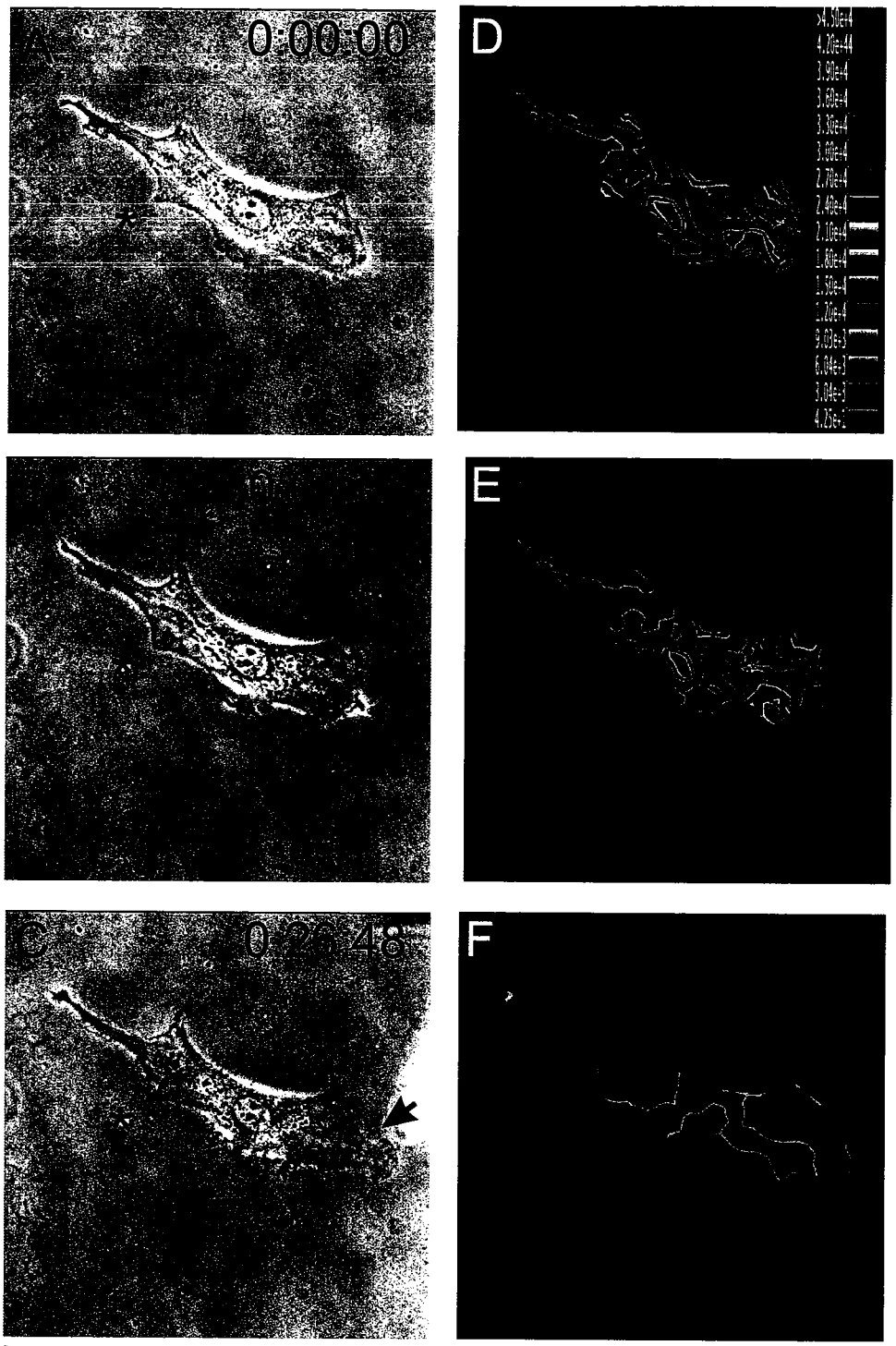

Figure 17. Response of cell migration and traction forces to local application of gadolinium near the leading edge

Figure 18. Response of cell migration and traction forces to local application of Gd^{3+} near the trailing edge

Phase contrast images (A-C) of a migrating NIH3T3 fibroblast, recorded immediately before (A) or at specified time points after the application of 100 μM Gd^{3+} near the trailing edge, showed no apparent effect on cell morphology or migration. Asterisks mark a fiduciary reference point on the substrate. The corresponding traction stress images (D-F), with different colors representing the magnitude from violet (7.63×10^1 dynes/cm^2) to red (> 4.75×10^4 dynes/cm^2), showed no apparent effect on traction stress following the local Gd^{3+} application. Scale bar, 20 μm.

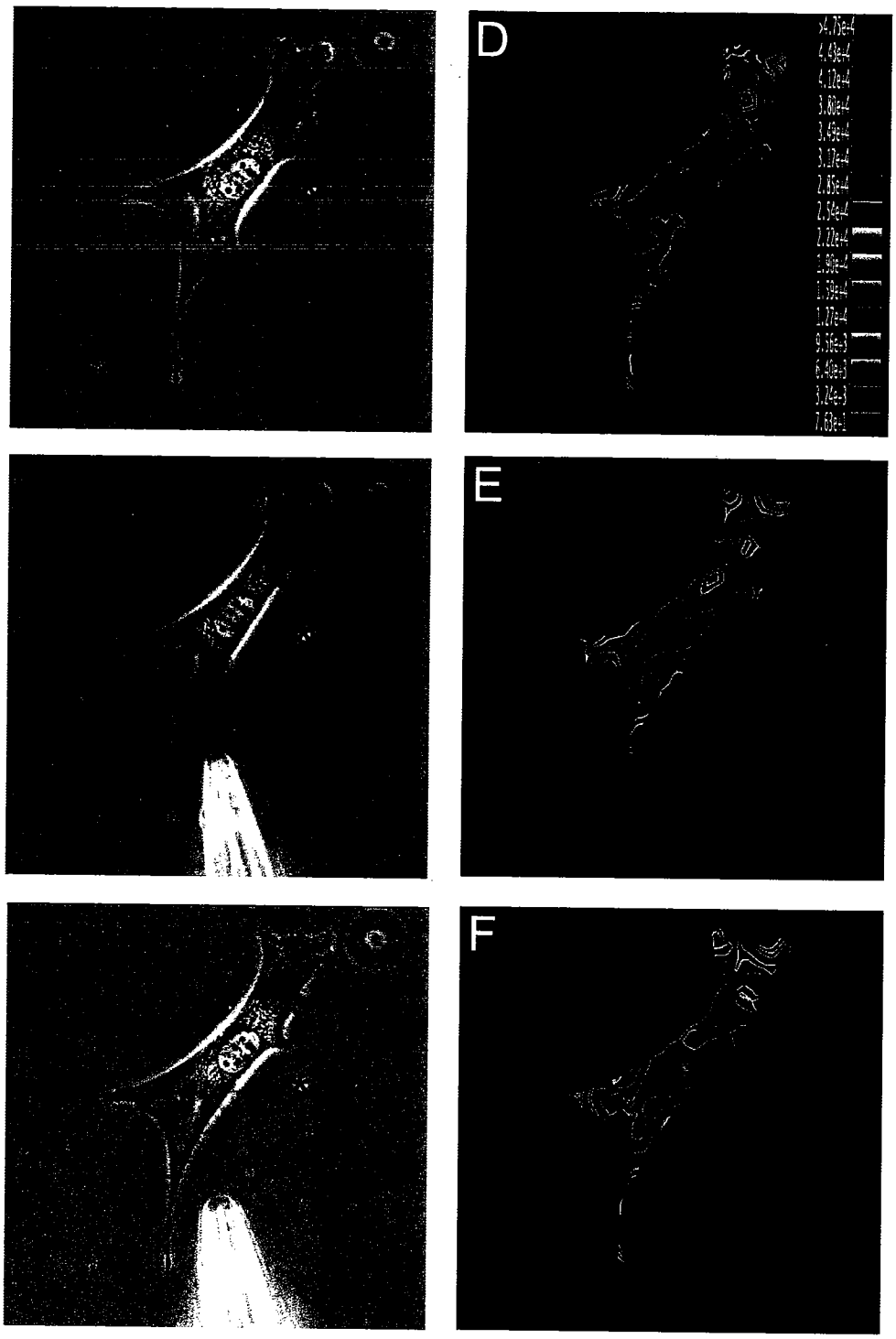

Figure 18. Response of cell migration and traction forces to local application of Gadolinium near the trailing edge

We found that only applications to the leading edge caused a decrease in traction forces and decrease in cell migration speed (Figures 15 and 17; n = 4). Local application of Gd^{3+} to the trailing edge caused no detectable effect on either traction forces or cell migration speed (Figures 15 and 18; n = 4).

Effects of Gd^{3+} on Focal Adhesions

To assess the mechanism underlying Gd^{3+}-induced inhibition of traction forces, we used IRM to monitor the pattern of substrate adhesions. The treatment caused a transient formation of dark, amorphous contact structures over a large portion of the ventral surface, which may reflect transient interactions of surface negative charges with Gd^{3+} (Figure 19B, arrows). However, at steady state, treated cells maintained focal adhesion-like structures (Figure 19C), consistent with their spread morphology despite the strong inhibition of traction forces. Compared to those in control cells, adhesion structures in Gd^{3+} treated cells appeared to be less elongated and more centrally localized (compare Figure 19A and 19C, and 20I and 20D).

To examine the structural organization of focal adhesions, we stained Gd^{3+} treated cells for vinculin and phosphotyrosine with immunofluorescence, and actin filaments with fluorescent phalloidin. The amount of both vinculin and phosphotyrosine decreased from focal adhesions (Figure 20A, F and E, J). The total level of phosphotyrosine was reduced by ~30 %, as estimated by integrating staining intensities of the entire cell (average of 40 cells). Gadolinium treated cells retained at least some stress fibers, although their size appeared reduced when compared to untreated cells (Figure 20B, G). Treatment of cells with Mn^{2+}, a heavy metal known to increase the integrin-ECM binding

affinity, only caused focal adhesions to appear more robust, and no qualitative difference was found in the IRM morphology of Mn^{2+} treated and control cells (data not shown).

Figure 19. Response of focal adhesions to Gd^{3+}

IRM images of a NIH3T3 cell were recorded immediately before (A), or after the treatment with 100 μM Gd^{3+}at indicated time points (B, C). Note the transient increase in the darkness of the image (B, arrows), before the image returned to a pattern similar to that before the treatment (C). However, the adhesion plaques appeared less elongated compared to those before treatment, and more adhesion plaques were found near the center of the cell (C, arrows). Scale bar, 20 μm.

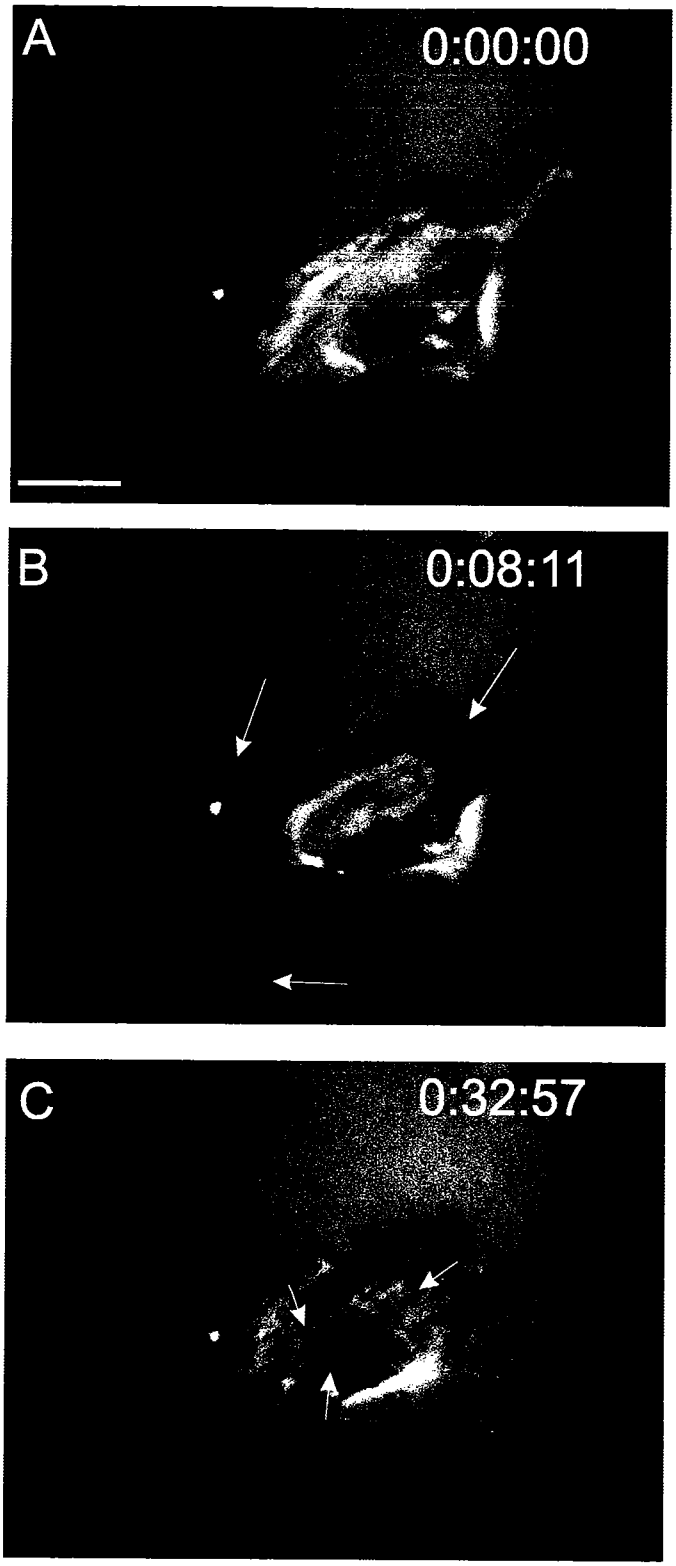

Figure 19. Response of focal adhesions to Gadolinium

Figure 20. Effects of Gd^{3+} on vinculin and phosphotyrosine organization

NIH3T3 cells were treated with 100 μM Gd^{3+} (A-E) or control buffer (F-J) for 30 min before processing for immunofluorescence staining of vinculin (A, F), actin filaments (B, G), or phosphotyrosine (E, J; in different cells). Panels C and H show combined actin-vinculin images. The control cell showed the characteristic localization of vinculin at focal adhesions (F), which were concentrated at the termini of stress fibers (H) and appeared as dark plaques in the IRM image (I). Gd^{3+} treated cell showed a reduction in stress fiber number and intensity, and an increase in cortical actin intensity (B). In addition, vinculin localization was much reduced at focal adhesions, and appeared primarily perinuclear (A). Staining of phosphotyrosine showed a similar decrease at focal adhesions in Gd^{3+} treated cells (E, J). IRM image of treated cell showed adhesion plaques throughout the cell, which appeared less elongated than those in control cells (D, I). Scale bar, 20 μm.

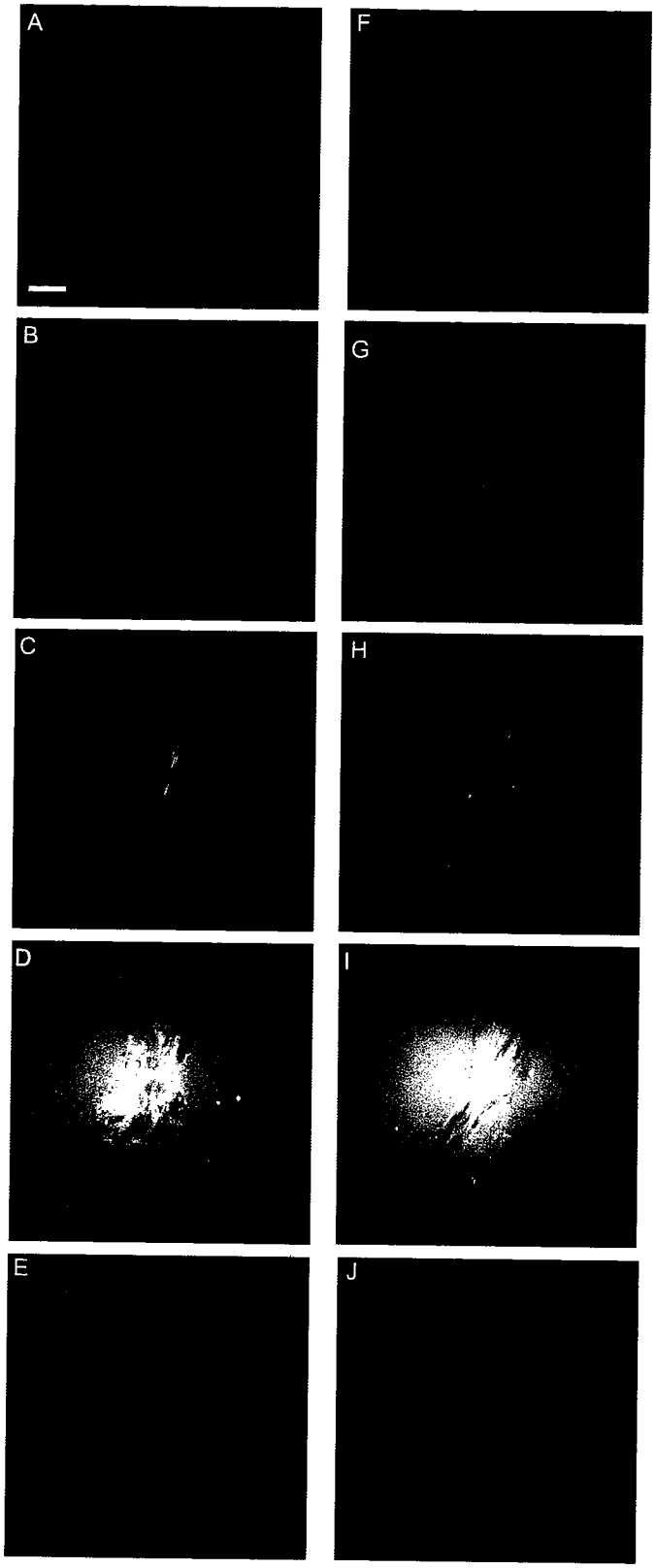

Figure 20. Effects of Gadolinium on Vinculin and Phospho-tyrosine organization

Discussion

Accumulating evidence indicates that cell motility is regulated not only by chemical factors but also by physical parameters. For example, endothelial cells show reorientation along the direction of fluid shear (Shirinsky et al., 1989). NIH 3T3 fibroblasts migrate preferentially toward stiff substrates or stretching forces (Lo et al., 2000). Such effects likely involve profound changes in the organization of the actin cytoskeleton and/or focal adhesions, as demonstrated by the increase in cortical rigidity (Chicurel et al., 1998; Glogauer et al., 1997), and in vinculin and zyxin concentration at focal adhesions (Riveline et al., 2001; Wang et al., 2000), upon the exertion of mechanical forces on integrin receptors. The mechano-sensitive responses have been implicated in regulating numerous physiological and pathological processes such as embryonic development, wound healing, and cancer metastasis (Ingber, 2002; Rabinovitz and Mercurio, 1996; Tomasek et al., 2002).

Calcium ion, with its multiple effects on the actin cytoskeleton, represents an attractive candidate for regulating cell migration. Previous experiments have demonstrated that the reorientation of eosinophils correlates with a surge in cytoplasmic Ca^{2+} (Brundage et al., 1991), while local activation of caged Ca^{2+} induces growth cone turning (Zheng, 2000). In the present study, we showed that Ca^{2+} plays an important role in mechano-sensing and in the generation/transmission of traction forces. We demonstrated that stretching forces caused an increase in intracellular Ca^{2+} concentration, and that such increases are inhibited by the stretch-activated channel blocker Gd^{3+} (Lee et al., 1999). We further demonstrated that the application of stretching forces caused a marked increase in cellular traction forces, while incubation with Gd^{3+} caused a striking

decrease in traction forces. Furthermore, the results with EGTA, which induced both loss of traction forces and retraction of cells, supported the notion that Ca^{2+} entry through membrane channels is critical for the maintenance of traction forces.

Detailed observations with phase, immunofluorescence, and IRM optics further indicated that inhibition of stretch-activated channels alone had no striking effect on the protrusive activities, the spread morphology, and only a transient effect on the physical contacts between cells and the substrate. However, the most intriguing observation was that Gd^{3+} caused a profound reduction of vinculin and phosphotyrosine from focal adhesions. The structural defects may cause disruptions in the mechanical interactions between focal adhesions and the cytoskeleton, leading to the precipitous drop in traction forces and cell migration activities. In addition, the decrease in Ca^{2+} may inhibit contractile activities of focal adhesion-associated cytoskeletal structures, which may in turn cause dissociation of focal adhesion proteins (Burridge and Chrzanowska-Wodnicka, 1996).

Using focal drug delivery (O'Connell et al., 2001), we have investigated the likely sites of action of stretch activated channels. Previous speculations have emphasized the possible regulation of cell de-adhesion and tail release by stretch-activated channels (Lee et al., 1999). It was proposed that cell migration causes tension to rise along the cell body, which in turn opens the stretch activated channels and triggers tail release. In contrast, we found that local application of Gd^{3+} to the leading edge resulted in a sharp decrease in traction forces and migration rate irrespective of the length of the cell, while applications to the cell body or the trailing edge caused no detectable effect on traction forces. Although it is possible that a Ca^{2+} sensitive mechanism may be involved in tail

release, we suspect that the previously reported cell elongation in Gd^{3+} may be due to the inhibition of retraction forces generated in the frontal region (Lee et al., 1999). Our results suggest that either stretch-activated channels are concentrated at the leading edge, or those channels located at the leading edge play a dominant role in regulating traction forces and cell migration.

Our observations may be understood in the context of the frontal towing model of cell migration (Munevar et al., 2001a). We proposed that the frontal region plays a critical role in both propelling the cell body and responding to guidance cues, whereas the rest of the cell behaves as a passive, resistive cargo. During fibroblast migration, frontal protrusion is followed by the formation of substrate adhesions and the development of active propulsive forces at these nascent focal adhesions (Beningo et al., 2001). The present results suggest that stretch-activated channels have no direct role in the steps of protrusion and substrate adhesion, but profound effects on the development of traction forces and possibly the subsequent maturation of focal adhesions.

In addition, Ca^{2+} entry through stretch-activated channels may be involved in maintaining the migrational directionality, and in mediating both passive and active responses to mechanical signals. Counter-forces to the strong traction forces at the front would cause Ca^{2+} entry through stretch-activated channels, which may in turn stimulate the local assembly of focal adhesions and the generation or transmission of traction forces. This mechano-sensitive modulation of mechanical forces would thus provide a positive feedback mechanism to stabilize the polarity of cell migration. Through a similar mechanism, migrating cells would turn toward stretching forces (Lo et al., 2000), by stimulating local adhesion structures and traction forces in the stretched region. In

addition, resistance of stiff substrate to traction forces may cause a similar opening of stretch-activated channels, and reorientation of the cell (Lo et al., 2000).

A number of intracellular Ca^{2+}-sensitive components may be involved in mediating the stretch response, including the myosin light chain kinase and caldesmon, which are regulated by Ca^{2+}-calmodulin (Walsh, 1994), and gelsolin and non-muscle α-actinin, which are regulated by direct Ca^{2+} binding (Rosenberg et al., 1981; Sun et al., 1999). These proteins are known to affect either the generation of contractile forces or the integrity of the cytoskeletal network for force transmission. However, it is not clear how Ca^{2+} entry affects vinculin and tyrosine phosphorylation at focal adhesions. One attractive mechanism involves the Ca^{2+} activated protease, calpain (Glading et al., 2002). At least some members of this family of proteases are associated with focal adhesions (Shim et al., 2001), and their putative targets include structural and regulatory components such as paxillin and Rho (Beckerle et al., 1987; Geiger and Bershadsky, 2001). Finally, focal adhesions are complex structures (Geiger and Bershadsky, 2001), and it is likely that additional mechano-chemical mechanisms, such as force-induced conformational responses of structural components, enzymes, or substrates, function in conjunction with stretch-activated channels. This has been suggested in a recent study indicating that Triton-extracted cytoskeletons maintained at least some of the abilities to respond to stretching forces (Sawada and Sheetz, 2002).

Chapter 5 – Discussion

Cell migration has proven to be a complex vital biological mechanism that performs numerous functions. Cell migration very simply consists of extension at the leading edge, adhesion to the underlying substrate, and retraction from the trailing edge (Bray, 2001). These steps do not occur in any set order and could occur simultaneously (Horwitz and Parsons, 1999). During the course of this study we have developed and applied a new imaging technique called traction force microscopy (Chapter 2), which has allowed us to map the mechanical forces generated by normal and H-ras transformed cells during migration (Chapter 2). The heart of this approach is the combination of flexible polyacrylamide substrates, digital imaging, and mathematical computation to deconvolve substrate deformation into a distribution of mechanical forces.

The overall results of this study revealed that propulsive traction forces generated by NIH 3T3 cells were concentrated near the tip of the lamellipodia and dropped off precipitously towards the center of the cell. The traction forces at the leading edge were shown not to correlate directly with local protrusive activities but rather with the overall direction of cell migration. We also found that protrusive regions that displayed persistent traction force generation tended to develop into dominant lamellipodia, and those exhibiting only transient traction force activities retracted quickly. Thus the polarity of cell migration is not determined by membrane protrusion *per se*, but through the subsequent development of strong substrate adhesions and traction forces.

The functional role of cell substrate adhesion interaction was further probed through the localized application of GRGDTP peptide, a competitive inhibitor of integrin-extracellular matrix binding. Using this approach we found that inhibition of

frontal adhesions resulted in a drastic and global decrease in traction forces, suggesting that the integrins and associated cytoskeleton in this region are specialized in their abilities to transmit active forces and to maintain the general tension throughout the cell. Conversely, release of the trailing edge resulted in no decrease in traction forces elsewhere in the cell, suggesting that these are passive forces that serve to anchor the cell to the underlying substrate and additionally resist forces generated in other regions of the cell transmitted throughout the cell body. Thus the trailing edge and elongated cell body may be maintained by one type of anchoring sites whereas the leading edge may constitute a mechanically distinct entity that serves to exert strong forces that tow the anchored cell body forward.

Important questions still remain concerning how mechanical forces are generated and where exactly in the cell they are generated. If the forces are generated in a location distal to the leading edge, how then are these forces transmitted from their origin to the leading edge? Also of great interest would be the elucidation of the molecular components that make up the different mechanical zones hypothesized in the frontal towing model. In addition, it is important to understand the mechanism that distinguishes between focal adhesions that serve to propel the cell forward during migration, from those that serve to anchor the cell onto the substrate.

H-ras transformed NIH 3T3 cells showed a greatly reduced magnitude in traction forces, although the duration of localized traction force activities at protrusions remained similar to that for normal NIH 3T3 fibroblasts. The forces exerted by H-ras transformed cells had also become radialy symmetric and appeared scattered in small pockets all along the cell, likely giving rise to the loss of a defined polarity. Also different in H-ras

transformed cells were the images of shear force as compared to normal cells. The H-ras transformed cells showed multiple small mechanically discrete zones with neither an organized front nor a well-defined tail. Questions remain why the transient protrusions, normally short lived in NIH 3T3 cells, tend to become amplified in H-ras transformed NIH 3T3 cells leading to their erratic motile activity. One potential hypothesis for this is that local traction forces and adhesive sites at the leading edge of normal cells may activate a positive feedback mechanism that maintains head to tail cell polarity while a negative feedback in distal regions of the cell act to suppress protrusive/adhesive activities elsewhere. These mechanisms may be disrupted in transformed cells. In support of this hypothesis previous studies have suggested that H-ras mediated signaling pathways may interact with those mediated by the small GTP-binding proteins, including rac and rho, which are known modulators of actin organization as well as myosin II contractility (Hall, 1998; Narumiya et al., 1997; Rottner et al., 1999b).

Having mapped the temporal and spatial distribution of traction forces during cell migration, I turned my attention to the regulation of cell motility via physical parameters. One potential mediator of this mechanical response is calcium ions given their multiple effects on the actin cytoskeleton as well as other intracellular components potentially involved in cell migration. Simple substrate stretching experiments have shown that mechanical stretching increased intracellular calcium ion concentration, an effect inhibited by the stretch-activated channel blocker gadolinium. Additionally stretching also resulted in a significant increase in cellular traction forces whereas gadolinium abolished this stretching response and caused the traction forces to drop to the baseline.

Electrophysiological studies of these cells in conjunction with additional pharmacological channel blocking analysis would serve to further elucidate the presence of stretch-activated channels in these cells. The present results could also be further extended using a peptide toxin from *Grammostola spatulata* spider venom which has been identified as a specific inhibitor of stretch-activated channels (Suchyna et al., 2000). In order to further relate changes in calcium ion concentration (either global or local) to increases in traction force magnitude and propagation (either globally or locally), it would be of great insight to be able to quantify force propagation and changes in intracellular calcium ion concentration simultaneously. The sensitivity of our system would also allow us to visualize if calcium ions increased locally at the site of stretching and if this correlated with localized traction force propagation. The study could be further extended using caged calcium ions to test any putative relationship between calcium ions and traction forces.

Our results using IRM and immuno-flourescence staining have shown that application of gadolinium resulted in a transient change in focal adhesion appearance as well as a sustained reduction of vinculin protein and phosphotyrosine from focal adhesions. To further our knowledge of the effects of stretch-activated channels on focal adhesions, cells transfected with GFP labeled vinculin, and/or other focal adhesion proteins (e.g. zyxin, talin) could be used to observe if gadolinium application results in the disassembly and/or miss-location of focal adhesion proteins during focal adhesion formation (Critchley, 2000). Previous studies have shown that cells appear to preferentially develop the strongest traction forces at new and nascent focal adhesion sites (Beningo et al., 2001). Utilizing cells transfected with GFP-labeled focal adhesion

proteins in conjunction with the localized application of gadolinium could shed important light on the assembly of focal adhesions relative to calcium entry into the cell.

The inter-relation between mechanical stimulus and cell signaling is a growing field with far reaching implications in a vast array of cellular functions. Further elucidation of the mechanisms by which cells send and receive mechanical signals, and translate this information into changes in migration behavior will further deepen our overall understanding of cell migration, as well as its role in both normal body functions and various pathological conditions.

References

Abercrombie, M., and G.A. Dunn. 1975. Adhesions of fibroblasts to substratum during contact inhibition observed by interference reflection microscopy. *Exp Cell Res.* 92:57-62.

Abercrombie, M., J.E. Heaysman, and S.M. Pegrum. 1970. The locomotion of fibroblasts in culture. I. Movements of the leading edge. *Exp Cell Res.* 59:393-8.

Abercrombie, M., J.E. Heaysman, and S.M. Pegrum. 1971. The locomotion of fibroblasts in culture. IV. Electron microscopy of the leading lamella. *Exp Cell Res.* 67:359-67.

Abraham, V.C., V. Krishnamurthi, D.L. Taylor, and F. Lanni. 1999. The actin-based nanomachine at the leading edge of migrating cells. *Biophys J.* 77:1721-32.

Albrecht-Buehler, G. 1980. Autonomous movements of cytoplasmic fragments. *Proc Natl Acad Sci U S A.* 77:6639-43.

Allen, R.D. 1981. Motility. *J Cell Biol.* 91:148s-155s.

Anderson, K.I., and R. Cross. 2000. Contact dynamics during keratocyte motility. *Curr Biol.* 10:253-60.

Balaban, N.Q., U.S. Schwarz, D. Riveline, P. Goichberg, G. Tzur, I. Sabanay, D. Mahalu, S. Safran, A. Bershadsky, L. Addadi, and B. Geiger. 2001. Force and focal adhesion assembly: a close relationship studied using elastic micropatterned substrates. *Nat Cell Biol.* 3:466-72.

Bear, J.E., J.J. Loureiro, I. Libova, R. Fassler, J. Wehland, and F.B. Gertler. 2000. Negative regulation of fibroblast motility by Ena/VASP proteins. *Cell.* 101:717-28.

Beauvais-Jouneau, A., and J.P. Thiery. 1997. Multiple roles for integrins during development. *Biol Cell.* 89:5-11.

Beckerle, M.C. 1997. Zyxin: zinc fingers at sites of cell adhesion. *Bioessays.* 19:949-57.

Beckerle, M.C., K. Burridge, G.N. DeMartino, and D.E. Croall. 1987. Colocalization of calcium-dependent protease II and one of its substrates at sites of cell adhesion. *Cell.* 51:569-77.

Beningo, K.A., M. Dembo, I. Kaverina, J.V. Small, and Y.L. Wang. 2001. Nascent focal adhesions are responsible for the generation of strong propulsive forces in migrating fibroblasts. *J Cell Biol.* 153:881-8.

Beningo, K.A., C.M. Lo, and Y.L. Wang. 2002. Flexible polyacrylamide substrata for the analysis of mechanical interactions at cell-substratum adhesions. *Methods Cell Biol.* 69:325-39.

Bondy, G.P., S. Wilson, and A.F. Chambers. 1985. Experimental metastatic ability of H-ras-transformed NIH3T3 cells. *Cancer Res.* 45:6005-9.

Borisy, G.G., and T.M. Svitkina. 2000. Actin machinery: pushing the envelope. *Curr Opin Cell Biol.* 12:104-12.

Boudreau, N.J., and P.L. Jones. 1999. Extracellular matrix and integrin signaling: the shape of things to come. *Biochem J.* 339 (Pt 3):481-8.

Bray, D. 2001. Cell Movements From Molecules to Motility. Garland Publishing, New York. 119-120.

Brown, A.F., V. Dugina, G.A. Dunn, and J.M. Vasiliev. 1989. A quantitative analysis of alterations in the shape of cultured fibroblasts induced by tumor-promoting phorbol ester. *Cell Biol Int Rep.* 13:357-66.

Brundage, R.A., K.E. Fogarty, R.A. Tuft, and F.S. Fay. 1991. Calcium gradients underlying polarization and chemotaxis of eosinophils. *Science.* 254:703-6.

Burton, K., J.H. Park, and D.L. Taylor. 1999. Keratocytes generate traction forces in two phases. *Mol Biol Cell.* 10:3745-69.

Burton, K., and D.L. Taylor. 1997. Traction forces of cytokinesis measured with optically modified elastic substrata. *Nature.* 385:450-4.

Byers, H.R., T. Etoh, J.R. Doherty, A.J. Sober, and M.C. Mihm, Jr. 1991. Cell migration and actin organization in cultured human primary, recurrent cutaneous and metastatic melanoma. Time-lapse and image analysis. *Am J Pathol.* 139:423-35.

Carpenter, C.L., and L.C. Cantley. 1996. Phosphoinositide kinases. *Curr Opin Cell Biol.* 8:153-8.

Carpenter, C.L., B.C. Duckworth, K.R. Auger, B. Cohen, B.S. Schaffhausen, and L.C. Cantley. 1990. Purification and characterization of phosphoinositide 3-kinase from rat liver. *J Biol Chem.* 265:19704-11.

Carter, S.B. 1967. Haptotaxis and the mechanism of cell motility. *Nature.* 213:256-60.

Chen, H.C., P.A. Appeddu, J.T. Parsons, J.D. Hildebrand, M.D. Schaller, and J.L. Guan. 1995. Interaction of focal adhesion kinase with cytoskeletal protein talin. *J Biol Chem.* 270:16995-9.

Chen, W.T. 1981. Surface changes during retraction-induced spreading of fibroblasts. *J Cell Sci.* 49:1-13.

Chicurel, M.E., C.S. Chen, and D.E. Ingber. 1998. Cellular control lies in the balance of forces. *Curr Opin Cell Biol.* 10:232-9.

Cooper, G.M. 1997. The Cell, A Molecular Approach. *In* The Cell, A Molecular Approach. ASM Press, Washinton. 599-608.

Cox, E.A., and A. Huttenlocher. 1998. Regulation of integrin-mediated adhesion during cell migration. *Microsc Res Tech.* 43:412-9.

Crawford, A.W., J.W. Michelsen, and M.C. Beckerle. 1992. An interaction between zyxin and alpha-actinin. *J Cell Biol.* 116:1381-93.

Critchley, D.R. 2000. Focal adhesions - the cytoskeletal connection. *Curr Opin Cell Biol.* 12:133-9.

Davies, P.F. 1995. Flow-mediated endothelial mechanotransduction. *Physiol Rev.* 75:519-60.

De Beus, E., and K. Jacobson. 1998. Integrin involvement in keratocyte locomotion. *Cell Motil Cytoskeleton.* 41:126-37.

De Nichilo, M.O., and K.M. Yamada. 1996. Integrin alpha v beta 5-dependent serine phosphorylation of paxillin in cultured human macrophages adherent to vitronectin. *J Biol Chem.* 271:11016-22.

Dedhar, S., E. Ruoslahti, and M.D. Pierschbacher. 1987. A cell surface receptor complex for collagen type I recognizes the Arg-Gly-Asp sequence. *J Cell Biol.* 104:585-93.

Dekker, L.V., and P.J. Parker. 1994. Protein kinase C--a question of specificity. *Trends Biochem Sci.* 19:73-7.

Dembo, M., T. Oliver, A. Ishihara, and K. Jacobson. 1996. Imaging the traction stresses exerted by locomoting cells with the elastic substratum method. *Biophys J.* 70:2008-22.

Dembo, M., and Y.L. Wang. 1999. Stresses at the cell-to-substrate interface during locomotion of fibroblasts. *Biophys J.* 76:2307-16.

DePasquale, J.A., and C.S. Izzard. 1987. Evidence for an actin-containing cytoplasmic precursor of the focal contact and the timing of incorporation of vinculin at the focal contact. *J Cell Biol.* 105:2803-9.

Diakonova, M., G. Bokoch, and J.A. Swanson. 2002. Dynamics of cytoskeletal proteins during Fc gamma receptor-mediated phagocytosis in macrophages. *Mol Biol Cell.* 13:402-11.

DiMilla, P.A., K. Barbee, and D.A. Lauffenburger. 1991. Mathematical model for the effects of adhesion and mechanics on cell migration speed. *Biophys J.* 60:15-37.

Drees, B.E., K.M. Andrews, and M.C. Beckerle. 1999. Molecular dissection of zyxin function reveals its involvement in cell motility. *J Cell Biol.* 147:1549-60.

Ebashi, S. 1991. Excitation-contraction coupling and the mechanism of muscle contraction. *Annu Rev Physiol.* 53:1-16.

Egan, S.E., G.A. McClarty, L. Jarolim, J.A. Wright, I. Spiro, G. Hager, and A.H. Greenberg. 1987. Expression of H-ras correlates with metastatic potential: evidence for direct regulation of the metastatic phenotype in 10T1/2 and NIH 3T3 cells. *Mol Cell Biol.* 7:830-7.

Elson, E.L., Felder, S. F., Jay, P. Y., Kolodney, M. S., and Pasternack, C. 1999. Forces in Cell Locomotion. *Biochemical Society Symposium.* Vol. 65. J.M. Lackie, G. A. Dunn, and G.E. Jones, editor, Oxford, England. 299-314.

Galbraith, C.G., and M.P. Sheetz. 1997. A micromachined device provides a new bend on fibroblast traction forces. *Proc Natl Acad Sci U S A.* 94:9114-8.

Galbraith, C.G., and M.P. Sheetz. 1998. Forces on adhesive contacts affect cell function. *Curr Opin Cell Biol.* 10:566-71.

Gehlsen, K.R., W.S. Argraves, M.D. Pierschbacher, and E. Ruoslahti. 1988. Inhibition of in vitro tumor cell invasion by Arg-Gly-Asp-containing synthetic peptides. *J Cell Biol.* 106:925-30.

Geiger, B. 1979. A 130K protein from chicken gizzard: its localization at the termini of microfilament bundles in cultured chicken cells. *Cell.* 18:193-205.

Geiger, B., and A. Bershadsky. 2001. Assembly and mechanosensory function of focal contacts. *Curr Opin Cell Biol.* 13:584-92.

Giancotti, F.G., and E. Ruoslahti. 1999. Integrin signaling. *Science.* 285:1028-32.

Glading, A., D.A. Lauffenburger, and A. Wells. 2002. Cutting to the chase: calpain proteases in cell motility. *Trends Cell Biol.* 12:46-54.

Glogauer, M., P. Arora, G. Yao, I. Sokholov, J. Ferrier, and C.A. McCulloch. 1997. Calcium ions and tyrosine phosphorylation interact coordinately with actin to regulate cytoprotective responses to stretching. *J Cell Sci.* 110 (Pt 1):11-21.

Glotzer, M. 2001. Animal cell cytokinesis. *Annu Rev Cell Dev Biol.* 17:351-86.

Goldschmidt-Clermont, P.J., R.M. Galbraith, D.L. Emerson, F. Marsot, A.E. Nel, and P. Arnaud. 1985. Distinct sites on the G-actin molecule bind group-specific component and deoxyribonuclease I. *Biochem J.* 228:471-7.

Grinnell, F., M. Zhu, M.A. Carlson, and J.M. Abrams. 1999. Release of mechanical tension triggers apoptosis of human fibroblasts in a model of regressing granulation tissue. *Exp Cell Res.* 248:608-19.

Guharay, F., and F. Sachs. 1984. Stretch-activated single ion channel currents in tissue-cultured embryonic chick skeletal muscle. *J Physiol.* 352:685-701.

Gumbiner, B.M. 1996. Cell adhesion: the molecular basis of tissue architecture and morphogenesis. *Cell.* 84:345-57.

Haffner, C., T. Jarchau, M. Reinhard, J. Hoppe, S.M. Lohmann, and U. Walter. 1995. Molecular cloning, structural analysis and functional expression of the proline-rich focal adhesion and microfilament-associated protein VASP. *Embo J.* 14:19-27.

Hall, A. 1998. Rho GTPases and the actin cytoskeleton. *Science.* 279:509-14.

Hanks, S.K., M.B. Calalb, M.C. Harper, and S.K. Patel. 1992. Focal adhesion protein-tyrosine kinase phosphorylated in response to cell attachment to fibronectin. *Proc Natl Acad Sci U S A.* 89:8487-91.

Hannigan, G.E., C. Leung-Hagesteijn, L. Fitz-Gibbon, M.G. Coppolino, G. Radeva, J. Filmus, J.C. Bell, and S. Dedhar. 1996. Regulation of cell adhesion and anchorage-dependent growth by a new beta 1-integrin-linked protein kinase. *Nature.* 379:91-6.

Harris, A.K., D. Stopak, and P. Wild. 1981. Fibroblast traction as a mechanism for collagen morphogenesis. *Nature.* 290:249-51.

Harris, A.K., P. Wild, and D. Stopak. 1980. Silicone rubber substrata: a new wrinkle in the study of cell locomotion. *Science.* 208:177-9.

Harte, M.T., J.D. Hildebrand, M.R. Burnham, A.H. Bouton, and J.T. Parsons. 1996. p130Cas, a substrate associated with v-Src and v-Crk, localizes to focal adhesions and binds to focal adhesion kinase. *J Biol Chem.* 271:13649-55.

Heath, J.P. 1983. Behavior and structure of the leading lamella in moving fibroblasts. I. Occurrence and centripetal movement of arc-shaped microfilament bundles beneath the dorsal cell surface. *J Cell Sci.* 60:331-54.

Hildebrand, J.D., M.D. Schaller, and J.T. Parsons. 1995. Paxillin, a tyrosine phosphorylated focal adhesion-associated protein binds to the carboxyl terminal domain of focal adhesion kinase. *Mol Biol Cell.* 6:637-47.

Hildebrand, J.D., J.M. Taylor, and J.T. Parsons. 1996. An SH3 domain-containing GTPase-activating protein for Rho and Cdc42 associates with focal adhesion kinase. *Mol Cell Biol.* 16:3169-78.

Hill, S.A., S. Wilson, and A.F. Chambers. 1988. Clonal heterogeneity, experimental metastatic ability, and p21 expression in H-ras-transformed NIH 3T3 cells. *J Natl Cancer Inst.* 80:484-90.

Hobert, O., J.W. Schilling, M.C. Beckerle, A. Ullrich, and B. Jallal. 1996. SH3 domain-dependent interaction of the proto-oncogene product Vav with the focal contact protein zyxin. *Oncogene.* 12:1577-81.

Horwitz, A.R., and J.T. Parsons. 1999. Cell migration--movin' on. *Science.* 286:1102-3.

Huber, P.A. 1997. Caldesmon. *Int J Biochem Cell Biol.* 29:1047-51.

Huttenlocher, A., S.P. Palecek, Q. Lu, W. Zhang, R.L. Mellgren, D.A. Lauffenburger, M.H. Ginsberg, and A.F. Horwitz. 1997. Regulation of cell migration by the calcium-dependent protease calpain. *J Biol Chem.* 272:32719-22.

Hyatt, S.L., L. Liao, C. Chapline, and S. Jaken. 1994. Identification and characterization of alpha-protein kinase C binding proteins in normal and transformed REF52 cells. *Biochemistry*. 33:1223-8.

Hynes, R.O. 1992. Integrins: versatility, modulation, and signaling in cell adhesion. *Cell*. 69:11-25.

Ilic, D., C.H. Damsky, and T. Yamamoto. 1997. Focal adhesion kinase: at the crossroads of signal transduction. *J Cell Sci*. 110 (Pt 4):401-7.

Ingber, D. 2002. Mechanical signaling. *Ann N Y Acad Sci*. 961:162-3.

Ishihara, A., B. Holifield, and K. Jacobson. 1988. Analysis of lateral redistribution of a plasma membrane glycoprotein-monoclonal antibody complex [corrected]. *J Cell Biol*. 106:329-43.

Izzard, C.S., and L.R. Lochner. 1976. Cell-to-substrate contacts in living fibroblasts: an interference reflexion study with an evaluation of the technique. *J Cell Sci*. 21:129-59.

Kamm, K.E., and J.T. Stull. 2001. Dedicated myosin light chain kinases with diverse cellular functions. *J Biol Chem*. 276:4527-30.

Ko, K.S., P.D. Arora, and C.A. McCulloch. 2001. Cadherins mediate intercellular mechanical signaling in fibroblasts by activation of stretch-sensitive calcium-permeable channels. *J Biol Chem*. 276:35967-77.

Kulkarni, S., T.C. Saido, K. Suzuki, and J.E. Fox. 1999. Calpain mediates integrin-induced signaling at a point upstream of Rho family members. *J Biol Chem*. 274:21265-75.

Lauffenburger, D.A., and A.F. Horwitz. 1996. Cell migration: a physically integrated molecular process. *Cell*. 84:359-69.

Leader, W.M., D. Stopak, and A.K. Harris. 1983. Increased contractile strength and tightened adhesions to the substratum result from reverse transformation of CHO cells by dibutyryl cyclic adenosine monophosphate. *J Cell Sci*. 64:1-11.

Lee, J., A. Ishihara, G. Oxford, B. Johnson, and K. Jacobson. 1999. Regulation of cell movement is mediated by stretch-activated calcium channels. *Nature*. 400:382-6.

Lee, J., M. Leonard, T. Oliver, A. Ishihara, and K. Jacobson. 1994. Traction forces generated by locomoting keratocytes. *J Cell Biol*. 127:1957-64.

Lee, W.M., and R.M. Galbraith. 1992. The extracellular actin-scavenger system and actin toxicity. *N Engl J Med*. 326:1335-41.

Leitinger, B., A. McDowall, P. Stanley, and N. Hogg. 2000. The regulation of integrin function by Ca(2+). *Biochim Biophys Acta*. 1498:91-8.

Li, Y., Hu, Z., and Li, C. 1993. New Methods for measuring Poisson's ration in polymer gels. *Journal of Applied Polymer Science*. 50:1107-1111.

Lo, C.M., H.B. Wang, M. Dembo, and Y.L. Wang. 2000. Cell movement is guided by the rigidity of the substrate. *Biophys J*. 79:144-52.

Lukashev, M.E., and Z. Werb. 1998. ECM signaling: orchestrating cell behavior and misbehavior. *Trends Cell Biol*. 8:437-41.

Malawista, S.E., and A. De Boisfleury Chevance. 1982. The cytokineplast: purified, stable, and functional motile machinery from human blood polymorphonuclear leukocytes. *J Cell Biol*. 95:960-73.

McKenna, N.M., and Y.L. Wang. 1989. Culturing cells on the microscope stage. *Methods Cell Biol*. 29:195-205.

McKenna, N.M., Y.L. Wang, and M.E. Konkel. 1989. Formation and movement of myosin-containing structures in living fibroblasts. *J Cell Biol.* 109:1163-72.
Mermall, V., P.L. Post, and M.S. Mooseker. 1998. Unconventional myosins in cell movement, membrane traffic, and signal transduction. *Science.* 279:527-33.
Munevar, S., Y. Wang, and M. Dembo. 2001a. Traction force microscopy of migrating normal and H-ras transformed 3T3 fibroblasts. *Biophys J.* 80:1744-57.
Munevar, S., Y.L. Wang, and M. Dembo. 2001b. Distinct roles of frontal and rear cell-substrate adhesions in fibroblast migration. *Mol Biol Cell.* 12:3947-54.
Mutsaers, S.E., J.E. Bishop, G. McGrouther, and G.J. Laurent. 1997. Mechanisms of tissue repair: from wound healing to fibrosis. *Int J Biochem Cell Biol.* 29:5-17.
Narumiya, S., T. Ishizaki, and N. Watanabe. 1997. Rho effectors and reorganization of actin cytoskeleton. *FEBS Lett.* 410:68-72.
Naruse, K., T. Yamada, and M. Sokabe. 1998. Involvement of SA channels in orienting response of cultured endothelial cells to cyclic stretch. *Am J Physiol.* 274:H1532-8.
O'Connell, C.B., A.K. Warner, and Y. Wang. 2001. Distinct roles of the equatorial and polar cortices in the cleavage of adherent cells. *Curr Biol.* 11:702-7.
Oliver, T., M. Dembo, and K. Jacobson. 1995. Traction forces in locomoting cells. *Cell Motil Cytoskeleton.* 31:225-40.
Oliver, T., M. Dembo, and K. Jacobson. 1999. Separation of propulsive and adhesive traction stresses in locomoting keratocytes. *J Cell Biol.* 145:589-604.
Oliver, T., K. Jacobson, and M. Dembo. 1998. Design and use of substrata to measure traction forces exerted by cultured cells. *Methods Enzymol.* 298:497-521.
Parsons, J.T. 1996. Integrin-mediated signaling: regulation by protein tyrosine kinases and small GTP-binding proteins. *Curr Opin Cell Biol.* 8:146-52.
Pelham, R.J., Jr., and Y. Wang. 1997. Cell locomotion and focal adhesions are regulated by substrate flexibility. *Proc Natl Acad Sci U S A.* 94:13661-5.
Pelham, R.J., Jr., and Y. Wang. 1999. High resolution detection of mechanical forces exerted by locomoting fibroblasts on the substrate. *Mol Biol Cell.* 10:935-45.
Perrin, B.J., and A. Huttenlocher. 2002. Calpain. *Int J Biochem Cell Biol.* 34:722-5.
Petit, V., and J.P. Thiery. 2000. Focal adhesions: structure and dynamics. *Biol Cell.* 92:477-94.
Pollard, T.D., and G.G. Borisy. 2003. Cellular motility driven by assembly and disassembly of actin filaments. *Cell.* 112:453-65.
Pytela, R., M.D. Pierschbacher, M.H. Ginsberg, E.F. Plow, and E. Ruoslahti. 1986. Platelet membrane glycoprotein IIb/IIIa: member of a family of Arg-Gly-Asp--specific adhesion receptors. *Science.* 231:1559-62.
Rabinovitz, I., and A.M. Mercurio. 1996. The integrin alpha 6 beta 4 and the biology of carcinoma. *Biochem Cell Biol.* 74:811-21.
Radmacher, M., R.W. Tillamnn, M. Fritz, and H.E. Gaub. 1992. From molecules to cells: imaging soft samples with the atomic force microscope. *Science.* 257:1900-5.
Reinhard, M., M. Halbrugge, U. Scheer, C. Wiegand, B.M. Jockusch, and U. Walter. 1992. The 46/50 kDa phosphoprotein VASP purified from human platelets is a novel protein associated with actin filaments and focal contacts. *Embo J.* 11:2063-70.

Reinhard, M., K. Jouvenal, D. Tripier, and U. Walter. 1995. Identification, purification, and characterization of a zyxin-related protein that binds the focal adhesion and microfilament protein VASP (vasodilator-stimulated phosphoprotein). *Proc Natl Acad Sci U S A.* 92:7956-60.

Riveline, D., E. Zamir, N.Q. Balaban, U.S. Schwarz, T. Ishizaki, S. Narumiya, Z. Kam, B. Geiger, and A.D. Bershadsky. 2001. Focal contacts as mechanosensors: externally applied local mechanical force induces growth of focal contacts by an mDia1-dependent and ROCK-independent mechanism. *J Cell Biol.* 153:1175-86.

Rosen, A., K.F. Keenan, M. Thelen, A.C. Nairn, and A. Aderem. 1990. Activation of protein kinase C results in the displacement of its myristoylated, alanine-rich substrate from punctate structures in macrophage filopodia. *J Exp Med.* 172:1211-5.

Rosenberg, S., A. Stracher, and K. Burridge. 1981. Isolation and characterization of a calcium-sensitive alpha-actinin-like protein from human platelet cytoskeletons. *J Biol Chem.* 256:12986-91.

Rottner, K., B. Behrendt, J.V. Small, and J. Wehland. 1999a. VASP dynamics during lamellipodia protrusion. *Nat Cell Biol.* 1:321-2.

Rottner, K., A. Hall, and J.V. Small. 1999b. Interplay between Rac and Rho in the control of substrate contact dynamics. *Curr Biol.* 9:640-8.

Sadoshima, J., and S. Izumo. 1993. Mechanical stretch rapidly activates multiple signal transduction pathways in cardiac myocytes: potential involvement of an autocrine/paracrine mechanism. *Embo J.* 12:1681-92.

Sai, X., K. Naruse, and M. Sokabe. 1999. Activation of pp60(src) is critical for stretch-induced orienting response in fibroblasts. *J Cell Sci.* 112 (Pt 9):1365-73.

Sawada, Y., and M.P. Sheetz. 2002. Force transduction by Triton cytoskeletons. *J Cell Biol.* 156:609-15.

Schaller, M.D., C.A. Borgman, B.S. Cobb, R.R. Vines, A.B. Reynolds, and J.T. Parsons. 1992. pp125FAK a structurally distinctive protein-tyrosine kinase associated with focal adhesions. *Proc Natl Acad Sci U S A.* 89:5192-6.

Schoenwaelder, S.M., and K. Burridge. 1999. Bidirectional signaling between the cytoskeleton and integrins. *Curr Opin Cell Biol.* 11:274-86.

Schwartz, M.A., and V. Baron. 1999. Interactions between mitogenic stimuli, or, a thousand and one connections. *Curr Opin Cell Biol.* 11:197-202.

Sheetz, M.P., D.P. Felsenfeld, and C.G. Galbraith. 1998. Cell migration: regulation of force on extracellular-matrix-integrin complexes. *Trends Cell Biol.* 8:51-4.

Shim, S.R., S. Kook, J.I. Kim, and W.K. Song. 2001. Degradation of focal adhesion proteins paxillin and p130cas by caspases or calpains in apoptotic rat-1 and L929 cells. *Biochem Biophys Res Commun.* 286:601-8.

Shin, E.Y., J.Y. Lee, M.K. Park, G.B. Jeong, E.G. Kim, and S.Y. Kim. 1999. H-Ras is a negative regulator of alpha3beta1 integrin expression in ECV304 endothelial cells. *Biochem Biophys Res Commun.* 257:95-9.

Shirinsky, V.P., A.S. Antonov, K.G. Birukov, A.V. Sobolevsky, Y.A. Romanov, N.V. Kabaeva, G.N. Antonova, and V.N. Smirnov. 1989. Mechano-chemical control of human endothelium orientation and size. *J Cell Biol.* 109:331-9.

Small, J.V., K. Rottner, I. Kaverina, and K.I. Anderson. 1998. Assembling an actin cytoskeleton for cell attachment and movement. *Biochim Biophys Acta.* 1404:271-81.

Small, J.V., T. Stradal, E. Vignal, and K. Rottner. 2002. The lamellipodium: where motility begins. *Trends Cell Biol.* 12:112-20.

Stossel, T.P. 1993. On the crawling of animal cells. *Science.* 260:1086-94.

Suchyna, T.M., J.H. Johnson, K. Hamer, J.F. Leykam, D.A. Gage, H.F. Clemo, C.M. Baumgarten, and F. Sachs. 2000. Identification of a peptide toxin from Grammostola spatulata spider venom that blocks cation-selective stretch-activated channels. *J Gen Physiol.* 115:583-98.

Sun, H.Q., M. Yamamoto, M. Mejillano, and H.L. Yin. 1999. Gelsolin, a multifunctional actin regulatory protein. *J Biol Chem.* 274:33179-82.

Svitkina, T.M., and G.G. Borisy. 1999. Progress in protrusion: the tell-tale scar. *Trends Biochem Sci.* 24:432-6.

Svitkina, T.M., A.B. Verkhovsky, K.M. McQuade, and G.G. Borisy. 1997. Analysis of the actin-myosin II system in fish epidermal keratocytes: mechanism of cell body translocation. *J Cell Biol.* 139:397-415.

Takagi, J., B.M. Petre, T. Walz, and T.A. Springer. 2002. Global conformational rearrangements in integrin extracellular domains in outside-in and inside-out signaling. *Cell.* 110:599-11.

Tomasek, J.J., G. Gabbiani, B. Hinz, C. Chaponnier, and R.A. Brown. 2002. Myofibroblasts and mechano-regulation of connective tissue remodeling. *Nat Rev Mol Cell Biol.* 3:349-63.

Tortora G., F., Brundell, C., Case. 1995. Microbiology an Introduction. Benjamin/Cummings Publishing Company, New York. 801 pp.

Turner, C.E., M.C. Brown, J.A. Perrotta, M.C. Riedy, S.N. Nikolopoulos, A.R. McDonald, S. Bagrodia, S. Thomas, and P.S. Leventhal. 1999. Paxillin LD4 motif binds PAK and PIX through a novel 95-kD ankyrin repeat, ARF-GAP protein: A role in cytoskeletal remodeling. *J Cell Biol.* 145:851-63.

Tuxworth, R.I., I. Weber, D. Wessels, G.C. Addicks, D.R. Soll, G. Gerisch, and M.A. Titus. 2001. A role for myosin VII in dynamic cell adhesion. *Curr Biol.* 11:318-29.

Tzima, E., M.A. del Pozo, S.J. Shattil, S. Chien, and M.A. Schwartz. 2001. Activation of integrins in endothelial cells by fluid shear stress mediates Rho-dependent cytoskeletal alignment. *Embo J.* 20:4639-47.

Van Baelen, H., R. Bouillon, and P. De Moor. 1980. Vitamin D-binding protein (Gc-globulin) binds actin. *J Biol Chem.* 255:2270-2.

Varani, J., S.E. Fligiel, and B. Wilson. 1986. Motility of rasH oncogene transformed NIH-3T3 cells. *Invasion Metastasis.* 6:335-46.

Verkhovsky, A.B., and G.G. Borisy. 1993. Non-sarcomeric mode of myosin II organization in the fibroblast lamellum. *J Cell Biol.* 123:637-52.

Verkhovsky, A.B., T.M. Svitkina, and G.G. Borisy. 1999. Self-polarization and directional motility of cytoplasm. *Curr Biol.* 9:11-20.

Volkmann, N., and D. Hanein. 2000. Actomyosin: law and order in motility. *Curr Opin Cell Biol.* 12:26-34.

Walsh, M.P. 1994. Calmodulin and the regulation of smooth muscle contraction. *Mol Cell Biochem.* 135:21-41.

Wang, H.B., M. Dembo, and Y.L. Wang. 2000. Substrate flexibility regulates growth and apoptosis of normal but not transformed cells. *Am J Physiol Cell Physiol.* 279:C1345-50.

Wang, Y.L. 1985. Exchange of actin subunits at the leading edge of living fibroblasts: possible role of tread milling. *J Cell Biol.* 101:597-602.

Wang, Y.L., and R.J. Pelham, Jr. 1998. Preparation of a flexible, porous polyacrylamide substrate for mechanical studies of cultured cells. *Methods Enzymol.* 298:489-96.

Wells, A.L., A.W. Lin, L.Q. Chen, D. Safer, S.M. Cain, T. Hasson, B.O. Carragher, R.A. Milligan, and H.L. Sweeney. 1999. Myosin VI is an actin-based motor that moves backwards. *Nature.* 401:505-8.

Yamada, K.M., and S. Miyamoto. 1995. Integrin transmembrane signaling and cytoskeletal control. *Curr Opin Cell Biol.* 7:681-9.

Yang, X.C., and F. Sachs. 1989. Block of stretch-activated ion channels in Xenopus oocytes by gadolinium and calcium ions. *Science.* 243:1068-71.

Zheng, J.Q. 2000. Turning of nerve growth cones induced by localized increases in intracellular calcium ions. *Nature.* 403:89-93.